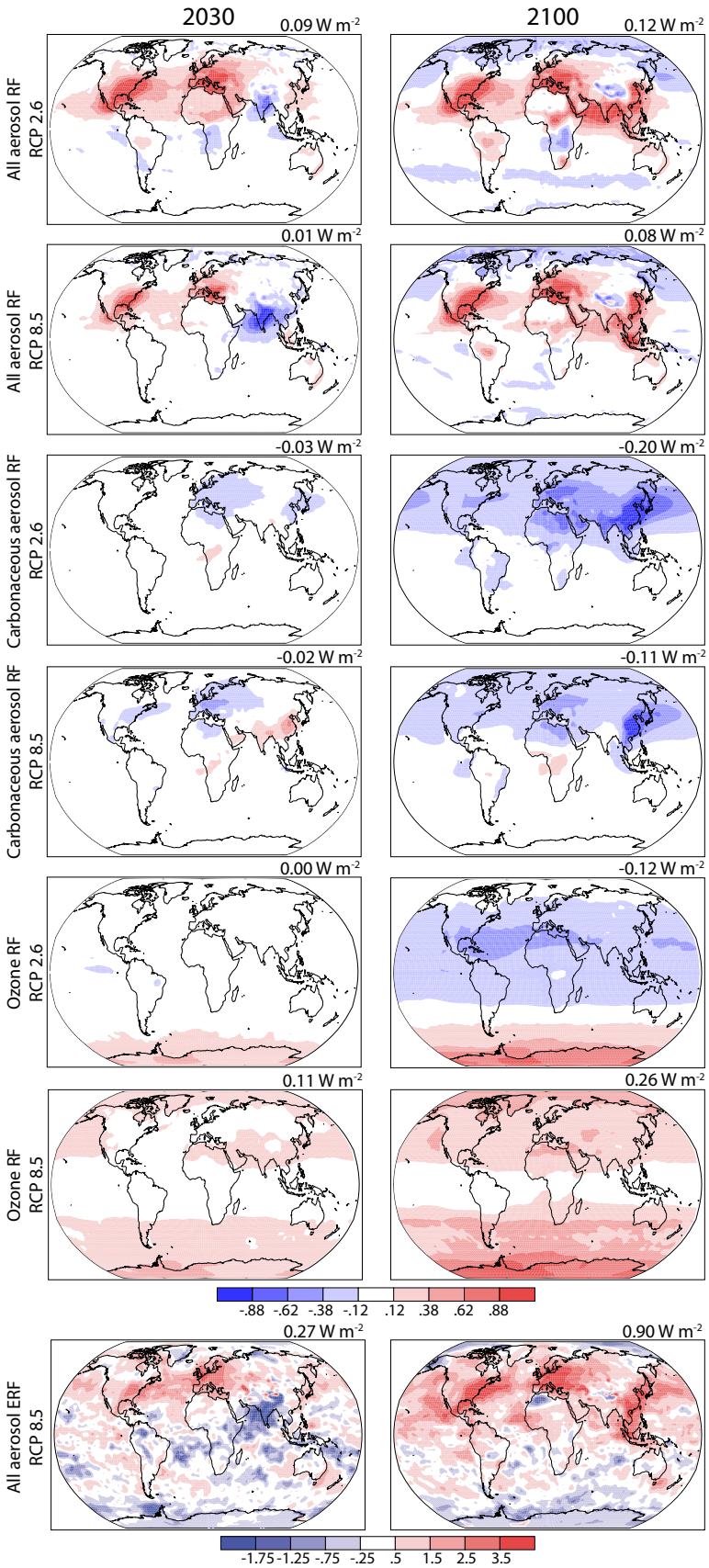

Figure 8.26 | Multi-model mean RF (W m^{-2}) due to aerosol–radiation interaction of all anthropogenic aerosols (first and second rows) and anthropogenic carbonaceous (BC+OC) aerosols (third and fourth rows), and total ozone (fifth and sixth rows) in 2030 (left) and 2100 (right) relative to 2000 for RCP2.6 (top each) and RCP8.5 (bottom each) based on the ACCMIP simulations. The seventh row shows multi-model mean ERF (W m^{-2}) by all anthropogenic aerosols in 2030 (left) and 2100 (right) relative to 2000 for RCP8.5. Global area-weighted means are given in the upper right of each panel.

8.7 Emission Metrics

8.7.1 Metric Concepts

8.7.1.1 Introduction

To quantify and compare the climate impacts of various emissions, it is necessary to choose a climate parameter by which to measure the effects; that is, RF, temperature response, and so forth. Thus, various choices are needed for the steps down the cause–effect chain from emissions to climate change and impacts (Figure 8.27 and Box 8.4). Each step in the cause effect chain requires a modelling framework. For assessments and evaluation one may—as an alternative to models that explicitly include physical processes resulting in forcing and responses—apply simpler measures or *metrics* that are based on results from complex models. Metrics are used to quantify the contributions to climate change of emissions of different substances and can thus act as 'exchange rates' in multi-component policies or comparisons of emissions from regions/countries or sources/sectors. Metrics are also used in areas such as Life Cycle Assessments and Integrated Assessment Modelling (e.g., by IPCC WGIII).

Metrics can be given in *absolute* terms (e.g., K kg^{-1}) or in *relative* terms by normalizing to a reference gas — usually CO_2. To transform the effects of different emissions to a common scale — often called 'CO_2 equivalent emissions'—the emission (E_i) of component *i* can be multiplied with the adopted normalized metric (M_i): $M_i \times E_i = CO_2\text{-eq}_i$. Ideally, the climate effects of the calculated CO_2 equivalent emissions should be the same regardless of the mix of components emitted. However, different components have different physical properties, and a metric that establishes equivalence with regard to one effect cannot guarantee equivalence with regard to other effects and over extended time periods, for example, Lauder et al. (2013), O'Neill (2000), Smith and Wigley (2000), Fuglestvedt et al. (2003).

Metrics do not define goals and policy—they are tools that enable evaluation and implementation of multi-component policies (i.e., which emissions to abate). The most appropriate metric will depend on which aspects of climate change are most important to a particular application, and different climate policy goals may lead to different conclusions about what is the most suitable metric with which to implement that policy, for example, Plattner et al. (2009); Tol et al. (2012). Metrics that have been proposed include physical metrics as well as more comprehensive metrics that account for both physical and economic dimensions (see 8.7.1.5 and WGIII, Chapter 3).

This section provides an assessment that focuses on the scientific aspects and utility of emission metrics. Extending such an assessment to include more policy-oriented aspects of their performance and usage such as simplicity, transparency, continuity, economic implications of usage of one metric over another, and so forth, is not given here as this is beyond the scope of WGI. However, consideration of such aspects is vital for user-assessments. In the following, the focus is on the more well-known Global Warming Potential (GWP) and Global Temperature change Potential (GTP), though other concepts are also briefly discussed.

8.7.1.2 The Global Warming Potential Concept

The Global Warming Potential (GWP) is defined as the time-integrated RF due to a pulse emission of a given component, relative to a pulse emission of an equal mass of CO_2 (Figure 8.28a and formula). The GWP was presented in the First IPCC Assessment (Houghton et al., 1990), stating 'It must be stressed that there is no universally accepted methodology for combining all the relevant factors into a single global warming potential for greenhouse gas emissions. A simple approach has been adopted here to illustrate the difficulties inherent in the concept, ...'. Further, the First IPCC Assessment gave no clear physical interpretation of the GWP.

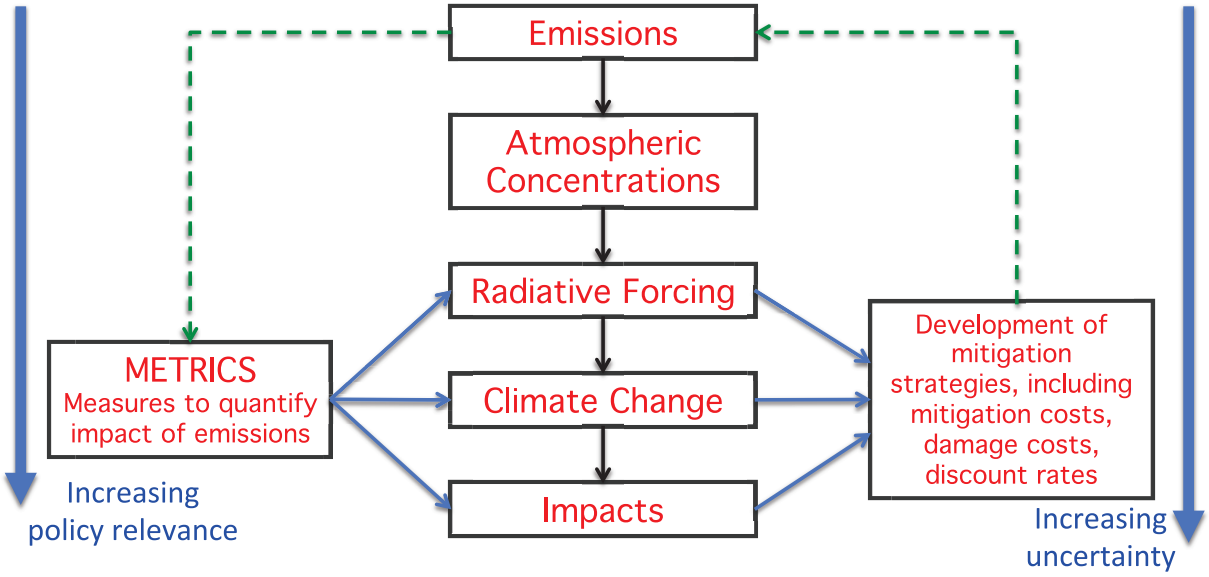

Figure 8.27 | The cause–effect chain from emissions to climate change and impacts showing how metrics can be defined to estimate responses to emissions (left) and for development of multi-component mitigation (right). The relevance of the various effects increases downwards but at the same time the uncertainty also increases. The dotted line on the left indicates that effects and impacts can be estimated directly from emissions, while the arrows on the right side indicate how these estimates can be used in development of strategies for reducing emissions. (Adapted from Fuglestvedt et al., 2003, and Plattner et al., 2009.)

Box 8.4 | Choices Required When Using Emission Metrics

Time frames: One can apply a *backward-looking* (i.e., historical) or a *forward-looking* perspective on the responses to emissions. In the forward-looking case one may use pulses of emissions, sustained emissions or emission scenarios. All choices of emission perturbations are somewhat artificial and idealized, and different choices serve different purposes. One may use the *level* (e.g., degrees Celsius) or *rate* of change (e.g., degrees Celsius per decade). Furthermore, the effects of emissions may be estimated at a particular time or be integrated over time up to a chosen time horizon. Alternatively, discounting of future effects may be introduced (i.e., a weighting of effects over time).

Type of effect or end-point: Radiative forcing, temperature change or sea level change, for example, could be examined (Figure 8.27). Metrics may also include eco/biological or socioeconomic damages. The choice of climate impact parameters is related to which aspects of climate change are considered relevant for interpretation of 'dangerous anthropogenic interference with the climate system' (UNFCCC Article 2).

Spatial dimension for emission and response: Equal-mass emissions of NTCFs from different regions can induce varying global mean climate responses, and the climate response also has a regional component irrespective of the regional variation in emissions. Thus, metrics may be given for region of *emission* as well as region of *response*.

Some of the choices involved in metrics are scientific (e.g., type of model, and how processes are included or parameterized in the models). Choices of time frames and climate impact are policy-related and cannot be based on science alone, but scientific studies can be used to analyse different approaches and policy choices.

A direct interpretation is that the GWP is an index of the total energy added to the climate system by a component in question relative to that added by CO_2. However, the GWP does not lead to equivalence with temperature or other climate variables (Fuglestvedt et al., 2000, 2003; O'Neill, 2000; Daniel et al., 2012; Smith and Wigley, 2000; Tanaka et al., 2009). Thus, the name 'Global Warming Potential' may be somewhat misleading, and 'relative cumulative forcing index' would be more appropriate. It can be shown that the GWP is approximately equal to the ratio (normalizing by the similar expression for CO_2) of the *equilibrium temperature response due to a sustained emission* of the species or to the *integrated temperature response for a pulse* emission (assuming efficacies are equal for the gases that are compared; O'Neill, 2000; Prather, 2002; Shine et al., 2005a; Peters et al., 2011a; Azar and Johansson, 2012).

The GWP has become the default metric for transferring emissions of different gases to a common scale; often called 'CO_2 equivalent emissions' (e.g., Shine, 2009). It has usually been integrated over 20, 100 or 500 years consistent with Houghton et al. (1990). Note, however that Houghton et al. presented these time horizons as 'candidates for discussion [that] should not be considered as having any special significance'. The GWP for a time horizon of 100 years was later adopted as a metric to implement the multi-gas approach embedded in the United Nations Framework Convention on Climate Change (UNFCCC) and made operational in the 1997 Kyoto Protocol. The choice of time horizon has a strong effect on the GWP values — and thus also on the calculated contributions of CO_2 equivalent emissions by component, sector or nation. There is no scientific argument for selecting 100 years compared with other choices (Fuglestvedt et al., 2003; Shine, 2009). The choice of time horizon is a value judgement because it depends

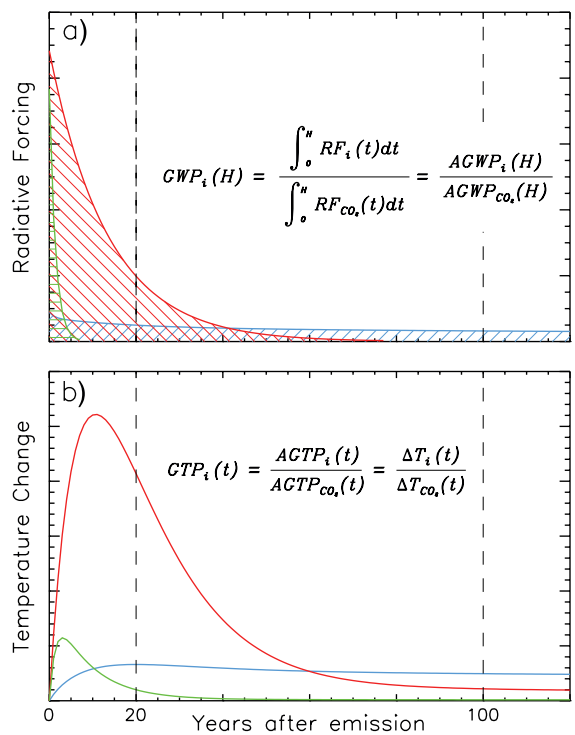

Figure 8.28 | (a) The Absolute Global Warming Potential (AGWP) is calculated by integrating the RF due to emission pulses over a chosen time horizon; for example, 20 and 100 years (vertical lines). The GWP is the ratio of AGWP for component *i* over AGWP for the reference gas CO_2. The blue hatched field represents the integrated RF from a pulse of CO_2, while the green and red fields represent example gases with 1.5 and 13 years lifetimes, respectively. (b) The Global Temperature change Potential (GTP) is based on the temperature response at a selected year after pulse emission of the same gases; e.g., 20 or 100 years (vertical lines). See Supplementary Material Section 8.SM.11 for equations for calculations of GWP and GTP.

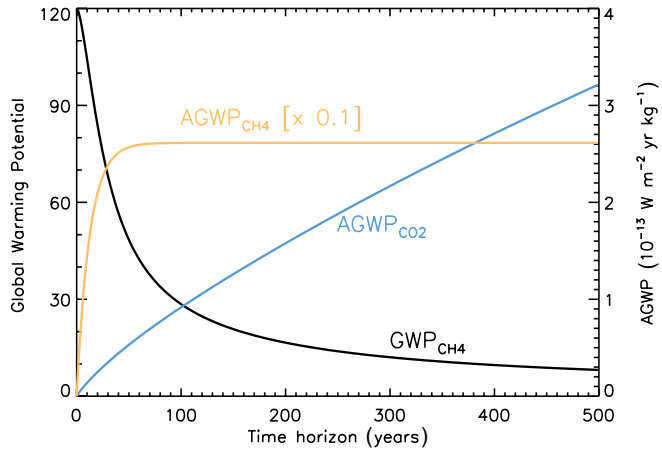

Figure 8.29 | Development of AGWP-CO_2, AGWP-CH_4 and GWP-CH_4 with time horizon. The yellow and blue curves show how the AGWPs changes with increasing time horizon. Because of the integrative nature the AGWP for CH_4 (yellow curve) reaches a constant level after about five decades. The AGWP for CO_2 continues to increase for centuries. Thus the ratio which is the GWP (black curve) falls with increasing time horizon.

on the relative weight assigned to effects at different times. Other important choices include the background atmosphere on which the GWP calculations are superimposed, and the way indirect effects and feedbacks are included (see Section 8.7.1.4).

For some gases the variation in GWP with time horizon mainly reflects properties of the reference gas, not the gas for which the GWP is calculated. The GWP for NTCFs decreases with increasing time horizon, as GWP is defined with the integrated RF of CO_2 in the denominator. As shown in Figure 8.29, after about five decades the development in the GWP for CH_4 is almost entirely determined by CO_2. However, for long-lived gases (e.g., SF_6) the development in GWP is controlled by both the increasing integrals of RF from the long-lived gas and CO_2.

8.7.1.3 The Global Temperature change Potential Concept

Compared to the GWP, the Global Temperature change Potential (GTP; Shine et al., 2005a) goes one step further down the cause–effect chain (Figure 8.27) and is defined as the *change in global mean surface temperature at a chosen point in time* in response to an emission pulse—relative to that of CO_2. Whereas GWP is integrated in time (Figure 8.28a), GTP is an end-point metric that is based on temperature change for a selected year, *t*, (see Figure 8.28b with formula). Like for the GWP, the impact from CO_2 is normally used as reference, hence, for a component *i*, $GTP(t)_i = AGTP(t)_i / AGTP(t)_{CO2} = \Delta T((t)_i / \Delta T(t)_{CO2}$, where AGTP is the absolute GTP giving temperature change per unit emission (see Supplementary Material Section 8.SM.11 for equations and parameter values). Shine et al. (2005a) presented the GTP for both pulse and sustained emission changes based on an energy balance model as well as analytical equations. A modification was later introduced (Shine et al., 2007) in which the time horizon is determined by the proximity to a target year as calculated by using scenarios and climate models (see Section 8.7.1.5).

Like GWP, the GTP values can be used for weighting the emissions to obtain 'CO_2 equivalents' (see Section 8.7.1.1). This gives the temperature effects of emissions relative to that of CO_2 for the chosen time horizon. As for GWP, the choice of time horizon has a strong effect on the metric values and the calculated contributions to warming.

In addition, the AGTP can be used to calculate the global mean temperature change due to any given emission scenario (assuming linearity) using a convolution of the emission scenarios and $AGTP_i$:

$$\Delta T(t) = \sum_i \int_0^t E_i(s) AGTP_i(t-s) ds \qquad (8.1)$$

where *i* is component, *t* is time, and *s* is time of emission (Berntsen and Fuglestvedt, 2008; Peters et al., 2011b; Shindell et al., 2011).

By accounting for the climate sensitivity and the exchange of heat between the atmosphere and the ocean, the GTP includes physical processes that the GWP does not. The GTP accounts for the slow response of the (deep) ocean, thereby prolonging the response to emissions beyond what is controlled by the decay time of the atmospheric concentration. Thus the GTP includes both the atmospheric adjustment time scale of the component considered and the response time scale of the climate system.

The GWP and GTP are fundamentally different by construction and different numerical values can be expected. In particular, the GWPs for NTCFs, over the same time frames, are higher than GTPs due to the integrative nature of the metric. The GTP values can be significantly affected by assumptions about the climate sensitivity and heat uptake by the ocean. Thus, the relative uncertainty ranges are wider for the GTP compared to GWP (see Section 8.7.1.4). The additional uncertainty is a typical trade-off when moving along the cause–effect chain to an effect of greater societal relevance (Figure 8.27). The formulation of the ocean response in the GTP has a substantial effect on the values; thus its characterization also represents a trade-off between simplicity and accuracy. As for GWP, the GTP is also influenced by the background atmosphere, and the way indirect effects and feedbacks are included (see Section 8.7.1.4).

8.7.1.4 Uncertainties and Limitations related to Global Warming Potential and Global Temperature change Potential

The uncertainty in the numerator of GWP; that is, the $AGWP_i$ (see formula in Figure 8.28a) is determined by uncertainties in lifetimes (or perturbation lifetimes) and radiative efficiency. Inclusion of indirect effects increases uncertainties (see below). For the reference gas CO_2, the uncertainty is dominated by uncertainties in the *impulse response function* (IRF) that describes the development in atmospheric concentration that follows from an emission pulse (Joos et al., 2013); see Box 6.2 and Supplementary Material Section 8.SM.12. The IRF is sensitive to model representation of the carbon cycle, pulse size and background CO_2 concentrations and climate.

Based on a multi-model study, Joos et al. (2013) estimate uncertainty ranges for the time-integrated IRF for CO_2 to be ±15% and ±25% (5 to 95% uncertainty range) for 20- and 100-year time horizons, respectively. Assuming quadratic error propagation, and ±10% uncertainty in radiative efficiency, the uncertainty ranges in AGWP for CO_2 were estimated to be ±18% and ±26% for 20 and 100 years. These

uncertainties affect all metrics that use CO_2 as reference. Reisinger et al. (2010) and Joos et al. (2013) show that these uncertainties increase with time horizon.

The same factors contribute to uncertainties in the GTP, with an additional contribution from the parameters describing the ocean heat uptake and climate sensitivity. In the first presentation of the GTP, Shine et al. (2005a) used one time constant for the climate response in their analytical expression. Improved approaches were used by Boucher and Reddy (2008), Collins et al. (2010) and Berntsen and Fuglestvedt (2008) that include more explicit representations of the deep ocean that increased the long-term response to a pulse forcing. Over the range of climate sensitivities from AR4, GTP_{50} for BC was found to vary by a factor of 2, the CH_4 GTP_{50} varied by about 50%, while for N_2O essentially no dependence was found (Fuglestvedt et al., 2010). AGTPs for CO_2 were also calculated in the multi-model study by Joos et al. (2013). They found uncertainty ranges in AGTP that are much larger than for AGWP; ±45% and ±90% for 20 and 100 years (5 to 95% uncertainty range). These uncertainty ranges also reflect the signal-to-noise ratio, and not only uncertainty in the physical mechanisms.

There are studies combining uncertainties in various input parameters. Reisinger et al. (2011) estimated the uncertainty in the GWP for CH_4 and found an uncertainty of –30 to +40% for the GWP_{100} and –50 to +75% for GTP_{100} of CH_4 (for 5 to 95% of the range). Boucher (2012) performed a Monte Carlo analysis with uncertainties in perturbation lifetime and radiative efficiency, and for GWP_{100} for CH_4 (assuming a constant background atmosphere) he found ±20%, and –40 to +65 for GTP_{100} (for 5 to 95% uncertainty range).

Here we estimate uncertainties in GWP values based on the uncertainties given for radiative efficiencies (Section 8.3.1), perturbation lifetimes, indirect effects and in the AGWP for the reference gas CO_2 (see Supplementary Material Section 8.SM.12). For CH_4 GWP we estimate an uncertainty of ±30% and ±40% for 20- and 100-year time horizons, respectively (for 5 to 95% uncertainty range). The uncertainty is dominated by AGWP for CO_2 and indirect effects. For gases with lifetimes of a century or more the uncertainties are of the order of ±20% and ±30% for 20- and 100-year horizons. The uncertainty in GWPs for gases with lifetimes of a few decades is estimated to be of the order of ±25% and ±35% for 20 and 100 years. For shorter-lived gases, the uncertainties in GWPs will be larger (see Supplementary Material Section 8.SM.12 for a discussion of contributions to the total uncertainty.) For GTP, few uncertainty estimates are available in the literature. Based on the results from Joos et al. (2013), Reisinger et al. (2010) and Boucher (2012) we assess the uncertainty to be of the order of ±75% for the CH_4 GTP_{100}.

The metric values are also strongly dependent on which processes are included in the definition of a metric. Ideally all indirect effects (Sections 8.2 and 8.3) should be taken into account in the calculation of metrics. The indirect effects of CH_4 on its own lifetime, tropospheric ozone and stratospheric water have been traditionally included in its GWP. Boucher et al. (2009) have quantified an indirect effect on CO_2 when fossil fuel CH_4 is oxidized in the atmosphere. Shindell et al. (2009) estimated the impact of reactive species emissions on both gaseous and aerosol forcing species and found that ozone precursors, including CH_4, had an additional substantial climate effect because they increased or decreased the rate of oxidation of SO_2 to sulphate aerosol. Studies with different sulphur cycle formulations have found lower sensitivity (Collins et al., 2010; Fry et al., 2012). Collins et al. (2010) postulated an additional component to their GWPs and GTPs for ozone precursors due to the decreased productivity of plants under higher levels of surface ozone. This was estimated to have the same magnitude as the ozone and CH_4 effects. This effect, however, has so far only been examined with one model. In a complex and interconnected system, feedbacks can become increasingly complex, and uncertainty of the magnitude and even direction of feedback increases the further one departs from the primary perturbation, resulting in a trade-off between completeness and robustness, and hence utility for decision-making.

Gillett and Matthews (2010) included climate–carbon feedbacks in calculations of GWP for CH_4 and N_2O and found that this increased the values by about 20% for 100 years. For GTP of CH_4 they found an increase of ~80%. They used numerical models for their studies and suggest that climate–carbon feedbacks should be considered and parameterized when used in simple models to derive metrics. Collins et al. (2013) parameterize the climate-carbon feedback based on Friedlingstein et al. (2006) and Arora et al. (2013) and find that this more than doubles the GTP_{100} for CH_4. Enhancement of the GTP for CH_4 due to carbon–climate feedbacks may also explain the higher GTP values found by Reisinger et al. (2010).

The inclusion of indirect effects and feedbacks in metric values has been inconsistent in the IPCC reports. In SAR and TAR, a carbon model without a coupling to a climate model was used for calculation of IRF for CO_2 (Joos et al., 1996), while in AR4 climate-carbon feedbacks were included for the CO_2 IRF (Plattner et al., 2008). For the time horizons 20 and 100 years, the $AGWP_{CO2}$ calculated with the Bern3D-LPJ model is, depending on the pulse size, 4 to 5% and 13 to 15% lower, respectively, when carbon cycle–climate feedbacks are not included (Joos et al., 2013). While the AGWP for the reference gas CO_2 included climate–carbon feedbacks, this is not the case for the non-CO_2 gas in the numerator of GWP, as recognized by Gillett and Matthews (2010), Joos et al. (2013), Collins et al. (2013) and Sarofim (2012). This means that the GWPs presented in AR4 may underestimate the relative impacts of non-CO_2 gases. The different inclusions of feedbacks partially represent the current state of knowledge, but also reflect inconsistent and ambiguous definitions. In calculations of AGWP for CO_2 in AR5 we use the IRF for CO_2 from Joos et al. (2013) which includes climate–carbon feedbacks. Metric values in AR5 are presented both with and without including climate–carbon feedbacks for non-CO_2 gases. This feedback is based on the carbon-cycle response in a similar set of models (Arora et al., 2013) as used for the reference gas (Collins et al., 2013).

The effect of including this feedback for the non-reference gas increases with time horizon due to the long-lived nature of the initiated CO_2 perturbation (Table 8.7). The relative importance also increases with decreasing lifetime of the component, and is larger for GTP than GWP due to the integrative nature of GWP. We calculate an increase in the CH_4 GWP_{100} of 20%. For GTP_{100}, however, the changes are much larger; of the order of 160%. For the shorter time horizons (e.g., 20 years) the effect of including this feedback is small (<5%) for both GWP

Table 8.7 | GWP and GTP with and without inclusion of climate–carbon feedbacks (cc fb) in response to emissions of the indicated non-CO_2 gases (climate-carbon feedbacks in response to the reference gas CO_2 are always included).

	Lifetime (years)		GWP_{20}	GWP_{100}	GTP_{20}	GTP_{100}
CH_4[b]	12.4[a]	No cc fb	84	28	67	4
		With cc fb	86	34	70	11
HFC-134a	13.4	No cc fb	3710	1300	3050	201
		With cc fb	3790	1550	3170	530
CFC-11	45.0	No cc fb	6900	4660	6890	2340
		With cc fb	7020	5350	7080	3490
N_2O	121.0[a]	No cc fb	264	265	277	234
		With cc fb	268	298	284	297
CF_4	50,000.0	No cc fb	4880	6630	5270	8040
		With cc fb	4950	7350	5400	9560

Notes:

Uncertainties related to the climate–carbon feedback are large, comparable in magnitude to the strength of the feedback for a single gas.

[a] Perturbation lifetime is used in the calculation of metrics.

[b] These values do not include CO_2 from methane oxidation. Values for fossil methane are higher by 1 and 2 for the 20 and 100 year metrics, respectively (Table 8.A.1).

and GTP. For the more long-lived gases the GWP_{100} values increase by 10 to 12%, while for GTP_{100} the increase is 20 to 30%. Table 8.A.1 gives metric values including the climate–carbon feedback for CO_2 only, while Supplementary Material Table 8.SM.16 gives values for all halocarbons that include the climate–carbon feedback. Though uncertainties in the carbon cycle are substantial, it is *likely* that including the climate–carbon feedback for non-CO_2 gases as well as for CO_2 provides a better estimate of the metric value than including it only for CO_2.

Emission metrics can be estimated based on a constant or variable background climate and this influences both the adjustment times and the concentration–forcing–temperature relationships. Thus, all metric values will need updating due to changing atmospheric conditions as well as improved input data. In AR5 we define the metric values with respect to a constant present-day condition of concentrations and climate. However, under non-constant background, Joos et al. (2013) found decreasing CO_2 $AGWP_{100}$ for increasing background levels (up to 23% for RCP8.5). This means that GWP for all non-CO_2 gases (except CH_4 and N_2O) would increase by roughly the same magnitude. Reisinger et al. (2011) found a reduction in AGWP for CO_2 of 36% for RCP8.5 from 2000 to 2100 and that the CH_4 radiative efficiency and AGWP also decrease with increasing CH_4 concentration. Accounting for both effects, the GWP_{100} for CH_4 would increase by 10 to 20% under low and mid-range RCPs by 2100, but would decrease by up to 10% by mid-century under the highest RCP. While these studies have focused on the background levels of GHGs, the same issues apply for temperature. Olivié et al. (2012) find different temperature IRFs depending on the background climate (and experimental set up).

User related choices (see Box 8.4) such as the time horizon can greatly affect the numerical values obtained for CO_2 equivalents. For a change in time horizon from 20 to 100 years, the GWP for CH_4 decreases by a factor of approximately 3 and its GTP by more than a factor of 10. Short-lived species are most sensitive to this choice. Some approaches have removed the time horizon from the metrics (e.g., Boucher, 2012), but discounting is usually introduced which means that a discount rate r (for the weighting function e^{-rt}) must be chosen instead. The choice of discount rate is also value based (see WGIII, Chapter 3).

For NTCFs the metric values also depend on the location and timing of emission and whether regional or global metrics are used for these gases is also a choice for the users. Metrics are usually calculated for pulses, but some studies also give metric values that assume constant emissions over the full time horizon (e.g., Shine et al., 2005a; Jacobson, 2010). It is important to be aware of the idealized assumption about constant future emissions (or change in emissions) of the compound being considered if metrics for sustained emissions are used.

8.7.1.5 New Metric Concepts

New metric concepts have been developed both to modify physical metrics to address shortcomings as well as to replace them with metrics that account for economic dimensions of problems to which metrics are applied. Modifications to physical metrics have been proposed to better represent CO_2 emissions from bioenergy, regional patterns of response, and for peak temperature limits.

Emissions of CO_2 from the combustion of biomass for energy in national emission inventories are currently assumed to have no net RF, based on the assumption that these emissions are compensated by biomass regrowth (IPCC, 1996). However, there is a time lag between combustion and regrowth, and while the CO_2 is resident in the atmosphere it leads to an additional RF. Modifications of the GWP and GTP for bioenergy (GWP_{bio}, GTP_{bio}) have been developed (Cherubini et al., 2011; Cherubini et al., 2012). The GWP_{bio} give values generally between zero (current default for bioenergy) and one (current for fossil fuel emissions) (Cherubini et al., 2011), and negative values are possible for GTP_{bio} due to the fast time scale of atmospheric–ocean CO_2 exchange relative to the growth cycle of biomass (Cherubini et al., 2012). GWP_{bio} and GTP_{bio} have been used in only a few applications, and more research is needed to assess their robustness and applicability. Metrics for biogeophysical effects, such as albedo changes, have been proposed (Betts, 2000; Rotenberg and Yakir, 2010) , but as for NTCFs regional variations

are important (Claussen et al., 2001) and the RF concept may not be adequate (Davin et al., 2007).

New concepts have also been developed to capture information about regional patterns of responses and cancelling effects that are lost when global mean metrics are used. The use of nonlinear damage functions to capture information on the spatial pattern of responses has been explored (Shine et al., 2005b; Lund et al., 2012). In addition, the Absolute Regional Temperature Potential (ARTP) (Shindell, 2012; Collins et al., 2013) has been developed to provide estimates of impacts at a sub-global scale. ARTP gives the time-dependent temperature response in four latitude bands as a function of the regional forcing imposed in all bands. These metrics, as well as new regional precipitation metrics (Shindell et al., 2012b), require additional studies to determine their robustness.

Alternatives to the single basket approach adopted by the Kyoto Protocol are a component-by-component approach or a multi-basket approach (Rypdal et al., 2005; Daniel et al., 2012; Sarofim, 2012; Jackson, 2009). Smith et al. (2012) show how peak temperature change is constrained by *cumulative emissions* (see 12.5.4) for gases with long lifetimes and *emissions rates* for shorter-lived gases (including CH_4). Thus, they divide gases into two baskets and present two metrics that can be used for estimating peak temperature for various emission scenarios. This division of gases into the two baskets is sensitive to the time of peak temperature in the different scenarios. The approach uses time invariant metrics that do not account for the timing of emissions relative to the target year. The choice of time horizon is implicit in the scenario assumed and this approach works only for a peak scenario.

A number of new metrics have been developed to add economic dimensions to purely physically based metrics such as the GWP and GTP. The use of physical metrics in policy contexts has been criticized by economists (Reilly and Richards, 1993; Schmalensee, 1993; Hammitt et al., 1996; Reilly et al., 1999; Bradford, 2001; De Cara et al., 2008). A prominent use of metrics is to set relative prices of gases when implementing a multi-gas policy. Once a particular policy has been agreed on, economic metrics can address policy goals more directly than physical metrics by accounting not only for physical dimensions but also for economic dimensions such as mitigation costs, damage costs and discount rates (see WGIII, Chapter 3; Deuber et al., 2013).

For example, if mitigation policy is set within a *cost-effectiveness* framework with the aim of making the least cost mix of emissions reductions across components to meet a global temperature target, the 'price ratio' (Manne and Richels, 2001), also called the Global Cost Potential (GCP) (Tol et al., 2012), most directly addresses the goal. The choice of target is a policy decision; metric values can then be calculated based on an agreed upon target. Similarly, if policy is set within a *cost–benefit* framework, the metric that directly addresses the policy goal is the ratio of the marginal damages from the emission of a gas (i.e., the damage costs to society resulting from an incremental increase in emissions) relative to the marginal damages of an emission of CO_2, known as the Global Damage Potential (GDP) (Kandlikar, 1995). Both types of metrics are typically determined within an integrated climate–economy model, since they are affected both by the response of the climate system as well as by economic factors.

If other indexes, such as the GWP, are used instead of an economic cost-minimizing index, costs to society will increase. Cost implications at the project or country level could be substantial under some circumstances (Godal and Fuglestvedt, 2002; Shine, 2009; Reisinger et al., 2013). However, under idealized conditions of full participation in mitigation policy, the increase is relatively small at the global level, particularly when compared to the cost savings resulting from a multi- (as opposed to single-) gas mitigation strategy even when based on an imperfect metric (O'Neill, 2003; Aaheim et al., 2006; Johansson et al., 2006; Johansson, 2012; Reisinger et al., 2013; Smith et al., 2013).

Purely physical metrics continue to be used in many contexts due at least in part to the added uncertainties in mitigation and damage costs, and therefore in the values of economic metrics (Boucher, 2012). Efforts have been made to view purely physical metrics such as GWPs and GTPs as approximations of economic indexes. GTPs, for example, can be interpreted as an approximation of a Global Cost Potential designed for use in a cost-effectiveness setting (Shine et al., 2007; Tol et al., 2012). Quantitative values for time-dependent GTPs reproduce in broad terms several features of the Global Cost Potential such as the rising value of metrics for short-lived gases as a climate policy target is approached (Tanaka et al., 2013). Figure 8.30 shows how contributions of N_2O, CH_4 and BC to warming in the target year changes over time. The contributions are given relative to CO_2 and show the effects of emission occurring at various times. Similarly, GWPs can be interpreted as approximations of the Global Damage Potential designed for a cost–benefit framework (Tol et al., 2012). These interpretations of the GTP and GWP imply that using even a purely physical metric in an economic policy context involves an implicit economic valuation.

In both cases, a number of simplifying assumptions must be made for these approximations to hold (Tol et al., 2012). For example, in the case of the GWP, the influence of emissions on RF, and therefore implicitly on costs to society, beyond the time horizon is not taken into account, and there are substantial numerical differences between GWP and GDP values (Marten and Newbold, 2012). In the case of the GTP, the influence of emissions on temperature change (and costs) is

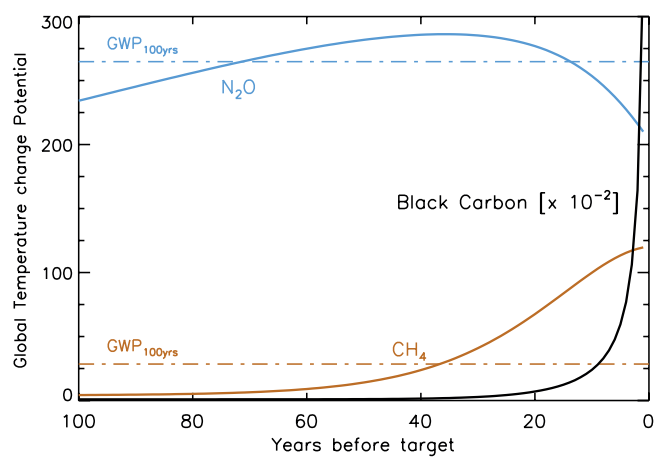

Figure 8.30 | Global Temperature change Potential (GTP(t)) for CH_4, nitrous oxide and BC for each year from year of emission to the time at which the temperature change target is reached. The (time-invariant) GWP_{100} is also shown for N_2O and CH_4 for comparison.

included only at the time the target is reached, but not before nor after. Other metrics have been developed to more closely approximate GCPs or GDPs. The Cost-Effective Temperature Potential (CETP) reproduces values of the GCP more closely than does the GTP (Johansson, 2012). It is similar to the GTP but accounts for post-target temperature effects based on an assumption about how to value costs beyond the time the target is reached. Metrics have also been proposed that take into account forcing or temperature effects that result from emissions trajectories over broad time spans, and that behave similarly to GCP and GTP (Tanaka et al., 2009; Manning and Reisinger, 2011) or to GWP (e.g., O'Neill, 2000; Peters et al., 2011a; Gillett and Matthews, 2010; Azar and Johansson, 2012).

8.7.1.6 Synthesis

In the application and evaluation of metrics, it is important to distinguish between two main sources of variation in metric values. While scientific choices of input data have to be made, there are also choices involving value judgements. For some metrics such choices are not always explicit and transparent. The choice of metric type and time horizon will for many components have a much larger effect than improved estimates of input parameters and can have strong effects on perceived impacts of emissions and abatement strategies.

In addition to progress in understanding of GWP, new concepts have been introduced or further explored since AR4. Time variant metrics introduce more dynamical views of the temporal contributions that accounts for the proximity to a prescribed target (in contrast to the traditional static GWP). Time variant metrics can be presented in a format that makes changing metric values over time predictable.

As metrics use parameters further down the cause effect chain the metrics become in general more policy relevant, but at the same time the uncertainties increase. Furthermore, metrics that account for regional variations in sensitivity to emissions or regional variation in response could give a very different emphasis to various emissions. Many species, especially NTCFs, produce distinctly regionally heterogeneous RF and climate response patterns. These aspects are not accounted for in the commonly used global scale metrics.

The GWPs and GTPs have had inconsistent treatment of indirect effects and feedbacks. The GWPs reported in AR4 include climate–carbon feedbacks for the reference gas CO_2 but not for the non-CO_2 gases. Such feedbacks may have significant impacts on metrics and should be treated consistently. More studies are needed to assess the importance of consistent treatment of indirect effects/feedbacks in metrics.

The weighting of effects over time—choice of time horizon in the case of GWP and GTP—is value based. Discounting is an alternative, which also includes value judgements and is equally controversial. The weighting used in the GWP is a weight equal to one up to the time horizon and zero thereafter, which is not in line with common approaches for evaluation of future effects in economics (e.g., as in WGIII, Chapter 3). Adoption of a fixed horizon of e.g., 20, 100 or 500 years will inevitably put no weight on the long-term effect of CO_2 beyond the time horizon (Figure 8.28 and Box 6.1). While GWP integrates the effects up to a chosen time horizon the GTP gives the temperature just for one chosen year with no weight on years before or after. The most appropriate metric depends on the particular application and which aspect of climate change is considered relevant in a given context. The GWP is not directly related to a temperature limit such as the 2°C target (Manne and Richels, 2001; Shine et al., 2007; Manning and Reisinger, 2011; Smith et al., 2012; Tol et al., 2012; Tanaka et al., 2013), whereas some economic metrics and physical end-point metrics like the GTP may be more suitable for this purpose.

To provide metrics that can be useful to the users and policymakers a more effective dialog and discussion on three topics is needed: (1) which applications particular metrics are meant to serve; (2) how comprehensive metrics need to be in terms of indirect effects and feedbacks, and economic dimensions; and—related to this (3) how important it is to have simple and transparent metrics (given by analytical formulations) versus more complex model-based and thus model-dependent metrics. These issues are also important to consider in a wider disciplinary context (e.g., across the IPCC Working Groups). Finally, it is important to be aware that all metric choices, even 'traditional' or 'widely used' metrics, contain implicit value judgements as well as large uncertainties.

8.7.2 Application of Metrics

8.7.2.1 Metrics for Carbon Dioxide, Methane, Nitrous Oxide, Halocarbons and Related Compounds

Updated (A)GWP and (A)GTP values for CO_2, CH_4, N_2O, CFCs, HCFCs, bromofluorocarbons, halons, HFCs, PFCs, SF_6, NF_3, and related halogen-containing compounds are given for some illustrative and tentative time horizons in Tables 8.7, 8.A.1 and Supplementary Material Table 8.SM.16. The input data and methods for calculations of GWPs and GTPs are documented in the Supplementary Material Section 8.SM.13. Indirect GWPs that account for the RF caused by depletion of stratospheric ozone (consistent with Section 8.3.3) are given for selected gases in Table 8.A.2.

The *confidence* in the ability to provide useful metrics at time scales of several centuries is *very low* due to nonlinear effects, large uncertainties for multi-century processes and strong assumptions of constant background conditions. Thus, we do not give metric values for longer time scales than 100 years (see discussion in Supplementary Material Section 8.SM.11). However, these time scales are important to consider for gases such as CO_2, SF_6 and PFCs. For CO_2, as much as 20 to 40% of the initial increase in concentration remains after 500 years. For PFC-14, 99% of an emission is still in the atmosphere after 500 years. The effects of emissions on these time scales are discussed in Chapter 12.

The GWP values have changed from previous assessments due to new estimates of lifetimes, impulse response functions and radiative efficiencies. These are updated due to improved knowledge and/or changed background levels. Because CO_2 is used as reference, any changes for this gas will affect all metric values via AGWP changes. Figure 8.31 shows how the values of radiative efficiency (RE), integrated impulse response function (IRF) and consequentially AGWP for CO_2 have changed from earlier assessments relative to AR5 values. The net effect of change in RE and IRF is an increase of approximately 1% and

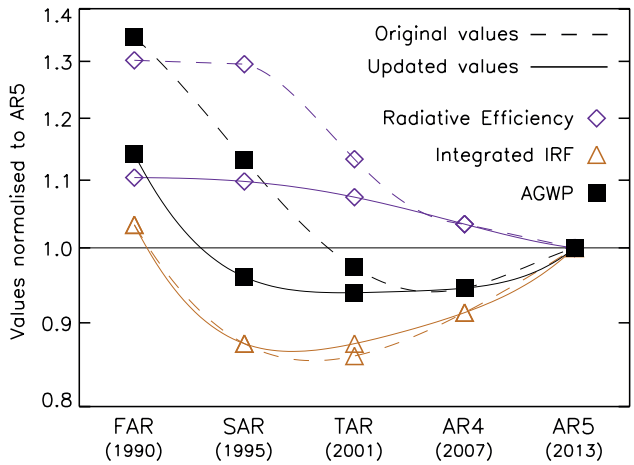

Figure 8.31 | Changes in the radiative efficiency (RE), integrated impulse response function (IRF) and Absolute Global Warming Potential (AGWP) for CO_2 for 100 years from earlier IPCC Assessment Reports normalized relative to the values given in AR5. The 'original' values are calculated based on the methods explained or value reported in each IPCC Assessment Report. The 'updated' values are calculated based on the methods used in AR5, but the input values from each Assessment Report. The difference is primarily in the formula for the RE, which was updated in TAR. The different integrated IRF in TAR relates to a different parameterisation of the same IRF (WMO, 1999). Changes represent both changes in scientific understanding and a changing background atmospheric CO_2 concentration (note that *y*-axis starts from 0.8). The lines connecting individual points are meant as a visual guide and not to represent the values between different Assessment Reports.

6% from AR4 to AR5 in AGWP for CO_2 for 20 and 100 years, respectively (see Supplementary Material Section 8.SM.12). These increases in the AGWP of the reference gas lead to corresponding decreases in the GWPs for all non-CO_2 gases. Continued increases in the atmospheric levels of CO_2 will lead to further changes in GWPs (and GTPs) in the future.

To understand the factors contributing to changes relative to AR4, comparisons are made here using the AR5 values that include climate–carbon feedbacks for CO_2 only. Relative to AR4 the CH_4 AGWP has changed due to changes in perturbation lifetime, a minor change in RE due to an increase in background concentration, and changes in the estimates of indirect effects. The indirect effects on O_3 and stratospheric H_2O are accounted for by increasing the effect of CH_4 by 50% and 15%, respectively (see Supplementary Material Table 8.SM.12). The ozone effect has doubled since AR4 taking into account more recent studies as detailed in Sections 8.3.3 and 8.5.1. Together with the changes in AGWP for CO_2 the net effect is increased GWP values of CH_4.

The GWPs for N_2O are lower here compared to AR4. A longer perturbation lifetime is used in AR5, while the radiative efficiency is lower due to increased abundances of CH_4 and N_2O. In addition, the reduction in CH_4 via stratospheric O_3, UV fluxes and OH levels due to increased N_2O abundance is included in GWPs and GTP. Owing to large uncertainties related to altitude of changes, we do not include the RF from stratospheric ozone changes as an indirect effect of N_2O.

Lifetimes for most of the halocarbons are taken from WMO (2011) and many of these have changed from AR4. The lifetimes of CFC-114, CFC-115 and HCF-161 are reduced by approximately 40%, while HFC-152 is reduced by one third. Among the hydrofluoroethers (HFEs) there are also several large changes in lifetimes. In addition, substantial updates of radiative efficiencies are made for several important gases; CFC-11, CFC-115, HCFC-124, HCFC-225cb, HFC-143a, HFC-245fa, CCl_4, $CHCl_3$, and SF_6. The radiative efficiency for carbon tetrachloride (CCl_4) is higher now and the GWP_{100} has increased by almost 25% from AR4. Uncertainties in metric values are given in Section 8.7.1.4. See also Supplementary Material Section 8.SM.12 and footnote to Table 8.A.1. As can be seen from Table 8.A.2, some ODS have strong indirect effects through stratospheric ozone forcing, which for some of the gases reduce their net GWP_{100} values substantially (and for the halons, to large negative values). Note that, consistent with Section 8.3.3, the uncertainties are large; ±100% for this indirect effect.

When climate-carbon feedbacks are included for both the non-CO_2 and reference gases, all metric values increase relative to the methodology used in AR4, sometimes greatly (Table 8.7, Supplementary Material Table 8.SM.16). Though the uncertainties range for these metric values is greater, as uncertainties in climate-carbon feedbacks are substantial, these calculations provide a more consistent methodology.

8.7.2.2 Metrics for Near-Term Climate Forcers

The GWP concept was initially used for the WMGHGs, but later for NTCFs as well. There are, however, substantial challenges related to calculations of GWP (and GTP) values for these components, which is reflected in the large ranges of values in the literature. Below we present and assess the current status of knowledge and quantification of metrics for various NTCFs.

8.7.2.2.1 Nitrogen oxides

Metric values for NO_X usually include the short-lived ozone effect, CH_4 changes and the CH_4-controlled O_3 response. NO_X also causes RF through nitrate formation, and via CH_4 it affects stratospheric H_2O and through ozone it influences CO_2. In addition, NO_x affects CO_2 through nitrogen deposition (fertilization effect). Due to high reactivity and the many nonlinear chemical interactions operating on different time scales, as well as heterogeneous emission patterns, calculation of *net* climate effects of NO_X is difficult. The net effect is a balance of large opposing effects with very different temporal behaviours. There is also a large spread in values among the regions due to variations in chemical and physical characteristics of the atmosphere.

As shown in Table 8.A.3 the GTP and GWP values are very different. This is due to the fundamentally different nature of these two metrics (see Figure 8.28) and the way they capture the temporal behaviour of responses to NO_x emissions. Time variation of GTP for NO_X is complex, which is not directly seen by the somewhat arbitrary choices of time horizon, and the net GTP is a fine balance between the contributing terms. The general pattern for NO_X is that the short-lived ozone forcing is always positive, while the CH_4-induced ozone forcing and CH_4 forcing are always negative (see Section 8.5.1). Nitrate aerosols from NO_x emission are not included in Table 8.A.3. For the GTP, all estimates for NO_X from surface sources give a negative net effect. As discussed in Section 8.7.1.4 Collins et al. (2010) and Shindell et al. (2009) implemented further indirect effects, but these are not included in Table

8.A.3 due to large uncertainties. The metric estimates for NO_X reflect the level of knowledge, but they also depend on experimental design, treatment of transport processes, and modelling of background levels. The multi-model study by Fry et al. (2012) shows the gaseous chemistry response to NO_X is relatively robust for European emissions, but that the uncertainty is so large that for some regions of emissions it is not possible to conclude whether NO_X causes cooling or warming.

8.7.2.2.2 Carbon monoxide and volatile organic compounds

Emissions of carbon monoxide (CO) and volatile organic compounds (VOCs) lead to production of ozone on short time scales. By affecting OH and thereby the levels of CH_4 they also initiate a positive long-term ozone effect. With its lifetime of 2 to 3 months, the effect of CO emissions is less dependent on location than is the case for NO_X (see Table 8.A.4). There is also less variation across models. However, Collins et al. (2010) found that inclusion of vegetation effects of O_3 increased the GTP values for CO by 20 to 50%. By including aerosol responses Shindell et al. (2009) found an increase in GWP_{100} by a factor of ~2.5. CO of fossil origin will also have a forcing effect by contributing to CO_2 levels. This effect adds 1.4 to 1.6 to the GWP_{100} for CO (Daniel and Solomon, 1998; Derwent et al., 2001). (The vegetation and aerosol effects are not included in the numbers in Table 8.A.4.)

VOC is not a well-defined group of hydrocarbons. This group of gases with different lifetimes is treated differently across models by lumping or using representative key species. However, the spread in metric values in Table 8.A.5 is moderate across regions, with highest values for emissions in South Asia (of the four regions studied). The effects via ozone and CH_4 cause warming, and the additional effects via interactions with aerosols and via the O_3–CO_2 link increase the warming effect further. Thus, the net effects of CO and VOC are less uncertain than for NO_X for which the net is a residual between larger terms of opposite sign. However, the formation of SOAs is usually not included in metric calculations for VOC, which introduces a cooling effect and increased uncertainty.

8.7.2.2.3 Black carbon and organic carbon

Most of the metric values for BC in the literature include the aerosol–radiation interaction and the snow/ice albedo effect of BC, though whether external or internal mixing is used varies between the studies. Bond et al. (2011) calculate GWPs and find that when the albedo effect is included the values increase by 5 to 15%. Studies have shown, however, that the climate response per unit forcing to this mechanism is stronger than for WMGHG (see Section 7.5).

Bond et al. (2013) assessed the current understanding of BC effects and calculated GWP and GTP for BC that includes aerosol–radiation interaction, aerosol–cloud interactions and albedo. As shown in Table 8.A.6 the uncertainties are wide for both metrics (for 90% uncertainty range) reflecting the current challenges related to understanding and quantifying the various effects (see Sections 7.5, 8.3.4 and 8.5.1). Their aerosol–radiation interaction effect is about 65% of the total effect while the albedo effect is approximately 20% of the aerosol–radiation interaction effect. Based on two studies (Rypdal et al., 2009; Bond et al., 2011), the GWP and GTP metrics were found to vary with the region where BC is emitted by about ±30% . For larger regions of emissions, Collins et al. (2013) calculated GWPs and GTPs for the direct effect of BC and found somewhat lower variations among the regions.

Several studies have focused on the effects of emissions of BC and OC from different regions (Bauer et al., 2007; Koch et al., 2007; Naik et al., 2007; Reddy and Boucher, 2007; Rypdal et al., 2009). However, examination of results from these models (Fuglestvedt et al., 2010) reveals that there is not a robust relationship between the region of emission and the metric value — hence, regions that yield the highest metric value in one study, do not, in general, do so in the other studies.

The metric values for OC are quite consistent across studies, but fewer studies are available (see Table 8.A.6). A brief overview of metric values for other components is given in the Supplementary Material Section 8.SM.14.

8.7.2.2.4 Summary of status of metrics for near-term climate forcers

The metrics provide a format for comparing the magnitudes of the various emissions as well as for comparing effects of emissions from different regions. They can also be used for comparing results from different studies. Much of the spread in results is due to differences in experimental design and how the models treat physical and chemical processes. Unlike most of the WMGHGs, many of the NTCFs are tightly coupled to the hydrologic cycle and atmospheric chemistry, leading to a much larger spread in results as these are highly complex processes that are difficult to validate on the requisite small spatial and short temporal scales. The confidence level is lower for many of the NTCF compared to WMGHG and much lower where aerosol–cloud interactions are important (see Section 8.5.1). There are particular difficulties for NO_X, because the net impact is a small residual of opposing effects with quite different spatial distributions and temporal behaviour. Although climate–carbon feedbacks for non-CO_2 emissions have not been included in the NTCF metrics (other than CH_4) presented here, they can greatly increase those values (Collins et al., 2013) and likely provide more realistic results.

8.7.2.3 Impact by Emitted Component

We now use the metrics evaluated here to estimate climate impacts of various components (in a forward looking perspective). Figure 8.32 shows global anthropogenic emissions of some selected components weighted by the GWP and GTP. The time horizons are chosen as examples and illustrate how the perceived impacts of components—relative to the impact of the reference gas—vary strongly as function of impact parameter (integrated RF in GWP or end-point temperature in GTP) and with time horizon.

We may also calculate the temporal development of the temperature responses to pulse or sustained emissions using the AGTP metric. Figure 8.33 shows that for a one-year pulse the impacts of NTCF decay quickly owing to their atmospheric adjustment times even if effects are prolonged due to climate response time (in the case of constant emissions the effects reach approximately constant levels since the emissions are replenished each year, except for CO_2, which has a fraction

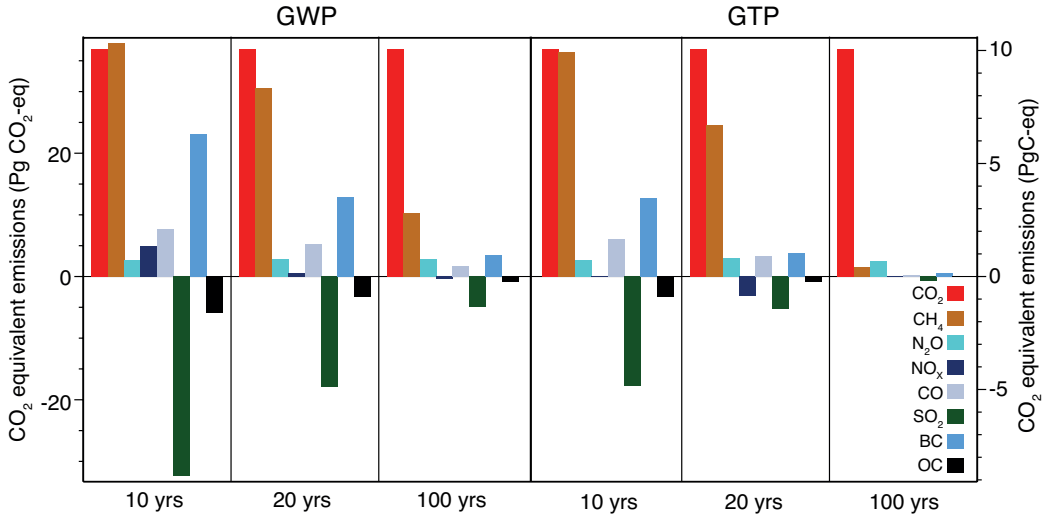

Figure 8.32 | Global anthropogenic emissions weighted by GWP and GTP for chosen time horizons (aerosol–cloud interactions are not included). Emission data for 2008 are taken from the EDGAR database. For BC and OC emissions for 2005 are from Shindell et al. (2012a). The units are 'CO_2 equivalents' which reflects equivalence only in the impact parameter of the chosen metric (integrated RF over the chosen time horizon for GWP; temperature change at the chosen point in time for GTP), given as $Pg(CO_2)_{eq}$ (left axis) and given as PgC_{eq} (right axis). There are large uncertainties related to the metric values and consequentially also to the calculated CO_2 equivalents (see text).

remaining in the atmosphere on time scales of centuries). Figure 8.33 also shows how some components have strong short-lived effects of both signs while CO_2 has a weaker initial effect but one that persists to create a long-lived warming effect. Note that there are large uncertainties related to the metric values (as discussed in Section 8.7.1.4); especially for the NTCFs.

These examples show that the outcome of comparisons of effects of emissions depends strongly on choice of time horizon and metric type. Such end-user choices will have a strong influence on the calculated contributions from NTCFs versus WMGHGs or non-CO_2 versus CO_2 emissions. Thus, each specific analysis should use a design chosen in light of the context and questions being asked.

8.7.2.4 Metrics and Impacts by Sector

While the emissions of WMGHGs vary strongly between sectors, the climate impacts of these gases are independent of sector. The latter is not the case for chemically active and short-lived components, due to the dependence of their impact on the emission location. Since most sectors have multiple co-emissions, and for NTCFs some of these are warming while others are cooling, the net impact of a given sector requires explicit calculations. Since AR4, there has been significant progress in the understanding and quantification of climate impacts of NTCFs from sectors such as transportation, power production and biomass burning (Berntsen and Fuglestvedt, 2008; Skeie et al., 2009; Stevenson and Derwent, 2009; Lee et al., 2010; Unger et al., 2010; Dahlmann et al., 2011). Supplementary Material Table 8.SM.18 gives an overview of recent published metric values for various components by sector.

The impact from sectors depends on choice of metric, time horizon, pulse versus sustained emissions and forward versus backward looking perspective (see Section 8.7.1 and Box 8.4). Unger et al. (2010) calculated RF for a set of components emitted from each sector. RF at chosen points in time (20 and 100 years) for *sustained* emissions was used by Unger et al. (2010) as the metric for comparison. This is comparable

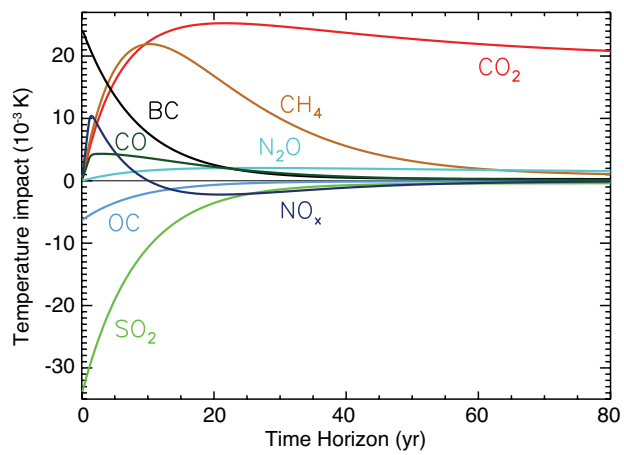

Figure 8.33 | Temperature response by component for total anthropogenic emissions for a 1-year pulse. Emission data for 2008 are taken from the EDGAR database and for BC and OC for 2005 from Shindell et al. (2012a). There are large uncertainties related to the AGTP values and consequentially also to the calculated temperature responses (see text).

to using integrated RF up to the chosen times for *pulse* emissions (as in GWPs). Such studies are relevant for policymaking that focuses on regulating the *total activity* of a sector or for understanding the contribution from a sector to climate change. On the other hand, the fixed mix of emissions makes it less general and relevant for emission scenarios. Alternatively, one may adopt a component-by-component view which is relevant for policies directed towards specific components (or sets of components, as controlling an individual pollutant in isolation is usually not practical). But this view will not capture interactions and non-linearities within the suite of components emitted by most sectors. The effects of specific emission control technologies or policies or projected societal changes on the mix of emissions is probably the most relevant type of analysis, but there are an enormous number of possible actions and regional details that could be investigated. Henze et al. (2012) demonstrate a method for providing highly spatially resolved

estimates of forcing per component, and caution that RF aggregated over regions or sectors may not represent the impacts of emissions changes on finer scales.

Metrics for individual land-based sectors are often similar to the global mean metric values (Shindell et al., 2008). In contrast, metrics for emissions from aviation and shipping usually show large differences from global mean metric values (Table 8.A.3 versus Table 8.SM.18). Though there can sometimes be substantial variation in the impact of land-based sectors across regions, and for a particular region even from one sector to another, variability between different land-based sources is generally smaller than between land, sea and air emissions.

NO_x from aviation is one example where the metric type is especially important. GWP_{20} values are positive due to the strong response of short-lived ozone. Reported GWP_{100} and GTP_{100} values are of either sign, however, due to the differences in balance between the individual effects modelled. Even if the models agree on the net effect of NO_X, the individual contributions can differ significantly, with large uncertainties stemming from the relative magnitudes of the CH_4 and O_3 responses (Myhre et al., 2011) and the background tropospheric concentrations of NO_X (Holmes et al., 2011; Stevenson and Derwent, 2009). Köhler et al. (2013), find strong regional sensitivity of ozone and CH_4 to NO_X particularly at cruise altitude. Generally, they find the strongest effects at low latitudes. For the aviation sector contrails and contrail induced cirrus are also important. Based on detailed studies in the literature, Fuglestvedt et al. (2010) produced GWP and GTP for contrails, water vapor and contrail-induced cirrus.

The GWP and GTPs for NO_X from shipping are strongly negative for all time horizons. The strong positive effect via O_3 due to the low-NO_X environment into which ships generally emit NO_X is outweighed by the stronger effect on CH_4 destruction due to the relatively lower latitudes of these emissions compared to land-based sources.

In addition to having large emissions of NO_X the shipping sector has large emission of SO_2. The direct GWP_{100} for shipping ranges from –11 to –43 (see Supplementary Material Table 8.SM.18). Lauer et al. (2007) reported detailed calculations of the indirect forcing specifically for this sector and found a wide spread of values depending on the emission inventory. Righi et al. (2011) and Peters et al. (2012) calculate indirect effects that are 30 to 50% lower than the indirect forcing reported by Lauer et al. (2007). The values from Shindell and Faluvegi (2010) for SO_2 from power generation are similar to those for shipping.

Although the various land transport sectors often are treated as one aggregate (e.g., road transport) there are important subdivisions. For instance, Bond et al. (2013) points out that among the BC-rich sectors they examined, diesel vehicles have the most clearly positive net impact on forcing. Studies delving even further have shown substantial differences between trucks and cars, gasoline and diesel vehicles, and low-sulphur versus high-sulphur fuels. Similarly, for power production there are important differences depending on fuel type (coal, oil, gas; e.g., Shindell and Faluvegi, 2010).

In the assessment of climate impacts of current emissions by sectors we give examples and apply a forward-looking perspective on effects in terms of temperature change. The AGTP concept can be used to study the effects of the various components for chosen time horizons. A single year's worth of current global emissions from the energy and industrial sectors have the largest contributions to warming after 100 years (see Figure 8.34a). Household fossil fuel and biofuel, biomass burning and on-road transportation are also relatively large contributors to warming over 100-year time scales. Those same sectors, along with sectors that emit large amounts of CH_4 (animal husbandry, waste/landfills and agriculture), are most important over shorter time horizons (about 20 years; see Figure 8.34b).

Analysing climate change impacts by using the net effect of particular activities or sectors may—compared to other perspectives—provide more insight into how societal actions influence climate. Owing to large variations in mix of short- and long-lived components, as well as cooling and warming effects, the results will also in these cases depend strongly on choice of time horizon and climate impact parameter. Improved understanding of aerosol–cloud interactions, and how those are attributed to individual components is clearly necessary to refine estimates of sectoral or emitted component impacts.

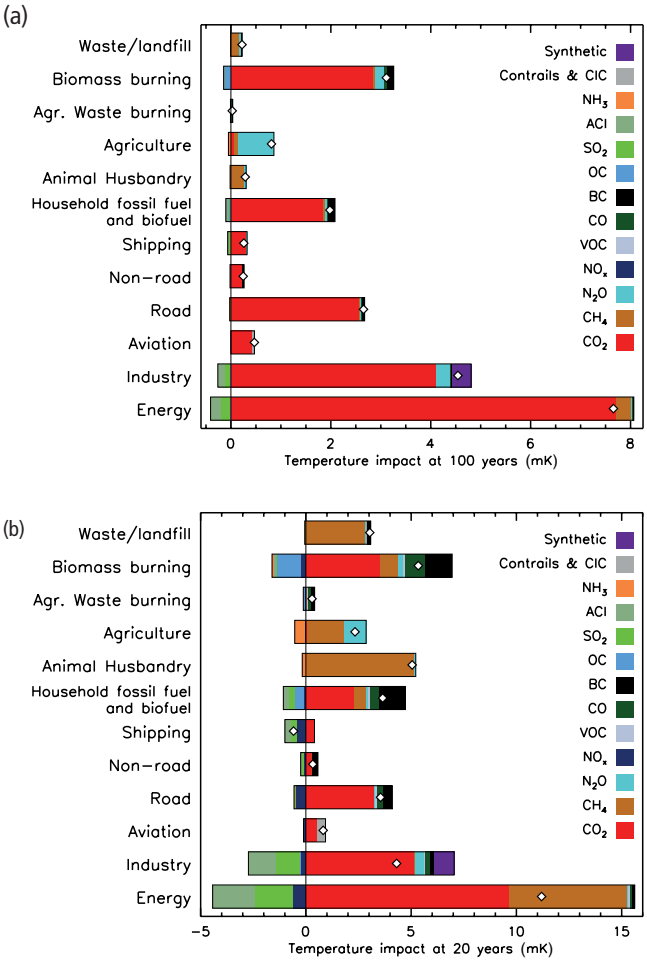

Figure 8.34 | Net global mean temperature change by source sector after (a) 100 and (b) 20 years (for 1-year pulse emissions). Emission data for 2008 are taken from the EDGAR database. For BC and OC anthropogenic emissions are from Shindell et al. (2012a) and biomass burning emissions are from Lamarque et al. (2010), see Supplementary Material Section 8.SM.17. There are large uncertainties related to the AGTP values and consequentially also to the calculated temperature responses (see text).

References

Aaheim, A., J. Fuglestvedt, and O. Godal, 2006: Costs savings of a flexible multi-gas climate policy. *Energy J.* (**Special Issue No. 3**), 485–501.

Abreu, J., J. Beer, F. Steinhilber, S. Tobias, and N. Weiss, 2008: For how long will the current grand maximum of solar activity persist? *Geophys. Res. Lett.*, **35**, L20109.

Ackerley, D., B. B. B. Booth, S. H. E. Knight, E. J. Highwood, D. J. Frame, M. R. Allen, and D. P. Rowell, 2011: Sensitivity of twentieth-century Sahel rainfall to sulfate aerosol and CO_2 forcing. *J. Clim.*, **24**, 4999–5014.

Allan, W., H. Struthers, and D. C. Lowe, 2007: Methane carbon isotope effects caused by atomic chlorine in the marine boundary layer: Global model results compared with Southern Hemisphere measurements. *J. Geophys. Res. Atmos.*, **112**, D04306.

Ammann, C. M., and P. Naveau, 2003: Statistical analysis of tropical explosive volcanism occurrences over the last 6 centuries. *Geophys. Res. Lett.*, **30**, 1210.

Ammann, C. M., and P. Naveau, 2010: A statistical volcanic forcing scenario generator for climate simulations. *J. Geophys. Res. Atmos.*, **115**, D05107.

Anchukaitis, K. J., B. M. Buckley, E. R. Cook, B. I. Cook, R. D. D'Arrigo, and C. M. Ammann, 2010: Influence of volcanic eruptions on the climate of the Asian monsoon region. *Geophys. Res. Lett.*, **37**, L22703.

Andersen, M., D. Blake, F. Rowland, M. Hurley, and T. Wallington, 2009: Atmospheric chemistry of sulfuryl fluoride: Reaction with OH radicals, CI atoms and O_3, atmospheric lifetime, IR spectrum, and global warming potential. *Environ. Sci. Technol.*, **43**, 1067–1070.

Andersen, M., V. Andersen, O. Nielsen, S. Sander, and T. Wallington, 2010: Atmospheric chemistry of $HCF_2O(CF_2CF_2O)(x)CF_2H$ (x=2–4): Kinetics and mechanisms of the chlorine-atom-initiated oxidation. *Chemphyschem*, **11**, 4035–4041.

Andrews, T., and P. M. Forster, 2008: CO_2 forcing induces semi-direct effects with consequences for climate feedback interpretations. *Geophys. Res. Lett.*, **35**, L04802.

Andrews, T., M. Doutriaux-Boucher, O. Boucher, and P. M. Forster, 2011: A regional and global analysis of carbon dioxide physiological forcing and its impact on climate. *Clim. Dyn.*, **36**, 783–792.

Andrews, T., J. Gregory, M. Webb, and K. Taylor, 2012a: Forcing, feedbacks and climate sensitivity in CMIP5 coupled atmosphere-ocean climate models. *Geophys. Res. Lett.*, **39**, L09712.

Andrews, T., P. Forster, O. Boucher, N. Bellouin, and A. Jones, 2010: Precipitation, radiative forcing and global temperature change. *Geophys. Res. Lett.*, **37**, doi:10.1029/2010GL043991, L14701.

Andrews, T., M. Ringer, M. Doutriaux-Boucher, M. Webb, and W. Collins, 2012b: Sensitivity of an Earth system climate model to idealized radiative forcing. *Geophys. Res. Lett.*, **39**, L10702.

Antuña, J. C., A. Robock, G. Stenchikov, J. Zhou, C. David, J. Barnes, and L. Thomason, 2003: Spatial and temporal variability of the stratospheric aerosol cloud produced by the 1991 Mount Pinatubo eruption. *J. Geophys. Res. Atmos.*, **108**, 4624.

Archibald, A. T., M. E. Jenkin, and D. E. Shallcross, 2010: An isoprene mechanism intercomparison. *Atmos. Environ.*, **44**, 5356–5364.

Archibald, A. T., et al., 2011: Impacts of HO(x) regeneration and recycling in the oxidation of isoprene: Consequences for the composition of past, present and future atmospheres. *Geophys. Res. Lett.*, **38**, L05804.

Arnold, T., et al., 2013: Nitrogen trifluoride global emissions estimated from updated atmospheric measurements, Proc. Natl. Acad. Sci. U.S.A, **110**, 2029-2034.

Arora, V. K., and A. Montenegro, 2011: Small temperature benefits provided by realistic afforestation efforts. *Nature Geosci.*, **4**, 514–518.

Arora, V. K., et al., 2013: Carbon-concentration and carbon-climate feedbacks in CMIP5 Earth system models. *J. Clim.*, **26**, 5289-5314.

Ashmore, M. R., 2005: Assessing the future global impacts of ozone on vegetation. *Plant Cell Environ.*, **28**, 949–964.

Azar, C., and D. J. A. Johansson, 2012: On the relationship between metrics to compare greenhouse gases—the case of IGTP, GWP and SGTP. *Earth Syst. Dynam.*, **3**, 139–147.

Baasandorj, M., A. R. Ravishankara, and J. B. Burkholder, 2011: Atmospheric chemistry of (Z)-$CF_3CH{=}CHCF_3$: OH radical reaction rate coefficient and global warming potential. *J. Phys. Chem. A*, **115**, 10539–10549.

Baasandorj, M., G. Knight, V. Papadimitriou, R. Talukdar, A. Ravishankara, and J. Burkholder, 2010: Rate coefficients for the gas-phase reaction of the hydroxyl radical with $CH_2 = CHF$ and $CH_2 = CF_2$. *J. Phys. Chem. A*, **114**, 4619–4633.

Bala, G., K. Caldeira, M. Wickett, T. J. Phillips, D. B. Lobell, C. Delire, and A. Mirin, 2007: Combined climate and carbon-cycle effects of large-scale deforestation. *Proc. Natl. Acad. Sci. U.S.A.*, **104**, 6550–6555.

Baliunas, S., and R. Jastrow, 1990: Evidence for long-term brightness changes of solar-type stars. *Nature*, **348**, 520–523.

Ball, W., Y. Unruh, N. Krivova, S. Solanki, T. Wenzler, D. Mortlock, and A. Jaffe, 2012: Reconstruction of total solar irradiance 1974–2009. *Astron. Astrophys.*, **541**, A27.

Ban-Weiss, G., L. Cao, G. Bala, and K. Caldeira, 2012: Dependence of climate forcing and response on the altitude of black carbon aerosols. *Clim. Dyn.*, **38**, 897–911.

Barnes, C. A., and D. P. Roy, 2008: Radiative forcing over the conterminous United States due to contemporary land cover land use albedo change. *Geophys. Res. Lett.*, **35**, L09706.

Bathiany, S., M. Claussen, V. Brovkin, T. Raddatz, and V. Gayler, 2010: Combined biogeophysical and biogeochemical effects of large-scale forest cover changes in the MPI earth system model. *Biogeosciences*, **7**, 1383–1399.

Bauer, S., D. Koch, N. Unger, S. Metzger, D. Shindell, and D. Streets, 2007: Nitrate aerosols today and in 2030: A global simulation including aerosols and tropospheric ozone. *Atmos. Chem. Phys.*, **7**, 5043–5059.

Bekki, S., J. A. Pyle, W. Zhong, R. Toumi, J. D. Haigh, and D. M. Pyle, 1996: The role of microphysical and chemical processes in prolonging the climate forcing of the Toba eruption. *Geophys. Res. Lett.*, **23**, 2669–2672.

Bellouin, N., J. Rae, A. Jones, C. Johnson, J. Haywood, and O. Boucher, 2011: Aerosol forcing in the Climate Model Intercomparison Project (CMIP5) simulations by HadGEM2–ES and the role of ammonium nitrate. *J. Geophys. Res. Atmos.*, **116**, D20206.

Bernier, P. Y., R. L. Desjardins, Y. Karimi-Zindashty, D. Worth, A. Beaudoin, Y. Luo, and S. Wang, 2011: Boreal lichen woodlands: A possible negative feedback to climate change in eastern North America. *Agr. Forest Meteorol.*, **151**, 521–528.

Berntsen, T., and J. Fuglestvedt, 2008: Global temperature responses to current emissions from the transport sectors. *Proc. Natl. Acad. Sci. U.S.A.*, **105**, 19154–19159.

Berntsen, T. K., et al., 1997: Effects of anthropogenic emissions on tropospheric ozone and its radiative forcing. *J. Geophys. Res. Atmos.*, **102**, 28101–28126.

Betts, R., 2000: Offset of the potential carbon sink from boreal forestation by decreases in surface albedo. *Nature*, **408**, 187–190.

Betts, R. A., P. D. Falloon, K. K. Goldewijk, and N. Ramankutty, 2007: Biogeophysical effects of land use on climate: Model simulations of radiative forcing and large-scale temperature change. *Agr. Forest Meteorol.*, **142**, 216–233.

Biasutti, M., and A. Giannini, 2006: Robust Sahel drying in response to late 20th century forcings. *Geophys. Res. Lett.*, **33**, L11706.

Blowers, P., K. F. Tetrault, and Y. Trujillo-Morehead, 2008: Global warming potential predictions for hydrofluoroethers with two carbon atoms. *Theor. Chem. Acc.*, **119**, 369–381.

Blowers, P., D. Moline, K. Tetrault, R. Wheeler, and S. Tuchawena, 2007: Prediction of radiative forcing values for hydrofluoroethers using density functional theory methods. *J. Geophys. Res. Atmos.*, **112**, D15108.

Boer, G. J., and B. Yu, 2003: Climate sensitivity and response. *Clim. Dyn.*, **20**, 415–429.

Bollasina, M. A., Y. Ming, and V. Ramaswamy, 2011: Anthropogenic aerosols and the weakening of the South Asian summer monsoon. *Science*, **334**, 502–505.

Bond, T., C. Zarzycki, M. Flanner, and D. Koch, 2011: Quantifying immediate radiative forcing by black carbon and organic matter with the Specific Forcing Pulse. *Atmos. Chem. Phys.*, **11**, 1505–1525.

Bond, T. C., et al., 2007: Historical emissions of black and organic carbon aerosol from energy-related combustion, 1850–2000. *Global Biogeochem. Cycles*, **21**, Gb2018.

Bond, T. C., et al., 2013: Bounding the role of black carbon in the climate system: A scientific assessment. *J. Geophys. Res. Atmos.*, **118**, doi:10.1002/jgrd.50171, 5380-5552.

Bonfils, C., and D. Lobell, 2007: Empirical evidence for a recent slowdown in irrigation-induced cooling. *Proc. Natl. Acad. Sci. U.S.A.*, **104**, 13582–13587.

Bonfils, C. J. W., T. J. Phillips, D. M. Lawrence, P. Cameron-Smith, W. J. Riley, and Z. M. Subin, 2012: On the influence of shrub height and expansion on northern high latitude climate. *Environ. Res. Lett.*, **7**, 015503.

Booth, B., N. Dunstone, P. Halloran, T. Andrews, and N. Bellouin, 2012: Aerosols implicated as a prime driver of twentieth-century North Atlantic climate variability. *Nature*, **485**, 534–534.

Boucher, O., 2012: Comparison of physically- and economically-based CO_2–equivalences for methane. *Earth Syst. Dyn.*, **3**, 49–61.

Boucher, O., and J. Haywood, 2001: On summing the components of radiative forcing of climate change. *Clim. Dyn.*, **18**, 297–302.

Boucher, O., and M. Reddy, 2008: Climate trade-off between black carbon and carbon dioxide emissions. *Energy Policy*, **36**, 193–200.

Boucher, O., P. Friedlingstein, B. Collins, and K. P. Shine, 2009: The indirect global warming potential and global temperature change potential due to methane oxidation. *Environ. Res. Lett.*, **4**, 044007.

Bourassa, A. E., et al., 2012: Large volcanic aerosol load in the stratosphere linked to Asian monsoon transport. *Science*, **337**, 78–81.

Bourassa, A. E., et al., 2013: Response to Comments on "Large Volcanic Aerosol Load in the Stratosphere Linked to Asian Monsoon Transport". *Science*, **339**, 6120.

Bowman, D., et al., 2009: Fire in the Earth System. *Science*, **324**, 481–484.

Bowman, K. W., et al., 2013: Evaluation of ACCMIP outgoing longwave radiation from tropospheric ozone using TES satellite observations. *Atmos. Chem. Phys.*, **13**, 4057–4072.

Bradford, D., 2001: Global change – Time, money and tradeoffs. *Nature*, **410**, 649–650.

Bravo, I., et al., 2010: Infrared absorption spectra, radiative efficiencies, and global warming potentials of perfluorocarbons: Comparison between experiment and theory. *J. Geophys. Res. Atmos.*, **115**, D24317.

Brovkin, V., et al., 2010: Sensitivity of a coupled climate-carbon cycle model to large volcanic eruptions during the last millennium. *Tellus B*, **62**, 674–681.

Calvin, K., et al., 2012: The role of Asia in mitigating climate change: Results from the Asia modeling exercise. *Energ. Econ.*, **34**, S251–S260.

Campra, P., M. Garcia, Y. Canton, and A. Palacios-Orueta, 2008: Surface temperature cooling trends and negative radiative forcing due to land use change toward greenhouse farming in southeastern Spain. *J. Geophys. Res. Atmos.*, **113**, D18109.

Carlton, A. G., R. W. Pinder, P. V. Bhave, and G. A. Pouliot, 2010: To what extent can biogenic SOA be controlled? *Environ. Sci. Technol.*, **44**, 3376–3380.

Carslaw, K. S., O. Boucher, D. V. Spracklen, G. W. Mann, J. G. L. Rae, S. Woodward, and M. Kulmala, 2010: A review of natural aerosol interactions and feedbacks within the Earth system. *Atmos. Chem. Phys.*, **10**, 1701–1737.

Chang, W. Y., H. Liao, and H. J. Wang, 2009: Climate responses to direct radiative forcing of anthropogenic aerosols, tropospheric ozone, and long-lived greenhouse gases in Eastern China over 1951–2000. *Adv. Atmos. Sci.*, **26**, 748–762.

Chen, W. T., A. Nenes, H. Liao, P. J. Adams, J. L. F. Li, and J. H. Seinfeld, 2010: Global climate response to anthropogenic aerosol indirect effects: Present day and year 2100. *J. Geophys. Res. Atmos.*, **115**, D12207.

Cherubini, F., G. Guest, and A. Strømman, 2012: Application of probablity distributions to the modelleing of biogenic CO_2 fluxes in life cycle assessment. *Global Change Biol.* , **4**, doi:10.1111/j.1757–1707.2011.01156.x, 784-798.

Cherubini, F., G. Peters, T. Berntsen, A. Stromman, and E. Hertwich, 2011: CO_2 emissions from biomass combustion for bioenergy: Atmospheric decay and contribution to global warming. *Global Change Biol. Bioenerg.*, **3**, 413–426.

Chung, C. E., and V. Ramanathan, 2006: Weakening of North Indian SST gradients and the monsoon rainfall in India and the Sahel. *J. Clim.*, **19**, 2036–2045.

Clark, H. L., M. L. Cathala, H. Teyssedre, J. P. Cammas, and V. H. Peuch, 2007: Cross-tropopause fluxes of ozone using assimilation of MOZAIC observations in a global CTM. *Tellus B*, **59**, 39–49.

Clarke, A. D., and K. J. Noone, 1985: Soot in the Arctic Snowpack—A cause for peturbations in radiative-transfer. *Atmos. Environ.*, **19**, 2045–2053.

Claussen, M., V. Brovkin, and A. Ganopolski, 2001: Biogeophysical versus biogeochemical feedbacks of large-scale land cover change. *Geophys. Res. Lett.*, **28**, 1011–1014.

Cofala, J., M. Amann, Z. Klimont, K. Kupiainen, and L. Hoglund-Isaksson, 2007: Scenarios of global anthropogenic emissions of air pollutants and methane until 2030. *Atmos. Environ.*, **41**, 8486–8499.

Collins, W., R. Derwent, C. Johnson, and D. Stevenson, 2002: The oxidation of organic compounds in the troposphere and their global warming potentials. *Clim. Change*, **52**, 453–479.

Collins, W. D., et al., 2006: Radiative forcing by well-mixed greenhouse gases: Estimates from climate models in the Intergovernmental Panel on Climate Change (IPCC) Fourth Assessment Report (AR4). *J. Geophys. Res. Atmos.*, **111**, D14317.

Collins, W. J., S. Sitch, and O. Boucher, 2010: How vegetation impacts affect climate metrics for ozone precursors. *J. Geophys. Res. Atmos.*, **115**, D23308.

Collins, W. J., M. M. Fry, H. Yu, J. S. Fuglestvedt, D. T. Shindell, and J. J. West, 2013: Global and regional temperature-change potentials for near-term climate forcers. *Atmos. Chem. Phys.*, **13**, 2471–2485.

Conley, A. J., J. F. Lamarque, F. Vitt, W. D. Collins, and J. Kiehl, 2013: PORT, a CESM tool for the diagnosis of radiative forcing. *Geosci. Model Dev.*, **6**, 469–476.

Cooper, O. R., et al., 2010: Increasing springtime ozone mixing ratios in the free troposphere over western North America. *Nature*, **463**, 344–348.

Cox, P. M., et al., 2008: Increasing risk of Amazonian drought due to decreasing aerosol pollution. *Nature*, **453**, 212–215.

Crook, J., and P. Forster, 2011: A balance between radiative forcing and climate feedback in the modeled 20th century temperature response. *J. Geophys. Res. Atmos.*, **116**, D17108.

Crowley, T. J., and M. B. Unterman, 2013: Technical details concerning development of a 1200 yr proxy index for global volcanism. *Earth Syst. Sci. Data*, **5**, 187-197.

Crutzen, P., 1973: Discussion of chemistry of some minor constituents in stratosphere and troposhere. *Pure Appl. Geophys.*, **106**, 1385–1399.

Dahlmann, K., V. Grewe, M. Ponater, and S. Matthes, 2011: Quantifying the contributions of individual NO_x sources to the trend in ozone radiative forcing. *Atmos. Environ.*, **45**, 2860–2868.

Daniel, J., and S. Solomon, 1998: On the climate forcing of carbon monoxide. *J. Geophys. Res. Atmos.*, **103**, 13249–13260.

Daniel, J., S. Solomon, and D. Abritton, 1995: On the evaluation of halocarbon radiative forcing and global warming potentials. *J. Geophys. Res. Atmos.*, **100**, 1271–1285.

Daniel, J., E. Fleming, R. Portmann, G. Velders, C. Jackman, and A. Ravishankara, 2010: Options to accelerate ozone recovery: Ozone and climate benefits. *Atmos. Chem. Phys.*, **10**, 7697–7707.

Daniel, J., S. Solomon, T. Sanford, M. McFarland, J. Fuglestvedt, and P. Friedlingstein, 2012: Limitations of single-basket trading: Lessons from the Montreal Protocol for climate policy. *Clim. Change*, **111**, 241–248.

Davin, E., N. de Noblet-Ducoudre, and P. Friedlingstein, 2007: Impact of land cover change on surface climate: Relevance of the radiative forcing concept. *Geophys. Res. Lett.*, **34**, L13702.

Davin, E. L., and N. de Noblet-Ducoudre, 2010: Climatic impact of global-scale deforestation: Radiative versus nonradiative orocesses. *J. Clim.*, **23**, 97–112.

De Cara, S., E. Galko, and P. Jayet, 2008: The global warming potential paradox: Implications for the design of climate policy. In: *Design of Climate Policy* [R. Guesnerie and H. Tulkens (eds.)]. The MIT Press, Cambridge, MA, USA, pp. 359–384.

de la Torre, L., et al., 2006: Solar influence on Northern Annular Mode spatial structure and QBO modulation. *Part. Accel. Space Plasma Phys. Sol. Radiat. Earth. Atmos. Clim.*, **37**, 1635–1639.

de Noblet-Ducoudre, N., et al., 2012: Determining robust impacts of land-use-induced land cover changes on surface climate over North America and Eurasia: Results from the first set of LUCID experiments. *J. Clim.*, **25**, 3261–3281.

DeAngelis, A., F. Dominguez, Y. Fan, A. Robock, M. D. Kustu, and D. Robinson, 2010: Evidence of enhanced precipitation due to irrigation over the Great Plains of the United States. *J. Geophys. Res. Atmos.*, **115**, D15115.

DeLand, M., and R. Cebula, 2012: Solar UV variations during the decline of Cycle 23. *J. Atmos. Sol. Terres. Phys.*, **77**, 225–234.

Delaygue, G., and E. Bard, 2011: An Antarctic view of Beryllium-10 and solar activity for the past millennium. *Clim. Dyn.*, **36**, 2201–2218.

Deligne, N. I., S. G. Coles, and R. S. J. Sparks, 2010: Recurrence rates of large explosive volcanic eruptions. *J. Geophys. Res. Sol. Earth*, **115**, B06203.

den Elzen, M., et al., 2005: Analysing countries' contribution to climate change: Scientific and policy-related choices. *Environ. Sci. Policy*, **8**, 614–636.

Denman, K. L., et al., 2007: Couplings between changes in the climate system and biogeochemistry. In: *Climate Change 2007: The Physical Science Basis. Contribution of Working Group I to the Fourth Assessment Report of the Intergovernmental Panel on Climate Change* [Solomon, S., D. Qin, M. Manning, Z. Chen, M. Marquis, K. B. Averyt, M. Tignor and H. L. Miller (eds.)] Cambridge University Press, Cambridge, United Kingdom and New York, NY, USA, 499-587.

Dentener, F., et al., 2006: The global atmospheric environment for the next generation. *Environ. Sci. Technol.*, **40**, 3586–3594.

Derwent, R., W. Collins, C. Johnson, and D. Stevenson, 2001: Transient behaviour of tropospheric ozone precursors in a global 3-D CTM and their indirect greenhouse effects. *Clim. Change*, **49**, 463–487.

Deuber, O., G. Luderer, and O. Edenhofer, 2013: Physico-economic evaluation of climate metrics: A conceptual framework. *Environ. Sci. Policy*, **29**, 37–45.

Dewitte, S., D. Crommelynck, S. Mekaoui, and A. Joukoff, 2004: Measurement and uncertainty of the long-term total solar irradiance trend. *Solar Phys.*, **224**, 209–216.

Dickinson, R., 1975: Solar variability and lower atmosphere. *Bull. Am. Meteorol. Soc.*, **56**, 1240–1248.

Doherty, S. J., S. G. Warren, T. C. Grenfell, A. D. Clarke, and R. E. Brandt, 2010: Light-absorbing impurities in Arctic snow. *Atmos. Chem. Phys.*, **10**, 11647–11680.

Doutriaux-Boucher, M., M. Webb, J. Gregory, and O. Boucher, 2009: Carbon dioxide induced stomatal closure increases radiative forcing via a rapid reduction in low cloud. *Geophys. Res. Lett.*, **36**, doi:10.1029/2008GL036273, L02703.

Ehhalt, D. H., and L. E. Heidt, 1973: Vertical profiles of CH_4 in troposphere and stratosphere. *J. Geophys. Res.*, **78**, 5265–5271.

Eliseev, A. V., and I.I. Mokhov, 2011: Effect of including land-use driven radiative forcing of the surface albedo of land on climate response in the 16th-21st centuries. *Izvestiya Atmos. Ocean. Phys.*, **47**, 15–30.

Engel, A., et al., 2009: Age of stratospheric air unchanged within uncertainties over the past 30 years. *Nature Geosci.*, **2**, 28–31.

Erlykin, A., and A. Wolfendale, 2011: Cosmic ray effects on cloud cover and their relevance to climate change. *J. Atmos. Sol. Terres. Phys.*, **73**, 1681–1686.

Ermolli, I., K. Matthes, T. Dudok de Wit, N. A. Krivova, K. Tourpali, M. Weber, Y. C. Unruh, L. Gray, U. Langematz, P. Pilewskie, E. Rozanov, W. Schmutz, A. Shapiro, S. K. Solanki, and T. N. Woods, 2013: Recent variability of the solar spectral irradiance and its impact on climate modelling, *Atmospheric Chemistry and Physics*, **13**, 3945-3977.

Esper, J., and F. H. Schweingruber, 2004: Large-scale treeline changes recorded in Siberia. *Geophys. Res. Lett.*, **31**, L06202.

Eyring, V., et al., 2010a: Sensitivity of 21st century stratospheric ozone to greenhouse gas scenarios. *Geophys. Res. Lett.*, **37**, L16807.

Eyring, V., et al., 2010b: Multi-model assessment of stratospheric ozone return dates and ozone recovery in CCMVal-2 models. *Atmos. Chem. Phys.*, **10**, 9451–9472.

Fan, F. X., M. E. Mann, and C. M. Ammann, 2009: Understanding changes in the Asian summer monsoon over the past millennium: Insights from a long-term coupled model simulation. *J. Clim.*, **22**, 1736–1748.

FAO, 2012: State of the world's forests. Food and Agriculture Organization of the United Nations, Rome, Italy, 60 pp.

Feng, X., and F. Zhao, 2009: Effect of changes of the HITRAN database on transmittance calculations in the near-infrared region. *J. Quant. Spectrosc. Radiat. Transfer*, **110**, 247–255.

Feng, X., F. Zhao, and W. Gao, 2007: Effect of the improvement of the HITIRAN database on the radiative transfer calculation. *J. Quant. Spectrosc. Radiat. Transfer*, **108**, 308–318.

Findell, K. L., E. Shevliakova, P. C. D. Milly, and R. J. Stouffer, 2007: Modeled impact of anthropogenic land cover change on climate. *J. Clim.*, **20**, 3621–3634.

Fioletov, V. E., G. E. Bodeker, A. J. Miller, R. D. McPeters, and R. Stolarski, 2002: Global and zonal total ozone variations estimated from ground-based and satellite measurements: 1964–2000. *J. Geophys. Res. Atmos.*, **107**, 4647.

Fiore, A. M., et al., 2009: Multimodel estimates of intercontinental source-receptor relationships for ozone pollution. *J. Geophys. Res. Atmos.*, **114**, D04301.

Fischer, E. M., J. Luterbacher, E. Zorita, S. F. B. Tett, C. Casty, and H. Wanner, 2007: European climate response to tropical volcanic eruptions over the last half millennium. *Geophys. Res. Lett.*, **34**, L05707.

Fishman, J., et al., 2010: An investigation of widespread ozone damage to the soybean crop in the upper Midwest determined from ground-based and satellite measurements. *Atmos. Environ.*, **44**, 2248–2256.

Flanner, M. G., C. S. Zender, J. T. Randerson, and P. J. Rasch, 2007: Present-day climate forcing and response from black carbon in snow. *J. Geophys. Res. Atmos.*, **112**, D11202.

Fletcher, C. G., P. J. Kushner, A. Hall, and X. Qu, 2009: Circulation responses to snow albedo feedback in climate change. *Geophys. Res. Lett.*, **36**, L09702.

Fomin, B. A., and V. A. Falaleeva, 2009: Recent progress in spectroscopy and its effect on line-by-line calculations for the validation of radiation codes for climate models. *Atmos. Oceanic Opt.*, **22**, 626–629.

Forster, P., and K. Shine, 1997: Radiative forcing and temperature trends from stratospheric ozone changes. *J. Geophys. Res. Atmos.*, **102**, 10841–10855.

Forster, P., et al., 2005: Resolution of the uncertainties in the radiative forcing of HFC-134a. *J. Quant. Spectrosc. Radiat. Transfer*, **93**, 447–460.

Forster, P., et al., 2007: Changes in Atmospheric Constituents and in Radiative Forcing. In: *Climate Change 2007: The Physical Science Basis. Contribution of Working Group I to the Fourth Assessment Report of the Intergovernmental Panel on Climate Change* [Solomon, S., D. Qin, M. Manning, Z. Chen, M. Marquis, K. B. Averyt, M. Tignor and H. L. Miller (eds.)] Cambridge University Press, Cambridge, United Kingdom and New York, NY, USA, 129-234.

Forster, P., et al., 2011a: Evaluation of radiation scheme performance within chemistry climate models. *J. Geophys. Res. Atmos.*, **116**, D10302.

Forster, P. M., T. Andrews, P. Good, J. M. Gregory, L. S. Jackson, and M. Zelinka, 2013: Evaluating adjusted forcing and model spread for historical and future scenarios in the CMIP5 generation of climate models. *J. Geophys. Res. Atmos.*, **118**, 1139–1150.

Forster, P. M., et al., 2011b: Stratospheric changes and climate. In: *Scientific Assessment of Ozone Depletion: 2010*. Global Ozone Research and Monitoring Project–Report No. 52, World Meteorological Organization, Geneva, Switzerland, 516 pp.

Fortuin, J. P. F., and H. Kelder, 1998: An ozone climatology based on ozonesonde and satellite measurements. *J. Geophys. Res. Atmos.*, **103**, 31709–31734.

Foukal, P., and J. Lean, 1988: Magnetic modulation of solar luminosity by phtospheric activity. *Astrophys. J.*, **328**, 347–357.

Fowler, D., et al., 2009: Atmospheric composition change: Ecosystems-atmosphere interactions. *Atmos. Environ.*, **43**, 5193–5267.

Frame, T., and L. Gray, 2010: The 11-yr solar cycle in ERA-40 data: An update to 2008. *J. Clim.*, **23**, 2213–2222.

Freckleton, R., E. Highwood, K. Shine, O. Wild, K. Law, and M. Sanderson, 1998: Greenhouse gas radiative forcing: Effects of averaging and inhomogeneities in trace gas distribution. *Q. J. R. Meteorol. Soc.*, **124**, 2099–2127.

Friedlingstein, P., et al., 2006: Climate-carbon cycle feedback analysis: Results from the C(4)MIP model intercomparison. *J. Clim.*, **19**, 3337–3353.

Frohlich, C., 2006: Solar irradiance variability since 1978—Revision of the PMOD composite during solar cycle 21. *Space Sci. Rev.*, **125**, 53–65.

Frohlich, C., 2009: Evidence of a long-term trend in total solar irradiance. *Astron. Astrophys.*, **501**, L27–L30.

Frolicher, T. L., F. Joos, and C. C. Raible, 2011: Sensitivity of atmospheric CO_2 and climate to explosive volcanic eruptions. *Biogeosciences*, **8**, 2317–2339.

Fromm, M., G. Nedoluha, and Z. Charvat, 2013: Comment on "Large Volcanic Aerosol Load in the Stratosphere Linked to Asian Monsoon Transport". *Science*, **339**, 647–c.

Fry, M., et al., 2012: The influence of ozone precursor emissions from four world regions on tropospheric composition and radiative climate forcing. *J. Geophys. Res. Atmos.*, **117**, D07306.

Fuglestvedt, J., T. Berntsen, O. Godal, and T. Skodvin, 2000: Climate implications of GWP-based reductions in greenhouse gas emissions. *Geophys. Res. Lett.*, **27**, 409–412.

Fuglestvedt, J., T. Berntsen, O. Godal, R. Sausen, K. Shine, and T. Skodvin, 2003: Metrics of climate change: Assessing radiative forcing and emission indices. *Clim. Change*, **58**, 267–331.

Fuglestvedt, J. S., et al., 2010: Transport impacts on atmosphere and climate: Metrics. *Atmos. Environ.*, **44**, 4648–4677.

Fung, I., J. John, J. Lerner, E. Matthews, M. Prather, L. P. Steele, and P. J. Fraser, 1991: 3-Dimensional model synthesis of the global methane cycle. *J. Geophys. Res. Atmos.*, **96**, 13033–13065.

Gaillard, M. J., et al., 2010: Holocene land-cover reconstructions for studies on land cover-climate feedbacks. *Clim. Past*, **6**, 483–499.

Gao, C. C., A. Robock, and C. Ammann, 2008: Volcanic forcing of climate over the past 1500 years: An improved ice core-based index for climate models. *J. Geophys. Res. Atmos.*, **113**, D23111.

Garcia, R. R., W. J. Randel, and D. E. Kinnison, 2011: On the determination of age of air trends from atmospheric trace species. *J. Atmos. Sci.*, **68**, 139–154.

Gerlach, T., 2011: Volcanic versus anthropogenic carbon dioxide. *Eos*, **92**, 201–202.

Gettelman, A., J. Holton, and K. Rosenlof, 1997: Mass fluxes of O_3, CH_4, N_2O and CF_2Cl_2 in the lower stratosphere calculated from observational data. *J. Geophys. Res. Atmos.*, **102**, 19149–19159.

Gillett, N., and H. Matthews, 2010: Accounting for carbon cycle feedbacks in a comparison of the global warming effects of greenhouse gases. *Environ. Res. Lett.*, **5**, 034011.

Ginoux, P., D. Garbuzov, and N. C. Hsu, 2010: Identification of anthropogenic and natural dust sources using Moderate Resolution Imaging Spectroradiometer (MODIS) Deep Blue level 2 data. *J. Geophys. Res. Atmos.*, **115**, D05204.

Godal, O., and J. Fuglestvedt, 2002: Testing 100-year global warming potentials: Impacts on compliance costs and abatement profile. *Clim. Change*, **52**, 93–127.

Goosse, H., et al., 2006: The origin of the European "Medieval Warm Period". *Clim. Past*, **2**, 99–113.

Granier, C., et al., 2011: Evolution of anthropogenic and biomass burning emissions of air pollutants at global and regional scales during the 1980–2010 period. *Clim. Change*, **109**, 163–190.

Gray, L., S. Rumbold, and K. Shine, 2009: Stratospheric temperature and radiative forcing response to 11-year solar cycle changes in irradiance and ozone. *J. Atmos. Sci.*, **66**, 2402–2417.

Gray, L., et al., 2010: Solar influences on climate. *Rev. Geophys.*, **48**, RG4001.

Gregory, J., and M. Webb, 2008: Tropospheric adjustment induces a cloud component in CO_2 forcing. *J. Clim.*, **21**, 58–71.

Gregory, J., et al., 2004: A new method for diagnosing radiative forcing and climate sensitivity. *Geophys. Res. Lett.*, **31**, L03205.

Gregory, J. M., 2010: Long-term effect of volcanic forcing on ocean heat content. *Geophys. Res. Lett.*, **37**, L22701.

Grewe, V., 2007: Impact of climate variability on tropospheric ozone. *Sci. Tot. Environ.*, **374**, 167–181.

Gusev, A. A., 2008: Temporal structure of the global sequence of volcanic eruptions: Order clustering and intermittent discharge rate. *Phys. Earth Planet. Inter.*, **166**, 203–218.

Haigh, J., 1994: The role of stratospheric ozone in modulating the solar radiative forcing of climate. *Nature*, **370**, 544–546.

Haigh, J., 1999: A GCM study of climate change in response to the 11-year solar cycle. *Q. J. R. Meteorol. Soc.*, **125**, 871–892.

Haigh, J. D., 1996: The impact of solar variability on climate. *Science*, **272**, 981–984.

Hall, J., and G. Lockwood, 2004: The chromospheric activity and variability of cycling and flat activity solar-analog stars. *Astrophys. J.*, **614**, 942–946.

Hallquist, M., et al., 2009: The formation, properties and impact of secondary organic aerosol: Current and emerging issues. *Atmos. Chem. Phys.*, **9**, 5155–5236.

Hammitt, J., A. Jain, J. Adams, and D. Wuebbles, 1996: A welfare-based index for assessing environmental effects of greenhouse-gas emissions. *Nature*, **381**, 301–303.

Hansen, J., and L. Nazarenko, 2004: Soot climate forcing via snow and ice albedos. *Proc. Natl. Acad. Sci. U.S.A.*, **101**, 423–428.

Hansen, J., et al., 2005: Efficacy of climate forcings. *J. Geophys. Res. Atmos.*, **110**, D18104.

Hansen, J., et al., 2007: Climate simulations for 1880–2003 with GISS modelE. *Clim. Dyn.*, **29**, 661–696.

Harder, J., J. Fontenla, P. Pilewskie, E. Richard, and T. Woods, 2009: Trends in solar spectral irradiance variability in the visible and infrared. *Geophys. Res. Lett.*, **36**, L07801.

Harrison, R., and M. Ambaum, 2010: Observing Forbush decreases in cloud at Shetland. *J. Atmos. Sol. Terres. Phys.*, **72**, 1408–1414.

Haywood, J., and M. Schulz, 2007: Causes of the reduction in uncertainty in the anthropogenic radiative forcing of climate between IPCC (2001) and IPCC (2007). *Geophys. Res. Lett.*, **34**, L20701.

Haywood, J. M., et al., 2010: Observations of the eruption of the Sarychev volcano and simulations using the HadGEM2 climate model. *J. Geophys. Res. Atmos.*, **115**, D21212.

Heathfield, A., C. Anastasi, A. McCulloch, and F. Nicolaisen, 1998: Integrated infrared absorption coefficients of several partially fluorinated ether compounds: CF_3OCF_2H, CF_2HOCF_2H, $CH_3OCF_2CF_2H$, CH_3OCF_2CFClH, $CH_3CH_2OCF_2CF_2H$, $CF_3CH_2OCF_2CF_2H$ AND $CH_2{=}CHCH_2OCF_2CF_2H$. *Atmos. Environ.*, **32**, 2825–2833.

Hegg, D. A., S. G. Warren, T. C. Grenfell, S. J. Doherty, T. V. Larson, and A. D. Clarke, 2009: Source attribution of black carbon in Arctic snow. *Environ. Sci. Technol.*, **43**, 4016–4021.

Hegglin, M. I., and T. G. Shepherd, 2009: Large climate-induced changes in ultraviolet index and stratosphere-to-troposphere ozone flux. *Nature Geosci.*, **2**, 687–691.

Helama, S., M. Fauria, K. Mielikainen, M. Timonen, and M. Eronen, 2010: Sub-Milankovitch solar forcing of past climates: Mid and late Holocene perspectives. *Geol. Soc. Am. Bull.*, **122**, 1981–1988.

Henze, D. K., et al., 2012: Spatially refined aerosol direct radiative forcing efficiencies. *Environ. Sci. Technol.*, **46**, 9511–9518.

Hohne, N., et al., 2011: Contributions of individual countries' emissions to climate change and their uncertainty. *Clim. Change*, **106**, 359–391.

Holmes, C., Q. Tang, and M. Prather, 2011: Uncertainties in climate assessment for the case of aviation NO. *Proc. Natl. Acad. Sci. U.S.A.*, **108**, 10997–11002.

Holmes, C. D., M. J. Prather, O. A. Sovde, and G. Myhre, 2013: Future methane, hydroxyl, and their uncertainties: Key climate and emission parameters for future predictions. *Atmos. Chem. Phys.*, **13**, 285–302.

Horowitz, L. W., 2006: Past, present, and future concentrations of tropospheric ozone and aerosols: Methodology, ozone evaluation, and sensitivity to aerosol wet removal. *J. Geophys. Res. Atmos.*, **111**, D22211.

Houghton, J. T., G. J. Jenkins, and J. J. Ephraums (eds.), 1990: *Climate Change. The IPCC Scientific Assessment*. Cambridge University Press, Cambridge, United Kingdom and New York, NY, USA, 364 pp.

Hoyle, C., et al., 2011: A review of the anthropogenic influence on biogenic secondary organic aerosol. *Atmos. Chem. Phys.*, **11**, 321–343.

Hsu, J., and M. J. Prather, 2009: Stratospheric variability and tropospheric ozone. *J. Geophys. Res. Atmos.*, **114**, D06102.

Huang, J., Q. Fu, W. Zhang, X. Wang, R. Zhang, H. Ye, and S. Warren, 2011: Dust and black carbon in seasonal snow across northern China. *Bull. Am. Meteorol. Soc.*, **92**, 175–181.

Huijnen, V., et al., 2010: The global chemistry transport model TM5: Description and evaluation of the tropospheric chemistry version 3.0. *Geosci. Model Dev.*, **3**, 445–473.

Hurst, D. F., et al., 2011: Stratospheric water vapor trends over Boulder, Colorado: Analysis of the 30 year Boulder record. *J. Geophys. Res. Atmos.*, **116**, D02306.

Hurtt, G. C., et al., 2006: The underpinnings of land-use history: Three centuries of global gridded land-use transitions, wood-harvest activity, and resulting secondary lands. *Global Change Biol.*, **12**, 1208–1229.

Iacono, M. J., J. S. Delamere, E. J. Mlawer, M. W. Shephard, S. A. Clough, and W. D. Collins, 2008: Radiative forcing by long-lived greenhouse gases: Calculations with the AER radiative transfer models. *J. Geophys. Res. Atmos.*, **113**, D13103.

Ineson, S., A. A. Scaife, J. R. Knight, J. C. Manners, N. J. Dunstone, L. J. Gray, and J. D. Haigh, 2011: Solar forcing of winter climate variability in the Northern Hemisphere. *Nature Geosci.*, **4**, 753–757.

IPCC, 1996: *Revised 1996 IPCC Guidelines for National Greenhouse Gas Inventories*. Intergovernmental Panel of Climate Change.

Isaksen, I., et al., 2009: Atmospheric composition change: Climate-chemistry interactions. *Atmos. Environ.*, **43**, 5138–5192.

Ito, A., and J. E. Penner, 2005: Historical emissions of carbonaceous aerosols from biomass and fossil fuel burning for the period 1870–2000. *Global Biogeochem. Cycles*, **19**, Gb2028.

Jackson, S., 2009: Parallel pursuit of near-term and long-term climate mitigation. *Science*, **326**, 526–527.

Jacobson, M., 2010: Short-term effects of controlling fossil-fuel soot, biofuel soot and gases, and methane on climate, Arctic ice, and air pollution health. *J. Geophys. Res. Atmos.*, **115**, D14209.

Jacobson, M., 2012: Investigating cloud absorption effects: Global absorption properties of black carbon, tar balls, and soil dust in clouds and aerosols. *J. Geophys. Res. Atmos.*, **117**, D06205.

Javadi, M., O. Nielsen, T. Wallington, M. Hurley, and J. Owens, 2007: Atmospheric chemistry of 2-ethoxy-3,3,4,4,5–pentafluorotetra-hydro-2,5-bis[1,2,2,2-tetrafluoro-1-(trifluoromethyl)ethyl]-furan: Kinetics, mechanisms, and products of CL atom and OH radical initiated oxidation. *Environ. Sci. Technol.*, **41**, 7389–7395.

Jin, M. L., R. E. Dickinson, and D. L. Zhang, 2005: The footprint of urban areas on global climate as characterized by MODIS. *J. Clim.*, **18**, 1551–1565.

Jin, Y., and D. P. Roy, 2005: Fire-induced albedo change and its radiative forcing at the surface in northern Australia. *Geophys. Res. Lett.*, **32**, L13401.

Jin, Y. F., J. T. Randerson, M. L. Goulden, and S. J. Goetz, 2012: Post-fire changes in net shortwave radiation along a latitudinal gradient in boreal North America. *Geophys. Res. Lett.*, **39**, L13403.

Johansson, D., 2012: Economics- and physical-based metrics for comparing greenhouse gases. *Clim. Change*, **110**, 123–141.

Johansson, D., U. Persson, and C. Azar, 2006: The cost of using global warming potentials: Analysing the trade off between CO_2, CH_4 and N_2O. *Clim. Change*, **77**, doi:10.1007/s10584-006-9054-1, 291–309.

Jones, G., M. Lockwood, and P. Stott, 2012: What influence will future solar activity changes over the 21st century have on projected global near-surface temperature changes? *J. Geophys. Res. Atmos.*, **117**, D05103.

Jones, G. S., J. M. Gregory, P. A. Stott, S. F. B. Tett, and R. B. Thorpe, 2005: An AOGCM simulation of the climate response to a volcanic super-eruption. *Clim. Dyn.*, **25**, 725–738.

Joos, F., M. Bruno, R. Fink, U. Siegenthaler, T. Stocker, and C. LeQuere, 1996: An efficient and accurate representation of complex oceanic and biospheric models of anthropogenic carbon uptake. *Tellus B*, **48**, 397–417.

Joos, F., et al., 2013: Carbon dioxide and climate impulse response functions for the computation of greenhouse gas metrics: A multi-model analysis. *Atmos. Chem. Phys.*, **13**, 2793–2825.

Joshi, M., and J. Gregory, 2008: Dependence of the land-sea contrast in surface climate response on the nature of the forcing. *Geophys. Res. Lett.*, **35**, L24802.

Joshi, M. M., and G. S. Jones, 2009: The climatic effects of the direct injection of water vapour into the stratosphere by large volcanic eruptions. *Atmos. Chem. Phys.*, **9**, 6109–6118.

Kandlikar, M., 1995: The relative role of trace gas emissions in greenhouse abatement policies. *Energ. Policy*, **23**, 879–883.

Kaplan, J. O., K. M. Krumhardt, E. C. Ellis, W. F. Ruddiman, C. Lemmen, and K. K. Goldewijk, 2011: Holocene carbon emissions as a result of anthropogenic land cover change. *Holocene*, **21**, 775–791.

Kasischke, E. S., and J. E. Penner, 2004: Improving global estimates of atmospheric emissions from biomass burning. *J. Geophys. Res. Atmos.*, **109**, D14S01.

Kawase, H., T. Nagashima, K. Sudo, and T. Nozawa, 2011: Future changes in tropospheric ozone under Representative Concentration Pathways (RCPs). *Geophys. Res. Lett.*, **38**, L05801.

Kawase, H., M. Abe, Y. Yamada, T. Takemura, T. Yokohata, and T. Nozawa, 2010: Physical mechanism of long-term drying trend over tropical North Africa. *Geophys. Res. Lett.*, **37**, L09706.

Kirkby, J., 2007: Cosmic rays and climate. *Surv. Geophys.*, **28**, 333–375.

Kirkby, J., et al., 2011: Role of sulphuric acid, ammonia and galactic cosmic rays in atmospheric aerosol nucleation. *Nature*, **476**, 429–433.

Kleinman, L. I., P. H. Daum, Y. N. Lee, L. J. Nunnermacker, S. R. Springston, J. Weinstein-Lloyd, and J. Rudolph, 2001: Sensitivity of ozone production rate to ozone precursors. *Geophys. Res. Lett.*, **28**, 2903–2906.

Knutti, R., et al., 2008: A review of uncertainties in global temperature projections over the twenty-first century. *J. Clim.*, **21**, 2651–2663.

Koch, D., and A. D. Del Genio, 2010: Black carbon semi-direct effects on cloud cover: Review and synthesis. *Atmos. Chem. Phys.*, **10**, 7685–7696.

Koch, D., T. Bond, D. Streets, N. Unger, and G. van der Werf, 2007: Global impacts of aerosols from particular source regions and sectors. *J. Geophys. Res. Atmos.*, **112**, D02205.

Koch, D., S. Menon, A. Del Genio, R. Ruedy, I. Alienov, and G. A. Schmidt, 2009a: Distinguishing aerosol impacts on climate over the past century. *J. Clim.*, **22**, 2659–2677.

Koch, D., et al., 2011: Coupled aerosol-chemistry-climate twentieth-century transient model investigation: Trends in short-lived species and climate responses. *J. Clim.*, **24**, 2693–2714.

Koch, D., et al., 2009b: Evaluation of black carbon estimations in global aerosol models. *Atmos. Chem. Phys.*, **9**, 9001–9026.

Koehler, M. O., G. Raedel, K. P. Shine, H. L. Rogers, and J. A. Pyle, 2013: Latitudinal variation of the effect of aviation NO_x emissions on atmospheric ozone and methane and related climate metrics. *Atmos. Environ.*, **64**, 1–9.

Koffi, B., et al., 2012: Application of the CALIOP layer product to evaluate the vertical distribution of aerosols estimated by global models: AeroCom phase I results. *J. Geophys. Res. Atmos.*, **117**, D10201.

Kopp, G., and J. Lean, 2011: A new, lower value of total solar irradiance: Evidence and climate significance. *Geophys. Res. Lett.*, **38**, L01706.

Kratz, D., 2008: The sensitivity of radiative transfer calculations to the changes in the HITRAN database from 1982 to 2004. *J. Quant. Spectrosc. Radiat. Transfer*, **109**, 1060–1080.

Kravitz, B., and A. Robock, 2011: Climate effects of high-latitude volcanic eruptions: Role of the time of year. *J. Geophys. Res. Atmos.*, **116**, D01105.

Kravitz, B., A. Robock, and A. Bourassa, 2010: Negligible climatic effects from the 2008 Okmok and Kasatochi volcanic eruptions. *J. Geophys. Res. Atmos.*, **115**, D00L05.

Kravitz, B., et al., 2011: Simulation and observations of stratospheric aerosols from the 2009 Sarychev volcanic eruption. *J. Geophys. Res. Atmos.*, **116**, D18211.

Kristjansson, J. E., T. Iversen, A. Kirkevag, O. Seland, and J. Debernard, 2005: Response of the climate system to aerosol direct and indirect forcing: Role of cloud feedbacks. *J. Geophys. Res. Atmos.*, **110**, D24206.

Krivova, N., L. Vieira, and S. Solanki, 2010: Reconstruction of solar spectral irradiance since the Maunder minimum. *J. Geophys. Res. Space Phys.*, **115**, A12112.

Kueppers, L. M., M. A. Snyder, and L. C. Sloan, 2007: Irrigation cooling effect: Regional climate forcing by land-use change. *Geophys. Res. Lett.*, **34**, L03703.

Kuroda, Y., and K. Kodera, 2005: Solar cycle modulation of the southern annular mode. *Geophys. Res. Lett.*, **32**, L13802.

Kvalevag, M. M., G. Myhre, G. Bonan, and S. Levis, 2010: Anthropogenic land cover changes in a GCM with surface albedo changes based on MODIS data. *Int. J. Climatol.*, **30**, 2105–2117.

Lacis, A. A., D. J. Wuebbles, J. A. Logan, 1990: Radiative forcing of climate by changes in the vertical-distribution of ozone, J. Geophys. Res., **95**, 9971-9981.

Lamarque, J., et al., 2011: Global and regional evolution of short-lived radiatively-active gases and aerosols in the Representative Concentration Pathways. *Clim. Change*, **109**, 191–212.

Lamarque, J., et al., 2010: Historical (1850–2000) gridded anthropogenic and biomass burning emissions of reactive gases and aerosols: Methodology and application. *Atmos. Chem. Phys.*, **10**, 7017–7039.

Lamarque, J. F., et al., 2013: The Atmospheric Chemistry and Climate Model Intercomparison Project (ACCMIP): Overview and description of models, simulations and climate diagnostics. *Geosci. Model Dev.*, **6**, 179–206.

Lau, K. M., M. K. Kim, and K. M. Kim, 2006: Asian summer monsoon anomalies induced by aerosol direct forcing: The role of the Tibetan Plateau. *Clim. Dyn.*, **26**, 855–864.

Lauder, A. R., I. G. Enting, J. O. Carter, N. Clisby, A. L. Cowie, B. K. Henry, and M. R. Raupach, 2013: Offsetting methane emissions—An alternative to emission equivalence metrics. *Int. J. Greenh. Gas Control*, **12**, 419–429.

Lauer, A., V. Eyring, J. Hendricks, P. Jockel, and U. Lohmann, 2007: Global model simulations of the impact of ocean-going ships on aerosols, clouds, and the radiation budget. *Atmos. Chem. Phys.*, **7**, 5061–5079.

Lawrence, P. J., and T. N. Chase, 2010: Investigating the climate impacts of global land cover change in the community climate system model. *Int. J. Climatol.*, **30**, 2066–2087.

Lean, J., 2000: Evolution of the sun's spectral irradiance since the Maunder Minimum. *Geophys. Res. Lett.*, **27**, 2425–2428.

Lean, J., and M. Deland, 2012: How does the sun's spectrum vary? *J. Clim.*, **25**, 2555–2560.

Lee, D. S., et al., 2010: Transport impacts on atmosphere and climate: Aviation. *Atmos. Environ.*, **44**, 4678–4734.

Lee, J., D. Shindell, and S. Hameed, 2009: The influence of solar forcing on tropical circulation. *J. Clim.*, **22**, 5870–5885.

Lee, R., M. Gibson, R. Wilson, and S. Thomas, 1995: Long-term total solar irradiance variability during sunspot cycle-22. *J. Geophys. Res. Space Phys.*, **100**, 1667–1675.

Lee, X., et al., 2011: Observed increase in local cooling effect of deforestation at higher latitudes. *Nature*, **479**, 384–387.

Lee, Y. H., et al., 2013: Evaluation of preindustrial to present-day black carbon and its albedo forcing from Atmospheric Chemistry and Climate Model Intercomparison Project (ACCMIP). *Atmos. Chem. Phys.*, **13**, 2607–2634.

Legras, B., O. Mestre, E. Bard, and P. Yiou, 2010: A critical look at solar-climate relationships from long temperature series. *Clim. Past*, **6**, 745–758.

Leibensperger, E. M., L. J. Mickley, and D. J. Jacob, 2008: Sensitivity of US air quality to mid-latitude cyclone frequency and implications of 1980–2006 climate change. *Atmos. Chem. Phys.*, **8**, 7075–7086.

Leibensperger, E. M., et al., 2012a: Climatic effects of 1950–2050 changes in US anthropogenic aerosols—Part 1: Aerosol trends and radiative forcing. *Atmos. Chem. Phys.*, **12**, 3333–3348.

Leibensperger, E. M., et al., 2012b: Climatic effects of 1950–2050 changes in US anthropogenic aerosols—Part 2: Climate response. *Atmos. Chem. Phys.*, **12**, 3349–3362.

Lelieveld, J., et al., 2008: Atmospheric oxidation capacity sustained by a tropical forest. *Nature*, **452**, 737–740.

Levy, H., 1971: Normal atmosphere—Large radical and formaldehyde concentrations predicted. *Science*, **173**, 141–143.

Liao, H., W. T. Chen, and J. H. Seinfeld, 2006: Role of climate change in global predictions of future tropospheric ozone and aerosols. *J. Geophys. Res. Atmos.*, **111**, D12304.

Lockwood, M., 2010: Solar change and climate: An update in the light of the current exceptional solar minimum. *Proc. R. Soc. London A*, **466**, 303–329.

Lockwood, M., and C. Frohlich, 2008: Recent oppositely directed trends in solar climate forcings and the global mean surface air temperature. II. Different reconstructions of the total solar irradiance variation and dependence on response time scale. *Proc. R. Soc. London A*, **464**, 1367–1385.

Lockwood, M., A. Rouillard, and I. Finch, 2009: The rise and fall of open solar flux during the current grand solar maximum. *Astrophys. J.*, **700**, 937–944.

Logan, J. A., 1999: An analysis of ozonesonde data for the troposphere: Recommendations for testing 3-D models and development of a gridded climatology for tropospheric ozone. *J. Geophys. Res. Atmos.*, **104**, 16115–16149.

Logan, J. A., M. J. Prather, S. C. Wofsy, and M. B. McElroy, 1981: Tropospheric chemistry—A global perspective. *J. Geophys. Res. Oceans Atmos.*, **86**, 7210–7254.

Logan, J. A., et al., 2012: Changes in ozone over Europe: Analysis of ozone measurements from sondes, regular aircraft (MOZAIC) and alpine surface sites. *J. Geophys. Res. Atmos.*, **117**, D09301.

Lohila, A., et al., 2010: Forestation of boreal peatlands: Impacts of changing albedo and greenhouse gas fluxes on radiative forcing. *J. Geophys. Res. Biogeosci.*, **115**, G04011.

Lohmann, U., et al., 2010: Total aerosol effect: Radiative forcing or radiative flux perturbation? *Atmos. Chem. Phys.*, **10**, 3235–3246.

Long, C. N., E. G. Dutton, J. A. Augustine, W. Wiscombe, M. Wild, S. A. McFarlane, and C. J. Flynn, 2009: Significant decadal brightening of downwelling shortwave in the continental United States. *J. Geophys. Res. Atmos.*, **114**, D00D06.

Long, D., and M. Collins, 2013: Quantifying global climate feedbacks, responses and forcing under abrupt and gradual CO_2 forcing. *Clim. Dyn.*, **41**, 2471-2479.

Lu, P., H. Zhang, and X. Jing, 2012: The effects of different HITRAN versions on calculated long-wave radiation and uncertainty evaluation. *Acta Meteorol. Sin.*, **26**, 389–398.

Lu, Z., Q. Zhang, and D. G. Streets, 2011: Sulfur dioxide and primary carbonaceous aerosol emissions in China and India, 1996–2010. *Atmos. Chem. Phys.*, **11**, 9839–9864.

Lund, M., T. Berntsen, J. Fuglestvedt, M. Ponater, and K. Shine, 2012: How much information is lost by using global-mean climate metrics? an example using the transport sector. *Clim. Change*, **113**, 949–963.

MacFarling Meure, C., et al., 2006: Law Dome CO_2, CH_4 and N_2O ice core records extended to 2000 years BP. *Geophys. Res. Lett.*, **33**, L14810.

MacMynowski, D., H. Shin, and K. Caldeira, 2011: The frequency response of temperature and precipitation in a climate model. *Geophys. Res. Lett.*, **38**, L16711.

Mader, J. A., J. Staehelin, T. Peter, D. Brunner, H. E. Rieder, and W. A. Stahel, 2010: Evidence for the effectiveness of the Montreal Protocol to protect the ozone layer. *Atmos. Chem. Phys.*, **10**, 12161–12171.

Mahowald, N. M., et al., 2010: Observed 20th century desert dust variability: Impact on climate and biogeochemistry. *Atmos. Chem. Phys.*, **10**, 10875–10893.

Mann, M., M. Cane, S. Zebiak, and A. Clement, 2005: Volcanic and solar forcing of the tropical Pacific over the past 1000 years. *J. Clim.*, **18**, 447–456.

Manne, A., and R. Richels, 2001: An alternative approach to establishing trade-offs among greenhouse gases. *Nature*, **410**, 675–677.

Manning, M., and A. Reisinger, 2011: Broader perspectives for comparing different greenhouse gases. *Philos. Trans. R. Soc. London A*, **369**, 1891–1905.

Marenco, A., H. Gouget, P. Nedelec, J. P. Pages, and F. Karcher, 1994: Evidence of a long-term increase in tropospheric ozone from PIC Du Midi Data Series—Consequences—Positive radiative forcing. *J. Geophys. Res. Atmos.*, **99**, 16617–16632.

Marten, A. L., and S. C. Newbold, 2012: Estimating the social cost of non-CO2 GHG emissions: Methane and nitrous oxide. *Energ. Policy*, **51**, 957–972.

Matthews, H. D., A. J. Weaver, K. J. Meissner, N. P. Gillett, and M. Eby, 2004: Natural and anthropogenic climate change: Incorporating historical land cover change, vegetation dynamics and the global carbon cycle. *Clim. Dyn.*, **22**, 461–479.

McComas, D., R. Ebert, H. Elliott, B. Goldstein, J. Gosling, N. Schwadron, and R. Skoug, 2008: Weaker solar wind from the polar coronal holes and the whole Sun. *Geophys. Res. Lett.*, **35**, L18103.

McLandress, C., T. G. Shepherd, J. F. Scinocca, D. A. Plummer, M. Sigmond, A. I. Jonsson, and M. C. Reader, 2011: Separating the dynamical effects of climate change and ozone depletion. Part II. Southern Hemisphere troposphere. *J. Clim.*, **24**, 1850–1868.

Meinshausen, M., T. Wigley, and S. Raper, 2011a: Emulating atmosphere-ocean and carbon cycle models with a simpler model, MAGICC6–Part 2: Applications. *Atmos. Chem. Phys.*, **11**, 1457–1471.

Meinshausen, M., et al., 2011b: The RCP greenhouse gas concentrations and their extensions from 1765 to 2300. *Clim. Change*, **109**, 213–241.

Mercado, L. M., N. Bellouin, S. Sitch, O. Boucher, C. Huntingford, M. Wild, and P. M. Cox, 2009: Impact of changes in diffuse radiation on the global land carbon sink. *Nature*, **458**, 1014–1017.

Merikanto, J., D. Spracklen, G. Mann, S. Pickering, and K. Carslaw, 2009: Impact of nucleation on global CCN. *Atmos. Chem. Phys.*, **9**, 8601–8616.

Mickley, L. J., E. M. Leibensperger, D. J. Jacob, and D. Rind, 2012: Regional warming from aerosol removal over the United States: Results from a transient 2010–2050 climate simulation. *Atmos. Environ.*, **46**, 545–553.

Miller, G. H., et al., 2012: Abrupt onset of the Little Ice Age triggered by volcanism and sustained by sea-ice/ocean feedbacks. *Geophys. Res. Lett.*, **39**, L02708.

Miller, R. L., I. Tegen, and J. Perlwitz, 2004: Surface radiative forcing by soil dust aerosols and the hydrologic cycle. *J. Geophys. Res. Atmos.*, **109**, D04203.

Mills, M. J., O. B. Toon, R. P. Turco, D. E. Kinnison, and R. R. Garcia, 2008: Massive global ozone loss predicted following regional nuclear conflict. *Proc. Natl. Acad. Sci. U.S.A.*, **105**, 5307–5312.

Ming, Y., and V. Ramaswamy, 2012: Nonlocal component of radiative flux perturbation. *Geophys. Res. Lett.*, **39**, L22706.

Ming, Y., V. Ramaswamy, and G. Persad, 2010: Two opposing effects of absorbing aerosols on global-mean precipitation. *Geophys. Res. Lett.*, **37**, L13701.

Ming, Y., V. Ramaswamy, and G. Chen, 2011: A model investigation of aerosol-induced changes in boreal winter extratropical circulation. *J. Clim.*, **24**, 6077–6091.

Ming, Y., V. Ramaswamy, L. J. Donner, V. T. J. Phillips, S. A. Klein, P. A. Ginoux, and L. W. Horowitz, 2007: Modeling the interactions between aerosols and liquid water clouds with a self-consistent cloud scheme in a general circulation model. *J. Atmos. Sci.*, **64**, 1189–1209.

Mirme, S., A. Mirme, A. Minikin, A. Petzold, U. Horrak, V.-M. Kerminen, and M. Kulmala, 2010: Atmospheric sub-3 nm particles at high altitudes. *Atm. Chem. Phys.*, **10**, 437–451.

Montzka, S. A., E. J. Dlugokencky, and J. H. Butler, 2011: Non-CO_2 greenhouse gases and climate change. *Nature*, **476**, 43–50.

Morrill, J., L. Floyd, and D. McMullin, 2011: The solar ultraviolet spectrum estimated using the Mg II Index and Ca II K disk activity. *Solar Physics*, **269**, 253–267.

Muhle, J., et al., 2009: Sulfuryl fluoride in the global atmosphere. *J. Geophys. Res. Atmos.*, **114**, D05306.

Mulitza, S., et al., 2010: Increase in African dust flux at the onset of commercial agriculture in the Sahel region. *Nature*, **466**, 226–228.

Murphy, D., and D. Fahey, 1994: An estimate of the flux of stratospheric reactive nitrogen and ozone into the troposphere. *J. Geophys. Res. Atmos.*, **99**, 5325–5332.

Myhre, G., M. M. Kvalevag, and C. B. Schaaf, 2005a: Radiative forcing due to anthropogenic vegetation change based on MODIS surface albedo data. *Geophys. Res. Lett.*, **32**, L21410.

Myhre, G., E. J. Highwood, K. P. Shine, and F. Stordal, 1998: New estimates of radiative forcing due to well mixed greenhouse gases. *Geophys. Res. Lett.*, **25**, 2715–2718.

Myhre, G., Y. Govaerts, J. M. Haywood, T. K. Berntsen, and A. Lattanzio, 2005b: Radiative effect of surface albedo change from biomass burning. *Geophys. Res. Lett.*, **32**, L20812.

Myhre, G., J. Nilsen, L. Gulstad, K. Shine, B. Rognerud, and I. Isaksen, 2007: Radiative forcing due to stratospheric water vapour from CH_4 oxidation. *Geophys. Res. Lett.*, **34**, L01807.

Myhre, G., et al., 2011: Radiative forcing due to changes in ozone and methane caused by the transport sector. *Atmos. Environ.*, **45**, 387–394.

Myhre, G., et al., 2013: Radiative forcing of the direct aerosol effect from AeroCom Phase II simulations. *Atmos. Chem. Phys.*, **13**, 1853–1877.

Nagai, T., B. Liley, T. Sakai, T. Shibata, and O. Uchino, 2010: Post-Pinatubo evolution and subsequent trend of the stratospheric aerosol layer observed by mid-latitude lidars in both hemispheres. *Sola*, **6**, 69–72.

Naik, V., D. L. Mauzerall, L. W. Horowitz, M. D. Schwarzkopf, V. Ramaswamy, and M. Oppenheimer, 2007: On the sensitivity of radiative forcing from biomass burning aerosols and ozone to emission location. *Geophys. Res. Lett.*, **34**, L03818.

Nair, U. S., D. K. Ray, J. Wang, S. A. Christopher, T. J. Lyons, R. M. Welch, and R. A. Pielke, 2007: Observational estimates of radiative forcing due to land use change in southwest Australia. *J. Geophys. Res. Atmos.*, **112**, D09117.

Neely, R. R., et al., 2013: Recent anthropogenic increases in SO_2 from Asia have minimal impact on stratospheric aerosol. *Geophys. Res. Lett.*, **40**, 999-1004.

O'ishi, R., A. Abe-Ouchi, I. Prentice, and S. Sitch, 2009: Vegetation dynamics and plant CO_2 responses as positive feedbacks in a greenhouse world. *Geophys. Res. Lett.*, **36**, L11706.

O'Neill, B., 2000: The jury is still out on global warming potentials. *Clim. Change*, **44**, 427–443.

O'Neill, B., 2003: Economics, natural science, and the costs of global warming potentials—An editorial comment. *Clim. Change*, **58**, 251–260.

Oleson, K. W., G. B. Bonan, and J. Feddema, 2010: Effects of white roofs on urban temperature in a global climate model. *Geophys. Res. Lett.*, **37**, L03701.

Olivié, D. J. L., G. Peters, and D. Saint-Martin, 2012: Atmosphere response time scales estimated from AOGCM experiments. *J. Climate*, **25**, 7956–7972.

Olsen, S. C., C. A. McLinden, and M. J. Prather, 2001: Stratospheric N_2O–NOy system: Testing uncertainties in a three-dimensional framework, *J. Geophys. Res.*, **106**, 28771.

Oreopoulos, L., et al., 2012: The Continual Intercomparison of Radiation Codes: Results from Phase I. *J. Geophys. Res. Atmos.*, **117**, D06118.

Osterman, G. B., et al., 2008: Validation of Tropospheric Emission Spectrometer (TES) measurements of the total, stratospheric, and tropospheric column abundance of ozone. *J. Geophys. Res. Atmos.*, **113**, D15S16.

Otterä, O. H., M. Bentsen, H. Drange, and L. L. Suo, 2010: External forcing as a metronome for Atlantic multidecadal variability. *Nature Geosci.*, **3**, 688–694.

Özdoğan, M., A. Robock, and C. J. Kucharik, 2013: Impacts of a nuclear war in South Asia on soybean and maize production in the Midwest United States. *Clim. Change*, **116**, 373–387.

Parrish, D. D., D. B. Millet, and A. H. Goldstein, 2009: Increasing ozone in marine boundary layer inflow at the west coasts of North America and Europe. *Atmos. Chem. Phys.*, **9**, 1303–1323.

Paulot, F., J. D. Crounse, H. G. Kjaergaard, A. Kurten, J. M. St Clair, J. H. Seinfeld, and P. O. Wennberg, 2009: Unexpected epoxide formation in the gas-phase photooxidation of isoprene. *Science*, **325**, 730–733.

Paynter, D., and V. Ramaswamy, 2011: An assessment of recent water vapor continuum measurements upon longwave and shortwave radiative transfer. *J. Geophys. Res. Atmos.*, **116**, D20302.

Pechony, O., and D. Shindell, 2010: Driving forces of global wildfires over the past millennium and the forthcoming century. *Proc. Natl. Acad. Sci. U.S.A.*, **107**, 19167–19170.

Peeters, J., T. L. Nguyen, and L. Vereecken, 2009: HO(x) radical regeneration in the oxidation of isoprene. *Phys. Chem. Chem. Phys.*, **11**, 5935–5939.

Penn, M., and W. Livingston, 2006: Temporal changes in sunspot umbral magnetic fields and temperatures. *Astrophys. J.*, **649**, L45–L48.

Penner, J., L. Xu, and M. Wang, 2011: Satellite methods underestimate indirect climate forcing by aerosols. *Proc. Natl. Acad. Sci. U.S.A.*, **108**, 13404–13408.

Penner, J., et al., 2006: Model intercomparison of indirect aerosol effects. *Atmos. Chem. Phys.*, **6**, 3391–3405.

Perlwitz, J., and R. L. Miller, 2010: Cloud cover increase with increasing aerosol absorptivity: A counterexample to the conventional semidirect aerosol effect. *J. Geophys. Res. Atmos.*, **115**, D08203.

Persad, G. G., Y. Ming, and V. Ramaswamy, 2012: Tropical tropospheric-only responses to absorbing aerosols. *J. Clim.*, **25**, 2471–2480.

Peters, G., B. Aamaas, T. Berntsen, and J. Fuglestvedt, 2011a: The integrated global temperature change potential (iGTP) and relationships between emission metrics. *Environ. Res. Lett.*, **6**, 044021.

Peters, G. P., B. Aamaas, M. T. Lund, C. Solli, and J. S. Fuglestvedt, 2011b: Alternative "Global Warming" metrics in life cycle assessment: A case study with existing transportation data. *Environ. Sci. Technol.*, **45**, 8633–8641.

Peters, K., P. Stier, J. Quaas, and H. Grassl, 2012: Aerosol indirect effects from shipping emissions: Sensitivity studies with the global aerosol-climate model ECHAM-HAM. *Atmos. Chem. Phys.*, **12**, 5985–6007.

Philipona, R., K. Behrens, and C. Ruckstuhl, 2009: How declining aerosols and rising greenhouse gases forced rapid warming in Europe since the 1980s. *Geophys. Res. Lett.*, **36**, L02806.

Pinto, J. P., R. P. Turco, and O. B. Toon, 1989: Self-limiting physical and chemical effects in volcanic-eruption clouds. *J. Geophys. Res. Atmos.*, **94**, 11165–11174.

Pitman, A. J., et al., 2009: Uncertainties in climate responses to past land cover change: First results from the LUCID intercomparison study. *Geophys. Res. Lett.*, **36**, L14814.

Plattner, G.-K., T. Stocker, P. Midgley, and M. Tignor, 2009: IPCC Expert Meeting on the Science of Alternative Metrics: Meeting Report. IPCC Working Group I, Technical Support Unit.

Plattner, G. K., et al., 2008: Long-term climate commitments projected with climate-carbon cycle models. *J. Clim.*, **21**, 2721–2751.

Pongratz, J., C. Reick, T. Raddatz, and M. Claussen, 2008: A reconstruction of global agricultural areas and land cover for the last millennium. *Global Biogeochem. Cycles*, **22**, Gb3018.

Pongratz, J., C. H. Reick, T. Raddatz, and M. Claussen, 2010: Biogeophysical versus biogeochemical climate response to historical anthropogenic land cover change. *Geophys. Res. Lett.*, **37**, L08702.

Pongratz, J., T. Raddatz, C. H. Reick, M. Esch, and M. Claussen, 2009: Radiative forcing from anthropogenic land cover change since AD 800. *Geophys. Res. Lett.*, **36**, L02709.

Pozzer, A., et al., 2012: Effects of business-as-usual anthropogenic emissions on air quality. *Atmos. Chem. Phys.*, **12**, 6915–6937.

Prather, M., 2002: Lifetimes of atmospheric species: Integrating environmental impacts. *Geophys. Res. Lett.*, **29**, 2063.

Prather, M., and J. Hsu, 2010: Coupling of nitrous oxide and methane by global atmospheric chemistry. *Science*, **330**, 952–954.

Prather, M. J., 1998: Time scales in atmospheric chemistry: Coupled perturbations to N_2O, NOy, and O_3. *Science*, **279**, 1339–1341.

Prather, M. J., C. D. Holmes, and J. Hsu, 2012: Reactive greenhouse gas scenarios: Systematic exploration of uncertainties and the role of atmospheric chemistry. *Geophys. Res. Lett.*, **39**, L09803.

Puma, M. J., and B. I. Cook, 2010: Effects of irrigation on global climate during the 20th century. *J. Geophys. Res. Atmos.*, **115**, D16120.

Quaas, J., O. Boucher, N. Bellouin, and S. Kinne, 2011: Which of satellite- or model-based estimates is closer to reality for aerosol indirect forcing? *Proc. Natl. Acad. Sci. U.S.A.*, **108**, E1099.

Quaas, J., et al., 2009: Aerosol indirect effects—general circulation model intercomparison and evaluation with satellite data. *Atmos. Chem. Phys.*, **9**, 8697–8717.

Rajakumar, B., R. Portmann, J. Burkholder, and A. Ravishankara, 2006: Rate coefficients for the reactions of OH with $CF_3CH_2CH_3$ (HFC-263fb), CF_3CHFCH_2F (HFC-245eb), and $CHF_2CHFCHF_2$ (HFC-245ea) between 238 and 375 K. *J. Phys. Chem. A*, **110**, 6724–6731.

Ramanathan, V., and G. Carmichael, 2008: Global and regional climate changes due to black carbon. *Nature Geosci.*, **1**, 221–227.

Ramanathan, V., et al., 2005: Atmospheric brown clouds: Impacts on South Asian climate and hydrological cycle. *Proc. Natl. Acad. Sci. U.S.A.*, **102**, 5326–5333.

Ramaswamy, V., et al., 2001: Radiative forcing of climate change. In: *Climate Change 2001: The Scientific Basis. Contribution of Working Group I to the Third Assessment Report of the Intergovernmntal Panel on Climate Change* [J. T. Houghton, Y. Ding, D. J. Griggs, M. Noquer, P. J. van der Linden, X. Dai, K. Maskell and C. A. Johnson (eds.)]. Cambride University Press, Cambridge, United Kingdom and New York, NY, USA, 349-416.

Randel, W., and F. Wu, 2007: A stratospheric ozone profile data set for 1979–2005: Variability, trends, and comparisons with column ozone data. *J. Geophys. Res. Atmos.*, **112**, D06313.

Randles, C. A., and V. Ramaswamy, 2008: Absorbing aerosols over Asia: A Geophysical Fluid Dynamics Laboratory general circulation model sensitivity study of model response to aerosol optical depth and aerosol absorption. *J. Geophys. Res. Atmos.*, **113**, D21203.

Rasch, P. J., et al., 2008: An overview of geoengineering of climate using stratospheric sulphate aerosols. *Philos. Trans. R. Soc. A*, **366**, 4007–4037.

Ravishankara, A. R., J. S. Daniel, and R. W. Portmann, 2009: Nitrous oxide (N_2O): The dominant ozone-depleting substance emitted in the 21st century. *Science*, **326**, 123–125.

Rechid, D., T. Raddatz, and D. Jacob, 2009: Parameterization of snow-free land surface albedo as a function of vegetation phenology based on MODIS data and applied in climate modelling. *Theor. Appl. Climatol.*, **95**, 245–255.

Reddy, M., and O. Boucher, 2007: Climate impact of black carbon emitted from energy consumption in the world's regions. *Geophys. Res. Lett.*, **34**, L11802.

Reilly, J., et al., 1999: Multi-gas assessment of the Kyoto Protocol. *Nature*, **401**, 549–555.

Reilly, J. M., and K. R. Richards, 1993: Climate-change damage and the trace-gas-index issue. *Environ. Resour. Econ.*, **3**, 41–61.

Reisinger, A., M. Meinshausen, and M. Manning, 2011: Future changes in global warming potentials under representative concentration pathways. *Environ. Res. Lett.*, **6**, 024020.

Reisinger, A., M. Meinshausen, M. Manning, and G. Bodeker, 2010: Uncertainties of global warming metrics: CO_2 and CH_4. *Geophys. Res. Lett.*, **37**, L14707.

Reisinger, A., P. Havlik, K. Riahi, O. Vliet, M. Obersteiner, and M. Herrero, 2013: Implications of alternative metrics for global mitigation costs and greenhouse gas emissions from agriculture. *Clim. Change*, **117**, 677-690.

Righi, M., C. Klinger, V. Eyring, J. Hendricks, A. Lauer, and A. Petzold, 2011: Climate impact of biofuels in shipping: global model studies of the aerosol indirect effect. *Environ. Sci. Technol.*, **45**, 3519–3525.

Rigozo, N., E. Echer, L. Vieira, and D. Nordemann, 2001: Reconstruction of Wolf sunspot numbers on the basis of spectral characteristics and estimates of associated radio flux and solar wind parameters for the last millennium. *Sol. Phys.*, **203**, 179–191.

Rigozo, N., D. Nordemann, E. Echer, M. Echer, and H. Silva, 2010: Prediction of solar minimum and maximum epochs on the basis of spectral characteristics for the next millennium. *Planet. Space Sci.*, **58**, 1971–1976.

Robock, A., 2000: Volcanic eruptions and climate. *Rev. Geophys.*, **38**, 191–219.

Robock, A., 2010: New START, Eyjafjallajökull, and Nuclear Winter. *Eos*, **91**, 444–445.

Robock, A., L. Oman, and G. L. Stenchikov, 2007a: Nuclear winter revisited with a modern climate model and current nuclear arsenals: Still catastrophic consequences. *J. Geophys. Res. Atmos.*, **112**, D13107.

Robock, A., L. Oman, and G. L. Stenchikov, 2008: Regional climate responses to geoengineering with tropical and Arctic SO_2 injections. *J. Geophys. Res. Atmos.*, **113**, D16101.

Robock, A., L. Oman, G. L. Stenchikov, O. B. Toon, C. Bardeen, and R. P. Turco, 2007b: Climatic consequences of regional nuclear conflicts. *Atmos. Chem. Phys.*, **7**, 2003–2012.

Robock, A., C. M. Ammann, L. Oman, D. Shindell, S. Levis, and G. Stenchikov, 2009: Did the Toba volcanic eruption of similar to 74 ka BP produce widespread glaciation? *J. Geophys. Res. Atmos.*, **114**, D10107.

Rogelj, J., et al., 2011: Emission pathways consistent with a 2 degrees C global temperature limit. *Nature Clim. Change*, **1**, 413–418.

Roscoe, H. K., and J. D. Haigh, 2007: Influences of ozone depletion, the solar cycle and the QBO on the Southern Annular Mode. *Q. J. R. Meteorol. Soc.*, **133**, 1855–1864.

Rotenberg, E., and D. Yakir, 2010: Contribution of semi-arid forests to the climate system. *Science*, **327**, 451–454.

Rothman, L., 2010: The evolution and impact of the HITRAN molecular spectroscopic database. *J. Quant. Spectrosc. Radiat. Transfer*, **111**, 1565–1567.

Rotstayn, L., and J. Penner, 2001: Indirect aerosol forcing, quasi forcing, and climate response. *J. Clim.*, **14**, 2960–2975.

Rotstayn, L. D., and U. Lohmann, 2002: Tropical rainfall trends and the indirect aerosol effect. *J. Clim.*, **15**, 2103–2116.

Rotstayn, L. D., B. F. Ryan, and J. E. Penner, 2000: Precipitation changes in a GCM resulting from the indirect effects of anthropogenic aerosols. *Geophys. Res. Lett.*, **27**, 3045–3048.

Rottman, G., 2006: Measurement of total and spectral solar irradiance. *Space Sci. Rev.*, **125**, 39–51.

Ruckstuhl, C., et al., 2008: Aerosol and cloud effects on solar brightening and the recent rapid warming. *Geophys. Res. Lett.*, **35**, L12708.

Russell, C., J. Luhmann, and L. Jian, 2010: How unprecedented a solar minimum? *Rev. Geophys.*, **48**, RG2004.

Rypdal, K., N. Rive, T. Berntsen, Z. Klimont, T. Mideksa, G. Myhre, and R. Skeie, 2009: Costs and global impacts of black carbon abatement strategies. *Tellus B.*, **61**, 625–641.

Rypdal, K., et al., 2005: Tropospheric ozone and aerosols in climate agreements: Scientific and political challenges. *Environ. Sci. Policy*, **8**, 29–43.

Salby, M. L., E. A. Titova, and L. Deschamps, 2012: Changes of the Antarctic ozone hole: Controlling mechanisms, seasonal predictability, and evolution. *J. Geophys. Res. Atmos.*, **117**, D10111.

Sarofim, M., 2012: The GTP of methane: Modeling analysis of temperature impacts of methane and carbon dioxide reductions. *Environ. Model. Assess.*, **17**, 231–239.

Sato, M., J. E. Hansen, M. P. McCormick, and J. B. Pollack, 1993: Stratospheric aerosol optical depths, 1850–1990. *J. Geophys. Res. Atmos.*, **98**, 22987–22994.

Schaaf, C., et al., 2002: First operational BRDF, albedo nadir reflectance products from MODIS. *Remote Sens. Environ.*, **83**, 135–148.

Schmalensee, R., 1993: Comparing greenhouse gases for policy purposes. *Energy J.*, **14**, 245–256.

Schmidt, A., K. S. Carslaw, G. W. Mann, M. Wilson, T. J. Breider, S. J. Pickering, and T. Thordarson, 2010: The impact of the 1783–1784 AD Laki eruption on global aerosol formation processes and cloud condensation nuclei. *Atmos. Chem. Phys.*, **10**, 6025–6041.

Schmidt, A., et al., 2012: Importance of tropospheric volcanic aerosol for indirect radiative forcing of climate. *Atmos. Chem. Phys.*, **12**, 7321–7339.

Schmidt, G., et al., 2011: Climate forcing reconstructions for use in PMIP simulations of the last millennium (v1.0). *Geosci. Model Dev.*, **4**, 33–45.

Schneider, D. P., C. M. Ammann, B. L. Otto-Bliesner, and D. S. Kaufman, 2009: Climate response to large, high-latitude and low-latitude volcanic eruptions in the Community Climate System Model. *J. Geophys. Res. Atmos.*, **114**, D15101.

Schultz, M. G., et al., 2008: Global wildland fire emissions from 1960 to 2000. *Global Biogeochem. Cycles*, **22**, Gb2002.

Seinfeld, J. H., and S. N. Pandis, 2006: *Atmospheric Chemistry and Physics: From Air Pollution to Climate Change.* John Wiley & Sons, Hoboken, NJ, USA.

Self, S., and S. Blake, 2008: Consequences of explosive supereruptions. *Elements*, **4**, 41–46.

Sharma, S., D. Lavoue, H. Cachier, L. Barrie, and S. Gong, 2004: Long-term trends of the black carbon concentrations in the Canadian Arctic. *J. Geophys. Res. Atmos.*, **109**, D15203.

Shibata, K., and K. Kodera, 2005: Simulation of radiative and dynamical responses of the middle atmosphere to the 11-year solar cycle. *J. Atmos. Sol. Terres. Phys.*, **67**, 125–143.

Shindell, D., and G. Faluvegi, 2009: Climate response to regional radiative forcing during the twentieth century. *Nature Geosci.*, **2**, 294–300.

Shindell, D., and G. Faluvegi, 2010: The net climate impact of coal-fired power plant emissions. *Atmos. Chem. Phys.*, **10**, 3247–3260.

Shindell, D., G. Schmidt, M. Mann, D. Rind, and A. Waple, 2001: Solar forcing of regional climate change during the maunder minimum. *Science*, **294**, 2149–2152.

Shindell, D., G. Faluvegi, A. Lacis, J. Hansen, R. Ruedy, and E. Aguilar, 2006a: Role of tropospheric ozone increases in 20th-century climate change. *J. Geophys. Res. Atmos.*, **111**, D08302.

Shindell, D., G. Faluvegi, R. Miller, G. Schmidt, J. Hansen, and S. Sun, 2006b: Solar and anthropogenic forcing of tropical hydrology. *Geophys. Res. Lett.*, **33**, L24706.

Shindell, D., M. Schulz, Y. Ming, T. Takemura, G. Faluvegi, and V. Ramaswamy, 2010: Spatial scales of climate response to inhomogeneous radiative forcing. *J. Geophys. Res. Atmos.*, **115**, D19110.

Shindell, D., et al., 2008: Climate forcing and air quality change due to regional emissions reductions by economic sector. *Atmos. Chem. Phys.*, **8**, 7101–7113.

Shindell, D., et al., 2011: Climate, health, agricultural and economic impacts of tighter vehicle-emission standards. *Nature Clim. Change*, **1**, 59–66.

Shindell, D., et al., 2013a: Attribution of historical ozone forcing to anthropogenic emissions. *Nature Clim. Change*, **3**, 567-570.

Shindell, D., et al., 2012a: Simultaneously mitigating near-term climate change and improving human health and food Security. *Science*, **335**, 183–189.

Shindell, D. T., 2012: Evaluation of the absolute regional temperature potential. *Atmos. Chem. Phys.*, **12**, 7955–7960.

Shindell, D. T., A. Voulgarakis, G. Faluvegi, and G. Milly, 2012b: Precipitation response to regional radiative forcing. *Atmos. Chem. Phys.*, **12**, 6969–6982.

Shindell, D. T., G. Faluvegi, D. M. Koch, G. A. Schmidt, N. Unger, and S. E. Bauer, 2009: Improved attribution of climate forcing to emissions. *Science*, **326**, 716–718.

Shindell, D. T., et al., 2006c: Simulations of preindustrial, present-day, and 2100 conditions in the NASA GISS composition and climate model G-PUCCINI. *Atmos. Chem. Phys.*, **6**, 4427–4459.

Shindell, D. T., et al., 2013b: Interactive ozone and methane chemistry in GISS-E2 historical and future climate simulations. *Atmos. Chem. Phys.*, **13**, 2653–2689.

Shindell, D. T., et al., 2013c: Radiative forcing in the ACCMIP historical and future climate simulations. *Atmos. Chem. Phys.*, **13**, 2939–2974.

Shine, K., 2009: The global warming potential-the need for an interdisciplinary retrial. *Clim. Change*, **96**, 467–472.

Shine, K., J. Cook, E. Highwood, and M. Joshi, 2003: An alternative to radiative forcing for estimating the relative importance of climate change mechanisms. *Geophys. Res. Lett.*, **30**, 2047.

Shine, K., J. Fuglestvedt, K. Hailemariam, and N. Stuber, 2005a: Alternatives to the global warming potential for comparing climate impacts of emissions of greenhouse gases. *Clim. Change*, **68**, 281–302.
Shine, K., T. Berntsen, J. Fuglestvedt, and R. Sausen, 2005b: Scientific issues in the design of metrics for inclusion of oxides of nitrogen in global climate agreements. *Proc. Natl. Acad. Sci. U.S.A.*, **102**, 15768–15773.
Shine, K., T. Berntsen, J. Fuglestvedt, R. Skeie, and N. Stuber, 2007: Comparing the climate effect of emissions of short- and long-lived climate agents. *Philos. Trans. R. Soc. A,* **365**, 1903–1914.
Shine, K. P., I. V. Ptashnik, and G. Raedel, 2012: The water vapour continuum: Brief history and recent developments. *Surv. Geophys.*, **33**, 535–555.
Siddaway, J. M., and S. V. Petelina, 2011: Transport and evolution of the 2009 Australian Black Saturday bushfire smoke in the lower stratosphere observed by OSIRIS on Odin. *J. Geophys. Res. Atmos.*, **116**, D06203.
Sitch, S., P. M. Cox, W. J. Collins, and C. Huntingford, 2007: Indirect radiative forcing of climate change through ozone effects on the land-carbon sink. *Nature*, **448**, 791–794.
Skeie, R., T. Berntsen, G. Myhre, K. Tanaka, M. Kvalevag, and C. Hoyle, 2011a: Anthropogenic radiative forcing time series from pre-industrial times until 2010. *Atmos. Chem. Phys.*, **11**, 11827–11857.
Skeie, R., T. Berntsen, G. Myhre, C. Pedersen, J. Strom, S. Gerland, and J. Ogren, 2011b: Black carbon in the atmosphere and snow, from pre-industrial times until present. *Atmos. Chem. Phys.*, **11**, 6809–6836.
Skeie, R. B., J. Fuglestvedt, T. Berntsen, M. T. Lund, G. Myhre, and K. Rypdal, 2009: Global temperature change from the transport sectors: Historical development and future scenarios. *Atmos. Environ.*, **43**, 6260–6270.
Smith, E., and A. Balogh, 2008: Decrease in heliospheric magnetic flux in this solar minimum: Recent Ulysses magnetic field observations. *Geophys. Res. Lett.*, **35**, L22103.
Smith, S., and M. Wigley, 2000: Global warming potentials: 1. Climatic implications of emissions reductions. *Clim. Change*, **44**, 445–457.
Smith, S., J. Karas, J. Edmonds, J. Eom, and A. Mizrahi, 2013: Sensitivity of multi-gas climate policy to emission metrics. *Clim. Change*, **117**, 663–675.
Smith, S. M., J. A. Lowe, N. H. A. Bowerman, L. K. Gohar, C. Huntingford, and M. R. Allen, 2012: Equivalence of greenhouse-gas emissions for peak temperature limits. *Nature Clim. Change*, **2**, 535–538.
Snow-Kropla, E., J. Pierce, D. Westervelt, and W. Trivitayanurak, 2011: Cosmic rays, aerosol formation and cloud-condensation nuclei: Sensitivities to model uncertainties. *Atmos. Chem. Phys.*, **11**, 4001–4013.
Solanki, S., and N. Krivova, 2004: Solar irradiance variations: From current measurements to long-term estimates. *Sol. Phys.*, **224**, 197–208.
Solomon, S., 1999: Stratospheric ozone depletion: A review of concepts and history. *Rev. Geophys.*, **37**, 275–316.
Solomon, S., J. S. Daniel, R. R. Neely, J. P. Vernier, E. G. Dutton, and L. W. Thomason, 2011: The persistently variable "background" stratospheric aerosol layer and global climate change. *Science*, **333**, 866–870.
Son, S. W., N. F. Tandon, L. M. Polvani, and D. W. Waugh, 2009: Ozone hole and Southern Hemisphere climate change. *Geophys. Res. Lett.*, **36**, L15705.
Soukharev, B., and L. Hood, 2006: Solar cycle variation of stratospheric ozone: Multiple regression analysis of long-term satellite data sets and comparisons with models. *J. Geophys. Res. Atmos.*, **111**, D20314.
Søvde, O., C. Hoyle, G. Myhre, and I. Isaksen, 2011: The HNO_3 forming branch of the HO_2 + NO reaction: Pre-industrial-to-present trends in atmospheric species and radiative forcings. *Atmos. Chem. Phys.*, **11**, 8929–8943.
Steinhilber, F., J. Beer, and C. Frohlich, 2009: Total solar irradiance during the Holocene. *Geophys. Res. Lett.*, **36**, L19704.
Stenchikov, G., A. Robock, V. Ramaswamy, M. D. Schwarzkopf, K. Hamilton, and S. Ramachandran, 2002: Arctic Oscillation response to the 1991 Mount Pinatubo eruption: Effects of volcanic aerosols and ozone depletion. *J. Geophys. Res. Atmos.*, **107**, 4803.
Stenchikov, G., T. L. Delworth, V. Ramaswamy, R. J. Stouffer, A. Wittenberg, and F. R. Zeng, 2009: Volcanic signals in oceans. *J. Geophys. Res. Atmos.*, **114**, D16104.
Stephens, G. L., N. B. Wood, and L. A. Pakula, 2004: On the radiative effects of dust on tropical convection. *Geophys. Res. Lett.*, **31**, L23112.
Stevenson, D., and R. Derwent, 2009: Does the location of aircraft nitrogen oxide emissions affect their climate impact? *Geophys. Res. Lett.*, **36**, L17810.
Stevenson, D. S., et al., 2013: Tropospheric ozone changes, radiative forcing and attribution to emissions in the Atmospheric Chemistry and Climate Model Intercomparison Project (ACCMIP). *Atmos. Chem. Phys.*, **13**, 3063–3085.
Stevenson, D. S., et al., 2006: Multimodel ensemble simulations of present-day and near-future tropospheric ozone. *J. Geophys. Res. Atmos.*, **111**, D08301.
Stiller, G. P., et al., 2012: Observed temporal evolution of global mean age of stratospheric air for the 2002 to 2010 period. *Atmos. Chem. Phys.*, **12**, 3311–3331.
Stothers, R. B., 2007: Three centuries of observation of stratospheric transparency. *Clim. Change*, **83**, 515–521.
Struthers, H., et al., 2011: The effect of sea ice loss on sea salt aerosol concentrations and the radiative balance in the Arctic. *Atmos. Chem. Phys.*, **11**, 3459–3477.
Swann, A. L. S., I. Y. Fung, and J. C. H. Chiang, 2012: Mid-latitude afforestation shifts general circulation and tropical precipitation. *Proc. Natl. Acad. Sci. U.S.A.*, **109**, 712–716.
Swingedouw, D., L. Terray, C. Cassou, A. Voldoire, D. Salas-Melia, and J. Servonnat, 2011: Natural forcing of climate during the last millennium: Fingerprint of solar variability. *Clim. Dyn.*, **36**, 1349–1364.
Takemura, T., 2012: Distributions and climate effects of atmospheric aerosols from the preindustrial era to 2100 along Representative Concentration Pathways (RCPs) simulated using the global aerosol model SPRINTARS. *Atmos. Chem. Phys.*, **12**, 11555–11572.
Tanaka, K., D. Johansson, B. O'Neill, and J. Fuglestvedt, 2013: Emission metrics under the 2°C climate stabilization. *Clim. Change Lett.* , **117**, 933-941.
Tanaka, K., B. O'Neill, D. Rokityanskiy, M. Obersteiner, and R. Tol, 2009: Evaluating Global Warming Potentials with historical temperature. *Clim. Change*, **96**, 443–466.
Taraborrelli, D., et al., 2012: Hydroxyl radical buffered by isoprene oxidation over tropical forests. *Nature Geosci.*, **5**, 190–193.
Taylor, P. C., R. G. Ellingson, and M. Cai, 2011: Seasonal variations of climate feedbacks in the NCAR CCSM3. *J. Clim.*, **24**, 3433–3444.
Textor, C., et al., 2006: Analysis and quantification of the diversities of aerosol life cycles within AeroCom. *Atmos. Chem. Phys.*, **6**, 1777–1813.
Thomason, L., and T. Peter, 2006: Assessment of Stratospheric Aerosol Properties (ASAP). *SPARC Reports*WCRP-124, WMO/TD- No. 1295, SPARC Report No. 4.
Thompson, D. W. J., S. Solomon, P. J. Kushner, M. H. England, K. M. Grise, and D. J. Karoly, 2011: Signatures of the Antarctic ozone hole in Southern Hemisphere surface climate change. *Nature Geosci.*, **4**, 741–749.
Thonicke, K., A. Spessa, I. C. Prentice, S. P. Harrison, L. Dong, and C. Carmona-Moreno, 2010: The influence of vegetation, fire spread and fire behaviour on biomass burning and trace gas emissions: Results from a process-based model. *Biogeosciences*, **7**, 1991–2011.
Tilmes, S., et al., 2012: Technical Note: Ozonesonde climatology between 1995 and 2011: Description, evaluation and applications. *Atmos. Chem. Phys.*, **12**, 7475–7497.
Timmreck, C., 2012: Modeling the climatic effects of large explosive volcanic eruptions. *Climate Change*, **3**, 545–564.
Timmreck, C., et al., 2010: Aerosol size confines climate response to volcanic super-eruptions. *Geophys. Res. Lett.*, **37**, L24705.
Tol, R., T. Berntsen, B. O'Neill, J. Fuglestvedt, and K. Shine, 2012: A unifying framework for metrics for aggregating the climate effect of different emissions. *Environ. Res. Lett.*, **7**, 044006.
Toon, O. B., A. Robock, and R. P. Turco, 2008: Environmental consequences of nuclear war. *Physics Today*, **61**, 37–42.
Trenberth, K. E., and A. Dai, 2007: Effects of Mount Pinatubo volcanic eruption on the hydrological cycle as an analog of geoengineering. *Geophys. Res. Lett.*, **34**, L15702.
Tsigaridis, K., and M. Kanakidou, 2007: Secondary organic aerosol importance in the future atmosphere. *Atmos. Environ.*, **41**, 4682–4692.
UNEP, 2011: Near-term Climate Protection and Clean Air Benefits: Actions for Controlling Short-Lived Climate Forcers. United Nations Environment Programme (UNEP), 78 pp.
Unger, N., T. C. Bond, J. S. Wang, D. M. Koch, S. Menon, D. T. Shindell, and S. Bauer, 2010: Attribution of climate forcing to economic sectors. *Proc. Natl. Acad. Sci. U.S.A.*, **107**, 3382–3387.
van der Molen, M. K., B. J. J. M. van den Hurk, and W. Hazeleger, 2011: A dampened land use change climate response towards the tropics. *Clim. Dyn.*, **37**, 2035–2043.
van der Werf, G. R., et al., 2010: Global fire emissions and the contribution of deforestation, savanna, forest, agricultural, and peat fires (1997–2009). *Atmos. Chem. Phys.*, **10**, 11707–11735.

van Vuuren, D., J. Edmonds, M. Kainuma, K. Riahi, and J. Weyant, 2011: A special issue on the RCPs. *Clim. Change*, **109**, 1–4.

Van Vuuren, D. P., et al., 2008: Temperature increase of 21st century mitigation scenarios. *Proc. Natl. Acad. Sci. U.S.A.*, **105**, 15258–15262.

Vasekova, E., E. Drage, K. Smith, and N. Mason, 2006: FTIR spectroscopy and radiative forcing of octafluorocyclobutane and octofluorocyclopentene. *J. Quant. Spectrosc. Radiat. Transfer*, **102**, 418–424.

Velders, G. J. M., D. W. Fahey, J. S. Daniel, M. McFarland, and S. O. Andersen, 2009: The large contribution of projected HFC emissions to future climate forcing. *Proc. Natl. Acad. Sci. U.S.A.*, **106**, 10949–10954.

Vernier, J. P., L. W. Thomason, T. D. Fairlie, P. Minnis, R. Palikonda, and K. M. Bedka, 2013: Comment on "Large Volcanic Aerosol Load in the Stratosphere Linked to Asian Monsoon Transport". *Science*, **339**, 647-d.

Vernier, J. P., et al., 2011: Major influence of tropical volcanic eruptions on the stratospheric aerosol layer during the last decade. *Geophys. Res. Lett.*, **38**, L12807.

Vial, J., J.-L. Dufresne, and S. Bony, 2013: On the interpretation of inter-model spread in CMIP5 climate sensitivity estimates. *Clim. Dyn.*, doi:10.1007/s00382-013-1725-9, in press.

Volz, A., and D. Kley, 1988: Evaluation of the Montsouris Series of ozone measurements made in the 19th century. *Nature*, **332**, 240–242.

Voulgarakis, A., and D. T. Shindell, 2010: Constraining the sensitivity of regional climate with the use of historical observations. *J. Clim.*, **23**, 6068–6073.

Voulgarakis, A., et al., 2013: Analysis of present day and future OH and methane lifetime in the ACCMIP simulations. *Atmos. Chem. Phys.*, **13**, 2563–2587.

Wang, C., D. Kim, A. Ekman, M. Barth, and P. Rasch, 2009: Impact of anthropogenic aerosols on Indian summer monsoon. *Geophys. Res. Lett.*, **36**, L21704.

Wang, M., and J. E. Penner, 2009: Aerosol indirect forcing in a global model with particle nucleation. *Atmos. Chem. Phys.*, **9**, 239–260.

Wang, X., S. J. Doherty, and J. Huang, 2013: Black carbon and other light-absorbing impurities in snow across Northern China. *J. Geophys. Res. Atmos.*, **118**, 1471–1492.

Wang, Y., J. Lean, and N. Sheeley, 2005: Modeling the sun's magnetic field and irradiance since 1713. *Astrophys. J.*, **625**, 522–538.

Warren, S., and W. Wiscombe, 1980: A model for the spectral albedo of snow. 2. Snow containing atmospheric aerosols. *J. Atmos. Sci.*, **37**, 2734–2745.

Weiss, R., J. Muhle, P. Salameh, and C. Harth, 2008: Nitrogen trifluoride in the global atmosphere. *Geophys. Res. Lett.*, **35**, L20821.

Wenzler, T., S. Solanki, and N. Krivova, 2009: Reconstructed and measured total solar irradiance: Is there a secular trend between 1978 and 2003? *Geophys. Res. Lett.*, **36**, L11102.

Wilcox, L., K. Shine, and B. Hoskins, 2012: Radiative forcing due to aviation water vapour emissions. *Atmos. Environ.*, **63**, 1–13.

Wild, M., 2009: How well do IPCC-AR4/CMIP3 climate models simulate global dimming/brightening and twentieth-century daytime and nighttime warming? *J. Geophys. Res. Atmos.*, **114**, D00D11.

Wild, O., 2007: Modelling the global tropospheric ozone budget: Exploring the variability in current models. *Atmos. Chem. Phys.*, **7**, 2643–2660.

Wild, O., and P. I. Palmer, 2008: How sensitive is tropospheric oxidation to anthropogenic emissions? *Geophys. Res. Lett.*, **35**, L22802.

Wild, O., M. Prather, and H. Akimoto, 2001: Indirect long-term global radiative cooling from NOx emissions. *Geophys. Res. Lett.*, **28**, 1719–1722.

Williams, K. D., A. Jones, D. L. Roberts, C. A. Senior, and M. J. Woodage, 2001: The response of the climate system to the indirect effects of anthropogenic sulfate aerosol. *Clim. Dyn.*, **17**, 845–856.

Willson, R., and A. Mordvinov, 2003: Secular total solar irradiance trend during solar cycles 21–23. *Geophys. Res. Lett.*, **30**, 1199.

WMO, 1999: *Scientific Assessment of Ozone Depletion: 1998*. Global Ozone Research and Monitoring Project. Report No. 44.World Meteorological Organization, Geneva, Switzerland.

WMO, 2011: *Scientific Assessment of Ozone Depletion: 2010*. Global Ozone Research and Monitoring Project-Report. World Meteorological Organisation, Geneva, Switzerland, 516 pp.

Worden, H., K. Bowman, S. Kulawik, and A. Aghedo, 2011: Sensitivity of outgoing longwave radiative flux to the global vertical distribution of ozone characterized by instantaneous radiative kernels from Aura-TES. *J. Geophys. Res. Atmos.*, **116**, D14115.

Worden, H., K. Bowman, J. Worden, A. Eldering, and R. Beer, 2008: Satellite measurements of the clear-sky greenhouse effect from tropospheric ozone. *Nature Geosci.*, **1**, 305–308.

Wright, J., 2004: Do we know of any Maunder minimum stars? *Astron. J.*, **128**, 1273–1278.

Wu, S. L., L. J. Mickley, D. J. Jacob, J. A. Logan, R. M. Yantosca, and D. Rind, 2007: Why are there large differences between models in global budgets of tropospheric ozone? *J. Geophys. Res. Atmos.*, **112**, D05302.

Xia, L. L., and A. Robock, 2013: Impacts of a nuclear war in South Asia on rice production in Mainland China. *Clim. Change*, **116**, 357–372.

Ye, H., R. Zhang, J. Shi, J. Huang, S. G. Warren, and Q. Fu, 2012: Black carbon in seasonal snow across northern Xinjiang in northwestern China. *Environ. Res. Lett.*, **7**, 044002.

Young, P. J., et al., 2013: Pre-industrial to end 21st century projections of tropospheric ozone from the Atmospheric Chemistry and Climate Model Intercomparison Project (ACCMIP). *Atmos. Chem. Phys.*, **13**, 2063–2090.

Zanchettin, D., et al., 2012: Bi-decadal variability excited in the coupled ocean-atmosphere system by strong tropical volcanic eruptions. *Clim. Dyn.*, **39**, 419–444.

Zarzycki, C. M., and T. C. Bond, 2010: How much can the vertical distribution of black carbon affect its global direct radiative forcing? *Geophys. Res. Lett.*, **37**, L20807.

Zeng, G., J. A. Pyle, and P. J. Young, 2008: Impact of climate change on tropospheric ozone and its global budgets. *Atmos. Chem. Phys.*, **8**, 369–387.

Zeng, G., O. Morgenstern, P. Braesicke, and J. A. Pyle, 2010: Impact of stratospheric ozone recovery on tropospheric ozone and its budget. *Geophys. Res. Lett.*, **37**, L09805.

Zhang, H., G. Y. Shi, and Y. Liu, 2005: A comparison between the two line-by-line integration algorithms. *Chin. J. Atmos. Sci.*, **29**, 581–593.

Zhang, H., G. Shi, and Y. Liu, 2008: The effects of line-wing cutoff in LBL integration on radiation calculations. *Acta Meteorol. Sin.*, **22**, 248–255.

Zhang, H., J. Wu, and P. Luc, 2011: A study of the radiative forcing and global warming potentials of hydrofluorocarbons. *J. Quant. Spectrosc. Radiat. Transfer*, **112**, 220–229.

Zhang, X. B., et al., 2007: Detection of human influence on twentieth-century precipitation trends. *Nature*, **448**, 461–465.

Zhong, Y., G. H. Miller, B. L. Otto-Bliesner, M. M. Holland, D. A. Bailey, D. P. Schneider, and A. Geirsdottir, 2011: Centennial-scale climate change from decadally-paced explosive volcanism: A coupled sea ice-ocean mechanism. *Clim. Dyn.*, **37**, 2373–2387.

Ziemke, J. R., S. Chandra, G. J. Labow, P. K. Bhartia, L. Froidevaux, and J. C. Witte, 2011: A global climatology of tropospheric and stratospheric ozone derived from Aura OMI and MLS measurements. *Atmos. Chem. Phys.*, **11**, 9237–9251.

Appendix 8.A: Lifetimes, Radiative Efficiencies and Metric Values

Table 8.A.1 | Radiative efficiencies (REs), lifetimes/adjustment times, AGWP and GWP values for 20 and 100 years, and AGTP and GTP values for 20, 50 and 100 years. Climate–carbon feedbacks are included for CO_2 while no climate feedbacks are included for the other components (see discussion in Sections 8.7.1.4 and 8.7.2.1, Supplementary Material and notes below the table; Supplementary Material Table 8.SM.16 gives analogous values including climate–carbon feedbacks for non-CO_2 emissions). For a complete list of chemical names and CAS numbers, and for accurate replications of metric values, see Supplementary Material Section 8.SM.13 and references therein.

Acronym, Common Name or Chemical Name	Chemical Formula	Lifetime (Years)	Radiative Efficiency ($W\ m^{-2}\ ppb^{-1}$)	AGWP 20-year ($W\ m^{-2}\ yr\ kg^{-1}$)	**GWP 20-year**	AGWP 100-year ($W\ m^{-2}\ yr\ kg^{-1}$)	**GWP 100-year**	AGTP 20-year ($K\ kg^{-1}$)	**GTP 20-year**	AGTP 50-year ($K\ kg^{-1}$)	**GTP 50-year**	AGTP 100-year ($K\ kg^{-1}$)	**GTP 100-year**
Carbon dioxide	CO_2	see*	1.37e-5	2.49e-14	**1**	9.17e-14	**1**	6.84e-16	**1**	6.17e-16	**1**	5.47e-16	**1**
Methane	CH_4	12.4†	3.63e-4	2.09e-12	**84**	2.61e-12	**28**	4.62e-14	**67**	8.69e-15	**14**	2.34e-15	**4**
Fossil methane‡	CH_4	12.4†	3.63e-4	2.11e-12	**85**	2.73e-12	**30**	4.68e-14	**68**	9.55e-15	**15**	3.11e-15	**6**
Nitrous Oxide	N_2O	121†	3.00e-3	6.58e-12	**264**	2.43e-11	**265**	1.89e-13	**277**	1.74e-13	**282**	1.28e-13	**234**
Chlorofluorocarbons													
CFC-11	CCl_3F	45.0	0.26	1.72e-10	**6900**	4.28e-10	**4660**	4.71e-12	**6890**	3.01e-12	**4890**	1.28e-12	**2340**
CFC-12	CCl_2F_2	100.0	0.32	2.69e-10	**10,800**	9.39e-10	**10,200**	7.71e-12	**11,300**	6.75e-12	**11,000**	4.62e-12	**8450**
CFC-13	$CClF_3$	640.0	0.25	2.71e-10	**10,900**	1.27e-09	**13,900**	7.99e-12	**11,700**	8.77e-12	**14,200**	8.71e-12	**15,900**
CFC-113	CCl_2FCClF_2	85.0	0.30	1.62e-10	**6490**	5.34e-10	**5820**	4.60e-12	**6730**	3.85e-12	**6250**	2.45e-12	**4470**
CFC-114	$CClF_2CClF_2$	190.0	0.31	1.92e-10	**7710**	7.88e-10	**8590**	5.60e-12	**8190**	5.56e-12	**9020**	4.68e-12	**8550**
CFC-115	$CClF_2CF_3$	1,020.0	0.20	1.46e-10	**5860**	7.03e-10	**7670**	4.32e-12	**6310**	4.81e-12	**7810**	4.91e-12	**8980**
Hydrochlorofluorocarbons													
HCFC-21	$CHCl_2F$	1.7	0.15	1.35e-11	**543**	1.35e-11	**148**	1.31e-13	**192**	1.59e-14	**26**	1.12e-14	**20**
HCFC-22	$CHClF_2$	11.9	0.21	1.32e-10	**5280**	1.62e-10	**1760**	2.87e-12	**4200**	5.13e-13	**832**	1.43e-13	**262**
HCFC-122	$CHCl_2CF_2Cl$	1.0	0.17	5.43e-12	**218**	5.43e-12	**59**	4.81e-14	**70**	6.25e-15	**10**	4.47e-15	**8**
HCFC-122a	$CHFClCFCl_2$	3.4	0.21	2.36e-11	**945**	2.37e-11	**258**	2.91e-13	**426**	2.99e-14	**48**	1.96e-14	**36**
HCFC-123	$CHCl_2CF_3$	1.3	0.15	7.28e-12	**292**	7.28e-12	**79**	6.71e-14	**98**	8.45e-15	**14**	6.00e-15	**11**
HCFC-123a	$CHClFCF_2Cl$	4.0	0.23	3.37e-11	**1350**	3.39e-11	**370**	4.51e-13	**659**	4.44e-14	**72**	2.81e-14	**51**
HCFC-124	$CHClFCF_3$	5.9	0.20	4.67e-11	**1870**	4.83e-11	**527**	7.63e-13	**1120**	7.46e-14	**121**	4.03e-14	**74**
HCFC-132c	CH_2FCFCl_2	4.3	0.17	3.07e-11	**1230**	3.10e-11	**338**	4.27e-13	**624**	4.14e-14	**67**	2.58e-14	**47**
HCFC-141b	CH_3CCl_2F	9.2	0.16	6.36e-11	**2550**	7.17e-11	**782**	1.27e-12	**1850**	1.67e-13	**271**	6.09e-14	**111**
HCFC-142b	CH_3CClF_2	17.2	0.19	1.25e-10	**5020**	1.82e-10	**1980**	3.01e-12	**4390**	8.46e-13	**1370**	1.95e-13	**356**
HCFC-225ca	$CHCl_2CF_2CF_3$	1.9	0.22	1.17e-11	**469**	1.17e-11	**127**	1.17e-13	**170**	1.38e-14	**22**	9.65e-15	**18**
HCFC-225cb	$CHClFCF_2CClF_2$	5.9	0.29	4.65e-11	**1860**	4.81e-11	**525**	7.61e-13	**1110**	7.43e-14	**120**	4.01e-14	**73**
(E)-1-Chloro-3,3,3-trifluoroprop-1-ene	trans-$CF_3CH{=}CHCl$	26.0 days	0.04	1.37e-13	**5**	1.37e-13	**1**	1.09e-15	**2**	1.54e-16	**<1**	1.12e-16	**<1**

(continued on next page)

Table 8.A.1 (continued)

Acronym, Common Name or Chemical Name	Chemical Formula	Lifetime (Years)	Radiative Efficiency (W m^{-2} ppb^{-1})	AGWP 20-year (W m^{-2} yr kg^{-1})	**GWP 20-year**	AGWP 100-year (W m^{-2} yr kg^{-1})	**GWP 100-year**	AGTP 20-year (K kg^{-1})	**GTP 20-year**	AGTP 50-year (K kg^{-1})	**GTP 50-year**	AGTP 100-year (K kg^{-1})	**GTP 100-year**
Hydrofluorocarbons													
HFC-23	CHF_3	222.0	0.18	2.70e-10	**10,800**	1.14e-09	**12,400**	7.88e-12	**11,500**	7.99e-12	**13,000**	6.95e-12	**12,700**
HFC-32	CH_2F_2	5.2	0.11	6.07e-11	**2430**	6.21e-11	**677**	9.32e-13	**1360**	8.93e-14	**145**	5.17e-14	**94**
HFC-41	CH_3F	2.8	0.02	1.07e-11	**427**	1.07e-11	**116**	1.21e-13	**177**	1.31e-14	**21**	8.82e-15	**16**
HFC-125	CHF_2CF_3	28.2	0.23	1.52e-10	**6090**	2.91e-10	**3170**	3.97e-12	**5800**	1.84e-12	**2980**	5.29e-13	**967**
HFC-134	CHF_2CHF_2	9.7	0.19	8.93e-11	**3580**	1.02e-10	**1120**	1.82e-12	**2660**	2.54e-13	**412**	8.73e-14	**160**
HFC-134a	CH_2FCF_3	13.4	0.16	9.26e-11	**3710**	1.19e-10	**1300**	2.09e-12	**3050**	4.33e-13	**703**	1.10e-13	**201**
HFC-143	CH_2FCHF_2	3.5	0.13	3.00e-11	**1200**	3.01e-11	**328**	3.76e-13	**549**	3.82e-14	**62**	2.49e-14	**46**
HFC-143a	CH_3CF_3	47.1	0.16	1.73e-10	**6940**	4.41e-10	**4800**	4.76e-12	**6960**	3.12e-12	**5060**	1.37e-12	**2500**
HFC-152	CH_2FCH_2F	0.4	0.04	1.51e-12	**60**	1.51e-12	**16**	1.25e-14	**18**	1.71e-15	**3**	1.24e-15	**2**
HFC-152a	CH_3CHF_2	1.5	0.10	1.26e-11	**506**	1.26e-11	**138**	1.19e-13	**174**	1.47e-14	**24**	1.04e-14	**19**
HFC-161	CH_3CH_2F	66.0 days	0.02	3.33e-13	**13**	3.33e-13	**4**	2.70e-15	**4**	3.76e-16	**<1**	2.74e-16	**<1**
HFC-227ca	$CF_3CF_2CHF_2$	28.2	0.27	1.27e-10	**5080**	2.42e-10	**2640**	3.31e-12	**4830**	1.53e-12	**2480**	4.41e-13	**806**
HFC-227ea	CF_3CHFCF_3	38.9	0.26	1.34e-10	**5360**	3.07e-10	**3350**	3.61e-12	**5280**	2.12e-12	**3440**	7.98e-13	**1460**
HFC-236cb	$CH_2FCF_2CF_3$	13.1	0.23	8.67e-11	**3480**	1.11e-10	**1210**	1.94e-12	**2840**	3.92e-13	**636**	1.01e-13	**185**
HFC-236ea	CHF_2CHFCF_3	11.0	0.30[a]	1.03e-10	**4110**	1.22e-10	**1330**	2.18e-12	**3190**	3.53e-13	**573**	1.06e-13	**195**
HFC-236fa	$CF_3CH_2CF_3$	242.0	0.24	1.73e-10	**6940**	7.39e-10	**8060**	5.06e-12	**7400**	5.18e-12	**8400**	4.58e-12	**8380**
HFC-245ca	$CH_2FCF_2CHF_2$	6.5	0.24[b]	6.26e-11	**2510**	6.56e-11	**716**	1.07e-12	**1570**	1.09e-13	**176**	5.49e-14	**100**
HFC-245cb	$CF_3CF_2CH_3$	47.1	0.24	1.67e-10	**6680**	4.24e-10	**4620**	4.58e-12	**6690**	3.00e-12	**4870**	1.32e-12	**2410**
HFC-245ea	$CHF_2CHFCHF_2$	3.2	0.16[c]	2.15e-11	**863**	2.16e-11	**235**	2.59e-13	**378**	2.70e-14	**44**	1.79e-14	**33**
HFC-245eb	$CH_2FCHFCF_3$	3.1	0.20[c]	2.66e-11	**1070**	2.66e-11	**290**	3.15e-13	**460**	3.31e-14	**54**	2.20e-14	**40**
HFC-245fa	$CHF_2CH_2CF_3$	7.7	0.24	7.29e-11	**2920**	7.87e-11	**858**	1.35e-12	**1970**	1.51e-13	**245**	6.62e-14	**121**
HFC-263fb	$CH_3CH_2CF_3$	1.2	0.10[c]	6.93e-12	**278**	6.93e-12	**76**	6.31e-14	**92**	8.02e-15	**13**	5.70e-15	**10**
HFC-272ca	$CH_3CF_2CH_3$	2.6	0.07	1.32e-11	**530**	1.32e-11	**144**	1.46e-13	**213**	1.61e-14	**26**	1.09e-14	**20**
HFC-329p	$CHF_2CF_2CF_2CF_3$	28.4	0.31	1.13e-10	**4510**	2.16e-10	**2360**	2.94e-12	**4290**	1.37e-12	**2220**	3.96e-13	**725**
HFC-365mfc	$CH_3CF_2CH_2CF_3$	8.7	0.22	6.64e-11	**2660**	7.38e-11	**804**	1.30e-12	**1890**	1.62e-13	**262**	6.24e-14	**114**
HFC-43-10mee	$CF_3CHFCHFCF_2CF_3$	16.1	0.42[b]	1.08e-10	**4310**	1.51e-10	**1650**	2.54e-12	**3720**	6.62e-13	**1070**	1.54e-13	**281**
HFC-1132a	$CH_2{=}CF_2$	4.0 days	0.004[d]	3.87e-15	**<1**	3.87e-15	**<1**	3.08e-17	**<1**	4.35e-18	**<1**	3.18e-18	**<1**
HFC-1141	$CH_2{=}CHF$	2.1 days	0.002[d]	1.54e-15	**<1**	1.54e-15	**<1**	1.23e-17	**<1**	1.73e-18	**<1**	1.27e-18	**<1**
(Z)-HFC-1225ye	$CF_3CF{=}CHF(Z)$	8.5 days	0.02	2.14e-14	**<1**	2.14e-14	**<1**	1.70e-16	**<1**	2.40e-17	**<1**	1.76e-17	**<1**
(E)-HFC-1225ye	$CF_3CF{=}CHF(E)$	4.9 days	0.01	7.25e-15	**<1**	7.25e-15	**<1**	5.77e-17	**<1**	8.14e-18	**<1**	5.95e-18	**<1**
(Z)-HFC-1234ze	$CF_3CH{=}CHF(Z)$	10.0 days	0.02	2.61e-14	**1**	2.61e-14	**<1**	2.08e-16	**<1**	2.93e-17	**<1**	2.14e-17	**<1**
HFC-1234yf	$CF_3CF{=}CH_2$	10.5 days	0.02	3.22e-14	**1**	3.22e-14	**<1**	2.57e-16	**<1**	3.62e-17	**<1**	2.65e-17	**<1**
(E)-HFC-1234ze	trans-$CF_3CH{=}CHF$	16.4 days	0.04	8.74e-14	**4**	8.74e-14	**<1**	6.98e-16	**<1**	9.82e-17	**<1**	7.18e-17	**<1**
(Z)-HFC-1336	$CF_3CH{=}CHCF_3(Z)$	22.0 days	0.07[d]	1.54e-13	**6**	1.54e-13	**2**	1.23e-15	**2**	1.73e-16	**<1**	1.26e-16	**<1**

(continued on next page)

Table 8.A.1 (continued)

Acronym, Common Name or Chemical Name	Chemical Formula	Lifetime (Years)	Radiative Efficiency (W m^{-2} ppb^{-1})	AGWP 20-year (W m^{-2} yr kg^{-1})	**GWP 20-year**	AGWP 100-year (W m^{-2} yr kg^{-1})	**GWP 100-year**	AGTP 20-year (K kg^{-1})	**GTP 20-year**	AGTP 50-year (K kg^{-1})	**GTP 50-year**	AGTP 100-year (K kg^{-1})	**GTP 100-year**
HFC-1243zf	$CF_3CH{=}CH_2$	7.0 days	0.01	1.37e-14	**1**	1.37e-14	**<1**	1.09e-16	**<1**	1.53e-17	**<1**	1.12e-17	**<1**
HFC-1345zfc	$C_2F_5CH{=}CH_2$	7.6 days	0.01	1.15e-14	**<1**	1.15e-14	**<1**	9.19e-17	**<1**	1.30e-17	**<1**	9.48e-18	**<1**
3,3,4,4,5,5,6,6,6-Nonafluorohex-1-ene	$C_4F_9CH{=}CH_2$	7.6 days	0.03	1.25e-14	**<1**	1.25e-14	**<1**	9.92e-17	**<1**	1.40e-17	**<1**	1.02e-17	**<1**
3,3,4,4,5,5,6,6,7,7,8,8,8-Tridecafluorooct-1-ene	$C_6F_{13}CH{=}CH_2$	7.6 days	0.03	9.89e-15	**<1**	9.89e-15	**<1**	7.87e-17	**<1**	1.11e-17	**<1**	8.12e-18	**<1**
3,3,4,4,5,5,6,6,7,7,8,8,9,9,10,10,10-Heptadecafluorodec-1-ene	$C_8F_{17}CH{=}CH_2$	7.6 days	0.03	8.52e-15	**<1**	8.52e-15	**<1**	6.79e-17	**<1**	9.57e-18	**<1**	7.00e-18	**<1**
Chlorocarbons and Hydrochlorocarbons													
Methyl chloroform	CH_3CCl_3	5.0	0.07	1.44e-11	**578**	1.47e-11	**160**	2.17e-13	**317**	2.07e-14	**34**	1.22e-14	**22**
Carbon tetrachloride	CCl_4	26.0	0.17	8.69e-11	**3480**	1.59e-10	**1730**	2.24e-12	**3280**	9.68e-13	**1570**	2.62e-13	**479**
Methyl chloride	CH_3Cl	1.0	0.01[a]	1.12e-12	**45**	1.12e-12	**12**	9.93e-15	**15**	1.29e-15	**2**	9.20e-16	**2**
Methylene chloride	CH_2Cl_2	0.4	0.03[b]	8.18e-13	**33**	8.18e-13	**9**	6.78e-15	**10**	9.26e-16	**2**	6.72e-16	**1**
Chloroform	$CHCl_3$	0.4	0.08	1.50e-12	**60**	1.50e-12	**16**	1.25e-14	**18**	1.70e-15	**3**	1.24e-15	**2**
1,2-Dichloroethane	CH_2ClCH_2Cl	65.0 days	0.01	8.24e-14	**3**	8.24e-14	**<1**	6.67e-16	**<1**	9.29e-17	**<1**	6.77e-17	**<1**
Bromocarbons, Hydrobromocarbons and Halons													
Methyl bromide	CH_3Br	0.8	0.004	2.16e-13	**9**	2.16e-13	**2**	1.87e-15	**3**	2.47e-16	**<1**	1.78e-16	**<1**
Methylene bromide	CH_2Br_2	0.3	0.01	9.31e-14	**4**	9.31e-14	**1**	7.66e-16	**1**	1.05e-16	**<1**	7.65e-17	**<1**
Halon-1201	$CHBrF_2$	5.2	0.15	3.37e-11	**1350**	3.45e-11	**376**	5.17e-13	**756**	4.96e-14	**80**	2.87e-14	**52**
Halon-1202	CBr_2F_2	2.9	0.27	2.12e-11	**848**	2.12e-11	**231**	2.43e-13	**356**	2.61e-14	**42**	1.75e-14	**32**
Halon-1211	$CBrClF_2$	16.0	0.29	1.15e-10	**4590**	1.60e-10	**1750**	2.70e-12	**3950**	6.98e-13	**1130**	1.62e-13	**297**
Halon-1301	$CBrF_3$	65.0	0.30	1.95e-10	**7800**	5.77e-10	**6290**	5.46e-12	**7990**	4.16e-12	**6750**	2.28e-12	**4170**
Halon-2301	CH_2BrCF_3	3.4	0.14	1.59e-11	**635**	1.59e-11	**173**	1.96e-13	**286**	2.01e-14	**33**	1.32e-14	**24**
Halon-2311 / Halothane	$CHBrClCF_3$	1.0	0.13	3.77e-12	**151**	3.77e-12	**41**	3.35e-14	**49**	4.34e-15	**7**	3.10e-15	**6**
Halon-2401	$CHFBrCF_3$	2.9	0.19	1.68e-11	**674**	1.68e-11	**184**	1.94e-13	**283**	2.07e-14	**34**	1.39e-14	**25**
Halon-2402	$CBrF_2CBrF_2$	20.0	0.31	8.59e-11	**3440**	1.35e-10	**1470**	2.12e-12	**3100**	7.08e-13	**1150**	1.66e-13	**304**
Fully Fluorinated Species													
Nitrogen trifluoride	NF_3	500.0	0.20	3.19e-10	**12,800**	1.47e-09	**16,100**	9.39e-12	**13,700**	1.02e-11	**16,500**	9.91e-12	**18,100**
Sulphur hexafluoride	SF_6	3,200.0	0.57	4.37e-10	**17,500**	2.16e-09	**23,500**	1.29e-11	**18,900**	1.47e-11	**23,800**	1.54e-11	**28,200**
(Trifluoromethyl) sulphur pentafluoride	SF_5CF_3	800.0	0.59	3.36e-10	**13,500**	1.60e-09	**17,400**	9.93e-12	**14,500**	1.10e-11	**17,800**	1.11e-11	**20,200**
Sulphuryl fluoride	SO_2F_2	36.0	0.20	1.71e-10	**6840**	3.76e-10	**4090**	4.58e-12	**6690**	2.55e-12	**4140**	9.01e-13	**1650**
PFC-14	CF_4	50,000.0	0.09	1.22e-10	**4880**	6.08e-10	**6630**	3.61e-12	**5270**	4.12e-12	**6690**	4.40e-12	**8040**
PFC-116	C_2F_6	10,000.0	0.25	2.05e-10	**8210**	1.02e-09	**11,100**	6.07e-12	**8880**	6.93e-12	**11,200**	7.36e-12	**13,500**
PFC-c216	c-C_3F_6	3,000.0	0.23[e]	1.71e-10	**6850**	8.44e-10	**9200**	5.06e-12	**7400**	5.74e-12	**9310**	6.03e-12	**11,000**
PFC-218	C_3F_8	2,600.0	0.28	1.66e-10	**6640**	8.16e-10	**8900**	4.91e-12	**7180**	5.56e-12	**9010**	5.83e-12	**10,700**
PFC-318	c-C_4F_8	3,200.0	0.32	1.77e-10	**7110**	8.75e-10	**9540**	5.25e-12	**7680**	5.96e-12	**9660**	6.27e-12	**11,500**

(continued on next page)

Table 8.A.1 (continued)

Acronym, Common Name or Chemical Name	Chemical Formula	Lifetime (Years)	Radiative Efficiency ($W\ m^{-2}\ ppb^{-1}$)	AGWP 20-year ($W\ m^{-2}\ yr\ kg^{-1}$)	**GWP 20-year**	AGWP 100-year ($W\ m^{-2}\ yr\ kg^{-1}$)	**GWP 100-year**	AGTP 20-year ($K\ kg^{-1}$)	**GTP 20-year**	AGTP 50-year ($K\ kg^{-1}$)	**GTP 50-year**	AGTP 100-year ($K\ kg^{-1}$)	**GTP 100-year**
PFC-31-10	C_4F_{10}	2,600.0	0.36	1.71e-10	**6870**	8.44e-10	**9200**	5.08e-12	**7420**	5.75e-12	**9320**	6.02e-12	**11,000**
Perfluorocyclopentene	$c\text{-}C_5F_8$	31.0 days	0.08[f]	1.71e-13	**7**	1.71e-13	**2**	1.37e-15	**2**	1.92e-16	**<1**	1.40e-16	**<1**
PFC-41-12	$n\text{-}C_5F_{12}$	4,100.0	0.41	1.58e-10	**6350**	7.84e-10	**8550**	4.69e-12	**6860**	5.33e-12	**8650**	5.62e-12	**10,300**
PFC-51-14	$n\text{-}C_6F_{14}$	3,100.0	0.44	1.47e-10	**5890**	7.26e-10	**7910**	4.35e-12	**6370**	4.94e-12	**8010**	5.19e-12	**9490**
PFC-61-16	$n\text{-}C_7F_{16}$	3,000.0	0.50	1.45e-10	**5830**	7.17e-10	**7820**	4.31e-12	**6290**	4.88e-12	**7920**	5.13e-12	**9380**
PFC-71-18	C_8F_{18}	3,000.0	0.55	1.42e-10	**5680**	6.99e-10	**7620**	4.20e-12	**6130**	4.76e-12	**7710**	5.00e-12	**9140**
PFC-91-18	$C_{10}F_{18}$	2,000.0	0.55	1.34e-10	**5390**	6.59e-10	**7190**	3.98e-12	**5820**	4.49e-12	**7290**	4.68e-12	**8570**
Perfluorodecalin (cis)	$Z\text{-}C_{10}F_{18}$	2,000.0	0.56	1.35e-10	**5430**	6.64e-10	**7240**	4.01e-12	**5860**	4.52e-12	**7340**	4.72e-12	**8630**
Perfluorodecalin (trans)	$E\text{-}C_{10}F_{18}$	2,000.0	0.48	1.18e-10	**4720**	5.77e-10	**6290**	3.48e-12	**5090**	3.93e-12	**6380**	4.10e-12	**7500**
PFC-1114	$CF_2{=}CF_2$	1.1 days	0.002	2.68e-16	**<1**	2.68e-16	**<1**	2.13e-18	**<1**	3.00e-19	**<1**	2.20e-19	**<1**
PFC-1216	$CF_3CF{=}CF_2$	4.9 days	0.01	6.42e-15	**<1**	6.42e-15	**<1**	5.11e-17	**<1**	7.21e-18	**<1**	5.27e-18	**<1**
Perfluorobuta-1,3-diene	$CF_2{=}CFCF{=}CF_2$	1.1 days	0.003	3.29e-16	**<1**	3.29e-16	**<1**	2.61e-18	**<1**	3.69e-19	**<1**	2.70e-19	**<1**
Perfluorobut-1-ene	$CF_3CF_2CF{=}CF_2$	6.0 days	0.02	8.38e-15	**<1**	8.38e-15	**<1**	6.67e-17	**<1**	9.41e-18	**<1**	6.88e-18	**<1**
Perfluorobut-2-ene	$CF_3CF{=}CFCF_3$	31.0 days	0.07	1.62e-13	**6**	1.62e-13	**2**	1.30e-15	**2**	1.82e-16	**<1**	1.33e-16	**<1**
Halogenated Alcohols and Ethers													
HFE-125	CHF_2OCF_3	119.0	0.41	3.10e-10	**12,400**	1.14e-09	**12,400**	8.91e-12	**13,000**	8.14e-12	**13,200**	5.97e-12	**10,900**
HFE-134 (HG-00)	CHF_2OCHF_2	24.4	0.44	2.90e-10	**11,600**	5.10e-10	**5560**	7.42e-12	**10,800**	3.02e-12	**4900**	7.83e-13	**1430**
HFE-143a	CH_3OCF_3	4.8	0.18	4.72e-11	**1890**	4.80e-11	**523**	6.95e-13	**1020**	6.66e-14	**108**	3.99e-14	**73**
HFE-227ea	$CF_3CHFOCF_3$	51.6	0.44	2.22e-10	**8900**	5.92e-10	**6450**	6.15e-12	**8980**	4.22e-12	**6850**	1.98e-12	**3630**
HCFE-235ca2 (enflurane)	CHF_2OCF_2CHFCl	4.3	0.41	5.30e-11	**2120**	5.35e-11	**583**	7.36e-13	**1080**	7.14e-14	**116**	4.44e-14	**81**
HCFE-235da2 (isoflurane)	$CHF_2OCHClCF_3$	3.5	0.42	4.49e-11	**1800**	4.50e-11	**491**	5.62e-13	**822**	5.72e-14	**93**	3.73e-14	**68**
HFE-236ca	$CHF_2OCF_2CHF_2$	20.8	0.56[g]	2.42e-10	**9710**	3.89e-10	**4240**	6.03e-12	**8820**	2.10e-12	**3400**	4.98e-13	**912**
HFE-236ea2 (desflurane)	$CHF_2OCHFCF_3$	10.8	0.45	1.39e-10	**5550**	1.64e-10	**1790**	2.93e-12	**4280**	4.64e-13	**753**	1.42e-13	**260**
HFE-236fa	$CF_3CH_2OCF_3$	7.5	0.36	8.35e-11	**3350**	8.98e-11	**979**	1.53e-12	**2240**	1.68e-13	**273**	7.54e-14	**138**
HFE-245cb2	$CF_3CF_2OCH_3$	4.9	0.33	5.90e-11	**2360**	6.00e-11	**654**	8.77e-13	**1280**	8.40e-14	**136**	4.99e-14	**91**
HFE-245fa1	$CHF_2CH_2OCF_3$	6.6	0.31	7.22e-11	**2900**	7.59e-11	**828**	1.25e-12	**1820**	1.27e-13	**206**	6.35e-14	**116**
HFE-245fa2	$CHF_2OCH_2CF_3$	5.5	0.36	7.25e-11	**2910**	7.45e-11	**812**	1.15e-12	**1670**	1.10e-13	**179**	6.21e-14	**114**
2,2,3,3,3-Pentafluoropropan-1-ol	$CF_3CF_2CH_2OH$	0.3	0.14	1.72e-12	**69**	1.72e-12	**19**	1.42e-14	**21**	1.95e-15	**3**	1.42e-15	**3**
HFE-254cb1	$CH_3OCF_2CHF_2$	2.5	0.26	2.76e-11	**1110**	2.76e-11	**301**	2.99e-13	**438**	3.34e-14	**54**	2.28e-14	**42**
HFE-263fb2	$CF_3CH_2OCH_3$	23.0 days	0.04	1.22e-13	**5**	1.22e-13	**1**	9.72e-16	**1**	1.37e-16	**<1**	9.98e-17	**<1**
HFE-263m1	$CF_3OCH_2CH_3$	0.4	0.13	2.70e-12	**108**	2.70e-12	**29**	2.25e-14	**33**	3.06e-15	**5**	2.22e-15	**4**
3,3,3-Trifluoropropan-1-ol	$CF_3CH_2CH_2OH$	12.0 days	0.02	3.57e-14	**1**	3.57e-14	**<1**	2.85e-16	**<1**	4.01e-17	**<1**	2.93e-17	**<1**
HFE-329mcc2	$CHF_2CF_2OCF_2CF_3$	22.5	0.53	1.68e-10	**6720**	2.81e-10	**3070**	4.23e-12	**6180**	1.59e-12	**2580**	3.93e-13	**718**
HFE-338mmz1	$(CF_3)_2CHOCHF_2$	21.2	0.44	1.48e-10	**5940**	2.40e-10	**2620**	3.70e-12	**5410**	1.31e-12	**2130**	3.14e-13	**575**

(continued on next page)

Table 8.A.1 (continued)

Acronym, Common Name or Chemical Name	Chemical Formula	Lifetime (Years)	Radiative Efficiency (W m^{-2} ppb^{-1})	AGWP 20-year (W m^{-2} yr kg^{-1})	**GWP 20-year**	AGWP 100-year (W m^{-2} yr kg^{-1})	**GWP 100-year**	AGTP 20-year (K kg^{-1})	**GTP 20-year**	AGTP 50-year (K kg^{-1})	**GTP 50-year**	AGTP 100-year (K kg^{-1})	**GTP 100-year**
HFE-338mcf2	$CF_3CH_2OCF_2CF_3$	7.5	0.44	7.93e-11	**3180**	8.52e-11	**929**	1.45e-12	**2120**	1.60e-13	**259**	7.16e-14	**131**
Sevoflurane (HFE-347mmz1)	$(CF_3)_2CHOCH_2F$	2.2	0.32	1.98e-11	**795**	1.98e-11	**216**	2.06e-13	**302**	2.37e-14	**38**	1.64e-14	**30**
HFE-347mcc3 (HFE-7000)	$CH_3OCF_2CF_2CF_3$	5.0	0.35	4.78e-11	**1910**	4.86e-11	**530**	7.18e-13	**1050**	6.87e-14	**111**	4.05e-14	**74**
HFE-347mcf2	$CHF_2CH_2OCF_2CF_3$	6.6	0.42	7.45e-11	**2990**	7.83e-11	**854**	1.29e-12	**1880**	1.31e-13	**212**	6.55e-14	**120**
HFE-347pcf2	$CHF_2CF_2OCH_2CF_3$	6.0	0.48[h]	7.86e-11	**3150**	8.15e-11	**889**	1.30e-12	**1900**	1.27e-13	**206**	6.81e-14	**124**
HFE-347mmy1	$(CF_3)_2CFOCH_3$	3.7	0.32	3.32e-11	**1330**	3.33e-11	**363**	4.27e-13	**624**	4.28e-14	**69**	2.76e-14	**51**
HFE-356mec3	$CH_3OCF_2CHFCF_3$	3.8	0.30	3.53e-11	**1410**	3.55e-11	**387**	4.60e-13	**673**	4.58e-14	**74**	2.94e-14	**54**
HFE-356mff2	$CF_3CH_2OCH_2CF_3$	105.0 days	0.17	1.54e-12	**62**	1.54e-12	**17**	1.26e-14	**18**	1.74e-15	**3**	1.26e-15	**2**
HFE-356pcf2	$CHF_2CH_2OCF_2CHF_2$	5.7	0.37	6.40e-11	**2560**	6.59e-11	**719**	1.03e-12	**1500**	9.97e-14	**162**	5.50e-14	**101**
HFE-356pcf3	$CHF_2OCH_2CF_2CHF_2$	3.5	0.38	4.08e-11	**1640**	4.09e-11	**446**	5.11e-13	**747**	5.20e-14	**84**	3.39e-14	**62**
HFE-356pcc3	$CH_3OCF_2CF_2CHF_2$	3.8	0.32	3.77e-11	**1510**	3.79e-11	**413**	4.91e-13	**718**	4.89e-14	**79**	3.14e-14	**57**
HFE-356mmz1	$(CF_3)_2CHOCH_3$	97.1 days	0.15	1.25e-12	**50**	1.25e-12	**14**	1.02e-14	**15**	1.41e-15	**2**	1.02e-15	**2**
HFE-365mcf3	$CF_3CF_2CH_2OCH_3$	19.3 days	0.05	8.51e-14	**3**	8.51e-14	**<1**	6.80e-16	**<1**	9.56e-17	**<1**	6.99e-17	**<1**
HFE-365mcf2	$CF_3CF_2OCH_2CH_3$	0.6	0.26[i]	5.35e-12	**215**	5.35e-12	**58**	4.53e-14	**66**	6.10e-15	**10**	4.40e-15	**8**
HFE-374pc2	$CHF_2CF_2OCH_2CH_3$	5.0	0.30	5.65e-11	**2260**	5.75e-11	**627**	8.48e-13	**1240**	8.12e-14	**132**	4.79e-14	**88**
4,4,4-Trifluorobutan-1-ol	$CF_3(CH_2)_2CH_2OH$	4.0 days	0.01	1.73e-15	**<1**	1.73e-15	**<1**	1.38e-17	**<1**	1.94e-18	**<1**	1.42e-18	**<1**
2,2,3,3,4,4,5,5-Octafluorocyclopentanol	$-(CF_2)_4CH(OH)-$	0.3	0.16	1.18e-12	**47**	1.18e-12	**13**	9.67e-15	**14**	1.33e-15	**2**	9.69e-16	**2**
HFE-43-10pccc124 (H-Galden 1040x, HG-11)	$CHF_2OCF_2OC_2F_4OCHF_2$	13.5	1.02	2.00e-10	**8010**	2.58e-10	**2820**	4.52e-12	**6600**	9.46e-13	**1530**	2.38e-13	**436**
HFE-449s1 (HFE-7100)	$C_4F_9OCH_3$	4.7	0.36	3.80e-11	**1530**	3.86e-11	**421**	5.54e-13	**809**	5.32e-14	**86**	3.21e-14	**59**
n-HFE-7100	$n\text{-}C_4F_9OCH_3$	4.7	0.42	4.39e-11	**1760**	4.45e-11	**486**	6.39e-13	**934**	6.14e-14	**99**	3.70e-14	**68**
i-HFE-7100	$i\text{-}C_4F_9OCH_3$	4.7	0.35	3.68e-11	**1480**	3.73e-11	**407**	5.35e-13	**783**	5.14e-14	**83**	3.10e-14	**57**
HFE-569sf2 (HFE-7200)	$C_4F_9OC_2H_5$	0.8	0.30	5.21e-12	**209**	5.21e-12	**57**	4.52e-14	**66**	5.97e-15	**10**	4.29e-15	**8**
n-HFE-7200	$n\text{-}C_4F_9OC_2H_5$	0.8	0.35[i]	5.92e-12	**237**	5.92e-12	**65**	5.14e-14	**75**	6.78e-15	**11**	4.87e-15	**9**
i-HFE-7200	$i\text{-}C_4F_9OC_2H_5$	0.8	0.24	4.06e-12	**163**	4.06e-12	**44**	3.52e-14	**52**	4.65e-15	**8**	3.34e-15	**6**
HFE-236ca12 (HG-10)	$CHF_2OCF_2OCHF_2$	25.0	0.65	2.75e-10	**11,000**	4.91e-10	**5350**	7.06e-12	**10,300**	2.94e-12	**4770**	7.75e-13	**1420**
HFE-338pcc13 (HG-01)	$CHF_2OCF_2CF_2OCHF_2$	12.9	0.86	2.10e-10	**8430**	2.67e-10	**2910**	4.69e-12	**6860**	9.28e-13	**1500**	2.42e-13	**442**
1,1,1,3,3,3-Hexafluoropropan-2-ol	$(CF_3)_2CHOH$	1.9	0.26	1.67e-11	**668**	1.67e-11	**182**	1.66e-13	**243**	1.97e-14	**32**	1.38e-14	**25**
HG-02	$HF_2C-(OCF_2CF_2)_2-OCF_2H$	12.9	1.24[i]	1.97e-10	**7900**	2.50e-10	**2730**	4.40e-12	**6430**	8.70e-13	**1410**	2.27e-13	**415**
HG-03	$HF_2C-(OCF_2CF_2)_3-OCF_2H$	12.9	1.76[i]	2.06e-10	**8270**	2.62e-10	**2850**	4.60e-12	**6730**	9.10e-13	**1480**	2.37e-13	**434**
HG-20	$HF_2C-(OCF_2)_2-OCF_2H$	25.0	0.92[i]	2.73e-10	**10,900**	4.86e-10	**5300**	7.00e-12	**10,200**	2.91e-12	**4730**	7.68e-13	**1400**
HG-21	$HF_2C-OCF_2CF_2OC-F_2OCF_2O-CF_2H$	13.5	1.71[i]	2.76e-10	**11,100**	3.57e-10	**3890**	6.23e-12	**9110**	1.31e-12	**2120**	3.29e-13	**602**

(continued on next page)

Table 8.A.1 (continued)

Acronym, Common Name or Chemical Name	Chemical Formula	Lifetime (Years)	Radiative Efficiency (W m^{-2} ppb^{-1})	AGWP 20-year (W m^{-2} yr kg^{-1})	**GWP 20-year**	AGWP 100-year (W m^{-2} yr kg^{-1})	**GWP 100-year**	AGTP 20-year (K kg^{-1})	**GTP 20-year**	AGTP 50-year (K kg^{-1})	**GTP 50-year**	AGTP 100-year (K kg^{-1})	**GTP 100-year**
HG-30	$HF_2C–(OCF_2)_3–OCF_2H$	25.0	1.65[i]	3.77e-10	**15,100**	6.73e-10	**7330**	9.68e-12	**14,100**	4.03e-12	**6530**	1.06e-12	**1940**
1-Ethoxy-1,1,2,2,3,3,3-heptafluoropropane	$CF_3CF_2CF_2OCH_2CH_3$	0.8	0.28[i]	5.56e-12	**223**	5.56e-12	**61**	4.80e-14	**70**	6.36e-15	**10**	4.57e-15	**8**
Fluoroxene	$CF_3CH_2OCH=CH_2$	3.6 days	0.01[i]	4.97e-15	**<1**	4.97e-15	**<1**	3.95e-17	**<1**	5.58e-18	**<1**	4.08e-18	**<1**
1,1,2,2-Tetrafluoro-1-(fluoromethoxy)ethane	$CH_2FOCF_2CF_2H$	6.2	0.34[i]	7.68e-11	**3080**	7.99e-11	**871**	1.29e-12	**1880**	1.28e-13	**207**	6.68e-14	**122**
2-Ethoxy-3,3,4,4,5-pentafluorotetrahydro-2,5-bis[1,2,2,2-tetrafluoro-1-(trifluoromethyl)ethyl]-furan	$C_{12}H_5F_{19}O_2$	1.0	0.49[j]	5.09e-12	**204**	5.09e-12	**56**	4.53e-14	**66**	5.86e-15	**10**	4.19e-15	**8**
Fluoro(methoxy)methane	CH_3OCH_2F	73.0 days	0.07[g]	1.15e-12	**46**	1.15e-12	**13**	9.34e-15	**14**	1.30e-15	**2**	9.46e-16	**2**
Difluoro(methoxy)methane	CH_3OCHF_2	1.1	0.17[g]	1.32e-11	**528**	1.32e-11	**144**	1.18e-13	**173**	1.52e-14	**25**	1.08e-14	**20**
Fluoro(fluoromethoxy)methane	CH_2FOCH_2F	0.9	0.19[g]	1.20e-11	**479**	1.20e-11	**130**	1.05e-13	**153**	1.37e-14	**22**	9.84e-15	**18**
Difluoro(fluoromethoxy)methane	CH_2FOCHF_2	3.3	0.30[g]	5.65e-11	**2260**	5.66e-11	**617**	6.88e-13	**1010**	7.11e-14	**115**	4.69e-14	**86**
Trifluoro(fluoromethoxy)methane	CH_2FOCF_3	4.4	0.33[g]	6.82e-11	**2730**	6.89e-11	**751**	9.59e-13	**1400**	9.27e-14	**150**	5.72e-14	**105**
HG′-01	$CH_3OCF_2CF_2OCH_3$	2.0	0.29	2.03e-11	**815**	2.03e-11	**222**	2.06e-13	**301**	2.42e-14	**39**	1.68e-14	**31**
HG′-02	$CH_3O(CF_2CF_2O)_2CH_3$	2.0	0.56	2.16e-11	**868**	2.16e-11	**236**	2.19e-13	**320**	2.57e-14	**42**	1.79e-14	**33**
HG′-03	$CH_3O(CF_2CF_2O)_3CH_3$	2.0	0.76	2.03e-11	**812**	2.03e-11	**221**	2.05e-13	**299**	2.41e-14	**39**	1.67e-14	**31**
HFE-329me3	$CF_3CFHCF_2OCF_3$	40.0	0.48	1.79e-10	**7170**	4.17e-10	**4550**	4.85e-12	**7090**	2.89e-12	**4690**	1.12e-12	**2040**
3,3,4,4,5,5,6,6,7,7,7-Undecafluoroheptan-1-ol	$CF_3(CF_2)_4CH_2CH_2OH$	20.0 days	0.06	3.91e-14	**2**	3.91e-14	**<1**	3.12e-16	**<1**	4.39e-17	**<1**	3.21e-17	**<1**
3,3,4,4,5,5,6,6,7,7,8,8,9,9,9-Pentadecafluorononan-1-ol	$CF_3(CF_2)_6CH_2CH_2OH$	20.0 days	0.07	3.00e-14	**1**	3.00e-14	**<1**	2.40e-16	**<1**	3.37e-17	**<1**	2.46e-17	**<1**
3,3,4,4,5,5,6,6,7,7,8,8,9,9,10,10,11,11,11-Nonadecafluoroundecan-1-ol	$CF_3(CF_2)_8CH_2CH_2OH$	20.0 days	0.05	1.72e-14	**<1**	1.72e-14	**<1**	1.37e-16	**<1**	1.93e-17	**<1**	1.41e-17	**<1**
2-Chloro-1,1,2-trifluoro-1-methoxyethane	CH_3OCF_2CHFCl	1.4	0.21	1.12e-11	**449**	1.12e-11	**122**	1.05e-13	**153**	1.31e-14	**21**	9.24e-15	**17**
PFPMIE (perfluoropolymethylisopropyl ether)	$CF_3OCF(CF_3)CF_2OCF_2OCF_3$	800.0	0.65	1.87e-10	**7500**	8.90e-10	**9710**	5.52e-12	**8070**	6.11e-12	**9910**	6.15e-12	**11,300**
HFE-216	$CF_3OCF=CF_2$	8.4 days	0.02	1.92e-14	**<1**	1.92e-14	**<1**	1.53e-16	**<1**	2.15e-17	**<1**	1.58e-17	**<1**
Trifluoromethyl formate	$HCOOCF_3$	3.5	0.31[i]	5.37e-11	**2150**	5.39e-11	**588**	6.73e-13	**984**	6.85e-14	**111**	4.47e-14	**82**
Perfluoroethyl formate	$HCOOCF_2CF_3$	3.5	0.44[i]	5.30e-11	**2130**	5.32e-11	**580**	6.64e-13	**971**	6.76e-14	**110**	4.41e-14	**81**
Perfluoropropyl formate	$HCOOCF_2CF_2CF_3$	2.6	0.50[i]	3.45e-11	**1380**	3.45e-11	**376**	3.80e-13	**555**	4.19e-14	**68**	2.85e-14	**52**
Perfluorobutyl formate	$HCOOCF_2CF_2CF_2CF_3$	3.0	0.56[i]	3.59e-11	**1440**	3.59e-11	**392**	4.19e-13	**613**	4.45e-14	**72**	2.97e-14	**54**
2,2,2-Trifluoroethyl formate	$HCOOCH_2CF_3$	0.4	0.16[i]	3.07e-12	**123**	3.07e-12	**33**	2.55e-14	**37**	3.48e-15	**6**	2.52e-15	**5**
3,3,3-Trifluoropropyl formate	$HCOOCH_2CH_2CF_3$	0.3	0.13[i]	1.60e-12	**64**	1.60e-12	**17**	1.31e-14	**19**	1.80e-15	**3**	1.31e-15	**2**
1,2,2,2-Tetrafluoroethyl formate	$HCOOCHFCF_3$	3.2	0.35[i]	4.30e-11	**1720**	4.31e-11	**470**	5.17e-13	**755**	5.39e-14	**87**	3.57e-14	**65**
1,1,1,3,3,3-Hexafluoropropan-2-yl formate	$HCOOCH(CF_3)_2$	3.2	0.33[i]	3.05e-11	**1220**	3.05e-11	**333**	3.66e-13	**535**	3.81e-14	**62**	2.53e-14	**46**
Perfluorobutyl acetate	$CH_3COOCF_2CF_2CF_2CF_3$	21.9 days	0.12[i]	1.52e-13	**6**	1.52e-13	**2**	1.21e-15	**2**	1.71e-16	**<1**	1.25e-16	**<1**
Perfluoropropyl acetate	$CH_3COOCF_2CF_2CF_3$	21.9 days	0.11[i]	1.59e-13	**6**	1.59e-13	**2**	1.27e-15	**2**	1.78e-16	**<1**	1.30e-16	**<1**
Perfluoroethyl acetate	$CH_3COOCF_2CF_3$	21.9 days	0.10[i]	1.89e-13	**8**	1.89e-13	**2**	1.51e-15	**2**	2.12e-16	**<1**	1.55e-16	**<1**
Trifluoromethyl acetate	CH_3COOCF_3	21.9 days	0.07[i]	1.90e-13	**8**	1.90e-13	**2**	1.52e-15	**2**	2.14e-16	**<1**	1.56e-16	**<1**

(continued on next page)

Table 8.A.1 (continued)

Acronym, Common Name or Chemical Name	Chemical Formula	Lifetime (Years)	Radiative Efficiency (W m^{-2} ppb^{-1})	AGWP 20-year (W m^{-2} yr kg^{-1})	**GWP 20-year**	AGWP 100-year (W m^{-2} yr kg^{-1})	**GWP 100-year**	AGTP 20-year (K kg^{-1})	**GTP 20-year**	AGTP 50-year (K kg^{-1})	**GTP 50-year**	AGTP 100-year (K kg^{-1})	**GTP 100-year**
Methyl carbonofluoridate	$FCOOCH_3$	1.8	0.07[i]	8.74e-12	**350**	8.74e-12	**95**	8.60e-14	**126**	1.03e-14	**17**	7.21e-15	**13**
1,1-Difluoroethyl carbonofluoridate	$FCOOCF_2CH_3$	0.3	0.17[i]	2.46e-12	**99**	2.46e-12	**27**	2.02e-14	**30**	2.78e-15	**5**	2.02e-15	**4**
1,1-Difluoroethyl 2,2,2-trifluoroacetate	$CF_3COOCF_2CH_3$	0.3	0.27[i]	2.83e-12	**113**	2.83e-12	**31**	2.33e-14	**34**	3.20e-15	**5**	2.32e-15	**4**
Ethyl 2,2,2-trifluoroacetate	$CF_3COOCH_2CH_3$	21.9 days	0.05[i]	1.26e-13	**5**	1.26e-13	**1**	1.00e-15	**1**	1.41e-16	**<1**	1.03e-16	**<1**
2,2,2-Trifluoroethyl 2,2,2-trifluoroacetate	$CF_3COOCH_2CF_3$	54.8 days	0.15[i]	6.27e-13	**25**	6.27e-13	**7**	5.06e-15	**7**	7.07e-16	**1**	5.15e-16	**<1**
Methyl 2,2,2-trifluoroacetate	CF_3COOCH_3	0.6	0.18[i]	4.80e-12	**192**	4.80e-12	**52**	4.08e-14	**60**	5.47e-15	**9**	3.95e-15	**7**
Methyl 2,2-difluoroacetate	HCF_2COOCH_3	40.1 days	0.05[i]	3.00e-13	**12**	3.00e-13	**3**	2.41e-15	**4**	3.38e-16	**<1**	2.47e-16	**<1**
Difluoromethyl 2,2,2-trifluoroacetate	$CF_3COOCHF_2$	0.3	0.24[i]	2.48e-12	**99**	2.48e-12	**27**	2.04e-14	**30**	2.81e-15	**5**	2.04e-15	**4**
2,2,3,3,4,4,4-Heptafluorobutan-1-ol	$C_3F_7CH_2OH$	0.6	0.20	3.10e-12	**124**	3.10e-12	**34**	2.61e-14	**38**	3.52e-15	**6**	2.55e-15	**5**
1,1,2-Trifluoro-2-(trifluoromethoxy)-ethane	$CHF_2CHFOCF_3$	9.8	0.35	9.91e-11	**3970**	1.14e-10	**1240**	2.03e-12	**2960**	2.88e-13	**467**	9.74e-14	**178**
1-Ethoxy-1,1,2,3,3,3-hexafluoropropane	$CF_3CHFCF_2OCH_2CH_3$	0.4	0.19	2.14e-12	**86**	2.14e-12	**23**	1.77e-14	**26**	2.43e-15	**4**	1.76e-15	**3**
1,1,1,2,2,3,3-Heptafluoro-3-(1,2,2,2-tetrafluoroethoxy)-propane	$CF_3CF_2CF_2OCHFCF_3$	67.0	0.58	1.98e-10	**7940**	5.95e-10	**6490**	5.57e-12	**8140**	4.29e-12	**6960**	2.39e-12	**4380**
2,2,3,3-Tetrafluoro-1-propanol	$CHF_2CF_2CH_2OH$	91.3 days	0.11	1.19e-12	**48**	1.19e-12	**13**	9.72e-15	**14**	1.35e-15	**2**	9.79e-16	**2**
2,2,3,4,4,4-Hexafluoro-1-butanol	$CF_3CHFCF_2CH_2OH$	94.9 days	0.19	1.56e-12	**63**	1.56e-12	**17**	1.27e-14	**19**	1.76e-15	**3**	1.28e-15	**2**
2,2,3,3,4,4,4-Heptafluoro-1-butanol	$CF_3CF_2CF_2CH_2OH$	0.3	0.16	1.49e-12	**60**	1.49e-12	**16**	1.23e-14	**18**	1.69e-15	**3**	1.23e-15	**2**
1,1,2,2-Tetrafluoro-3-methoxy-propane	$CHF_2CF_2CH_2OCH_3$	14.2 days	0.03	4.82e-14	**2**	4.82e-14	**<1**	3.84e-16	**<1**	5.41e-17	**<1**	3.96e-17	**<1**
perfluoro-2-methyl-3-pentanone	$CF_3CF_2C(O)CF(CF_3)_2$	7.0 days	0.03	9.14e-15	**<1**	9.14e-15	**<1**	7.27e-17	**<1**	1.03e-17	**<1**	7.51e-18	**<1**
3,3,3-Trifluoro-propanal	CF_3CH_2CHO	2.0 days	0.004	9.86e-16	**<1**	9.86e-16	**<1**	7.84e-18	**<1**	1.11e-18	**<1**	8.10e-19	**<1**
2-Fluoroethanol	CH_2FCH_2OH	20.4 days	0.02	8.07e-14	**3**	8.07e-14	**<1**	6.45e-16	**<1**	9.07e-17	**<1**	6.63e-17	**<1**
2,2-Difluoroethanol	CHF_2CH_2OH	40.0 days	0.04	2.78e-13	**11**	2.78e-13	**3**	2.23e-15	**3**	3.12e-16	**<1**	2.28e-16	**<1**
2,2,2-Trifluoroethanol	CF_3CH_2OH	0.3	0.10	1.83e-12	**73**	1.83e-12	**20**	1.50e-14	**22**	2.07e-15	**3**	1.50e-15	**3**
1,1′-Oxybis[2-(difluoromethoxy)-1,1,2,2-tetrafluoroethane	$HCF_2O(CF_2CF_2O)_2CF_2H$	26.0	1.15[k]	2.47e-10	**9910**	4.51e-10	**4920**	6.38e-12	**9320**	2.75e-12	**4460**	7.45e-13	**1360**
1,1,3,3,4,4,6,6,7,7,9,9,10,10,12,12-hexadecafluoro-2,5,8,11-Tetraoxadodecane	$HCF_2O(CF_2CF_2O)_3CF_2H$	26.0	1.43[k]	2.26e-10	**9050**	4.12e-10	**4490**	5.83e-12	**8520**	2.51e-12	**4080**	6.81e-13	**1250**
1,1,3,3,4,4,6,6,7,7,9,9,10,10,12,12,13,13,15,15-eicosafluoro-2,5,8,11,14-Pentaoxapentadecane	$HCF_2O(CF_2CF_2O)_4CF_2H$	26.0	1.46[k]	1.83e-10	**7320**	3.33e-10	**3630**	4.71e-12	**6880**	2.03e-12	**3300**	5.50e-13	**1010**

Notes:

For CH_4 we estimate an uncertainty of ±30% and ±40% for 20- and 100-year time horizon, respectively (for 90% uncertainty range). The uncertainty is dominated by AGWP for CO_2 and indirect effects. The uncertainty in GWP for N_2O is estimated to ±20% and ±30% for 20- and 100-year time horizon, with the largest contributions from CO_2. The uncertainty in GWP for HFC-134a is estimated to ±25% and ±35% for 20- and 100-year time horizons while for CFC-11 the GWP the corresponding numbers are approximately ±20% and ±35% (not accounting for the indirect effects). For CFC-12 the corresponding numbers are ±20 and ±30. The uncertainties estimated for HFC-134a and CFC-11 are assessed as representative for most other gases with similar or longer lifetimes. For shorter-lived gases, the uncertainties will be larger. For GTP, few estimates are available in the literature. The uncertainty is assessed to be of the order of ±75% for the methane GTP_{100}.

* No single lifetime can be given. The impulse response function for CO_2 from Joos et al. (2013) has been used. See also Supplementary Material Section 8.SM.11.

† Perturbation lifetime is used in calculation of metrics, not the lifetime of the atmospheric burden.

(continued on next page)

Table 8.A.1 Notes (continued)

‡ Metric values for CH_4 of fossil origin include the oxidation to CO_2 (based on Boucher et al., 2009). In applications of these values, inclusion of the CO_2 effect of fossil methane must be done with caution to avoid any double-counting because CO_2 emissions numbers are often based on total carbon content. Methane values without the CO_2 effect from fossil methane are thus appropriate for fossil methane sources for which the carbon has been accounted for elsewhere, or for biospheric methane sources for which there is abalance between CO_2 taken up by the biosphere and CO_2 produced from CH_4 oxidization. The addition effect on GWP and GTP represents lower limits from Boucher et al. (2009) and assume 50% of the carbon is deposited as formaldehyde to the surface and is then lost. The upper limit in Boucher et al. (2009) made the assumption that this deposited formaldehyde was subsequently further oxidized to CO_2 .

[a] RE is unchanged since AR4.

[b] RE is unchanged since AR4 except the absolute forcing is increased by a factor of 1.04 to account for the change in the recommended RE of CFC-11.

[c] Based on Rajakumar et al. (2006) (lifetime correction factor has been applied to account for non-homogeneous horizontal and vertical mixing).

[d] Based on instantaneous RE from Baasandorj et al. (2010); Baasandorj et al. (2011) (correction factors have been applied to account for stratospheric temperature adjustment and non-homogeneous horizontal and vertical mixing).

[e] Based on instantaneous RE from *ab initio* study of Bravo et al. (2010) (a factor 1.10 has been applied to account for stratospheric temperature adjustment).

[f] Based on average instantaneous RE reported in literature (Vasekova et al., 2006; Bravo et al., 2010) (correction factors have been applied to account for stratospheric temperature adjustment and non-homogeneous horizontal and vertical mixing).

[g] Based on instantaneous RE from *ab initio* studies of Blowers et al. (2007, 2008)(correction factors have been applied to account for stratospheric temperature adjustment and non-homogeneous horizontal and vertical mixing).

[h] Based on instantaneous RE from Heathfield et al. (1998) (correction factors have been applied to account for stratospheric temperature adjustment and non-homogeneous horizontal and vertical mixing).

[i] Note that calculation of RE is based on calculated (*ab initio*) absorption cross-section and uncertainties are therefore larger than for calculations using experimental absorption cross section.

[j] Based on instantaneous RE from Javadi et al. (2007) (correction factors have been applied to account for stratospheric temperature adjustment and non-homogeneous horizontal and vertical mixing).

[k] Based on instantaneous RE from Andersen et al. (2010) (correction factors have been applied to account for stratospheric temperature adjustment and non-homogeneous horizontal and vertical mixing).

The GTP values are calculated with a temperature impulse response function taken from Boucher and Reddy (2008). See also Supplementary Material Section 8.SM.11.

Table 8.A.2 | Halocarbon indirect GWPs from ozone depletion using the EESC-based method described in WMO (2011), adapted from Daniel et al. (1995). A radiative forcing in year 2011 of –0.15 (–0.30 to 0.0) W m^{-2} relative to preindustrial times is used (see Section 8.3.3). Uncertainty on the indirect AGWPs due to the ozone forcing uncertainty is ±100%.

Gas	GWP_{100}
CFC-11	–2640
CFC-12	–2100
CFC-113	–2150
CFC-114	–914
CFC-115	–223
HCFC-22	–98
HCFC-123	–37
HCFC-124	–46
HCFC-141b	–261
HCFC-142b	–152
CH_3CCl_3	–319
CCl_4	–2110
CH_3Br	–1250
Halon-1211	–19,000
Halon-1301	–44,500
Halon-2402	–32,000
HCFC-225ca	–40
HCFC-225cb	–60

Table 8.A.3 | GWP and GTP for NO_X from surface sources for time horizons of 20 and 100 years from the literature. All values are on a per kilogram of nitrogen basis. Uncertainty for numbers from Fry et al. (2012) and Collins et al. (2013) refer to 1-σ. For the reference gas CO_2, RE and IRF from AR4 are used in the calculations. The GWP_{100} and GTP_{100} values can be scaled by 0.94 and 0.92, respectively, to account for updated values for the reference gas CO_2. For 20 years the changes are negligible.

	GWP		GTP	
	H = 20	H = 100	H = 20	H = 100
NO_X East Asia[a]	6.4 (±38.1)	–5.3 (±11.5)	–55.6 (±23.8)	–1.3 (±2.1)
NO_X EU + North Africa[a]	–39.4 (±17.5)	–15.6 (±5.8)	–48.0 (±14.9)	–2.5 (±1.3)
NO_X North America[a]	–2.4 (±30.3)	–8.2 (±10.3)	–61.9 (±27.8)	–1.7 (±2.1)
NO_X South Asia[a]	–40.7 (±88.3)	–25.3 (±29.0)	–124.6 (±67.4)	–4.6 (±5.1)
NO_X four above regions[a]	–15.9 (±32.7)	–11.6 (±10.7)	–62.1 (±26.2)	–2.2 (±2.1)
Mid-latitude NOx[c]	–43 to +23	–18 to +1.6	–55 to –37	–2.9 to –0.02
Tropical NO_x[c]	43 to 130	–28 to –10	–260 to –220	–6.6 to –5.4
NO_X global[b]	19	–11	–87	–2.9
NO_X global[d]	–108 ± 35 –335 ± 110 –560 ± 279	–31 ± 10 –95 ± 31 –159 ± 79		

Notes:

[a] Fry et al. (2012) (updated by including stratospheric H_2O) and Collins et al. (2013).

[b] Fuglestvedt et al. (2010); based on Wild et al. (2001).

[c] Fuglestvedt et al. (2010).

[d] Shindell et al. (2009). Three values are given: First, without aerosols, second, direct aerosol effect included (sulfate and nitrate), third, direct and indirect aerosol effects included. Uncertainty ranges from Shindell et al. (2009) are given for 95% confidence levels.

Table 8.A.4 | GWP and GTP for CO for time horizons of 20 and 100 years from the literature. Uncertainty for numbers from Fry et al. (2012) and Collins et al. (2013) refer to 1-σ. For the reference gas CO_2, RE and IRF from AR4 are used in the calculations. The GWP_{100} and GTP_{100} values can be scaled by 0.94 and 0.92, respectively, to account for updated values for the reference gas CO_2. For 20 years the changes are negligible.

	GWP		GTP	
	H = 20	H = 100	H = 20	H = 100
CO East Asia[a]	5.4 (±1.7)	1.8 (±0.6)	3.5 (±1.3)	0.26 (±0.12)
CO EU + North Africa[a]	4.9 (±1.5)	1.6 (±0.5)	3.2 (±1.2)	0.24 (±0.11)
CO North America[a]	5.6 (±1.8)	1.8 (±0.6)	3.7 (±1.3)	0.27 (±0.12)
CO South Asia[a]	5.7 (±1.3)	1.8 (±0.4)	3.4 (±1.0)	0.27 (±0.10)
CO four regions above[a]	5.4 (±1.6)	1.8 (±0.5)	3.5 (±1.2)	0.26 (±0.11)
CO global[b]	6 to 9.3	2 to 3.3	3.7 to 6.1	0.29 to 0.55
CO global[c]	7.8 ± 2.0 11.4 ± 2.9 18.6 ± 8.3	2.2 ± 0.6 3.3 ± 0.8 5.3 ± 2.3		

Notes:

[a] Fry et al. (2012) (updated by including stratospheric H_2O) and Collins et al. (2013).

[b] Fuglestvedt et al. (2010).

[c] Shindell et al. (2009). Three values are given: First, without aerosols, second, direct aerosol effect included, third, direct and indirect aerosol effects included. Uncertainty ranges from Shindell et al. (2009) are given for 95% confidence levels.

Table 8.A.5 | GWP and GTP for VOCs for time horizons of 20 and 100 years from the literature. Uncertainty for numbers from Fry et al. (2012) and Collins et al. (2013) refer to 1-σ. For the reference gas CO_2, RE and IRF from AR4 are used in the calculations. The GWP_{100} and GTP_{100} values can be scaled by 0.94 and 0.92, respectively, to account for updated values for the reference gas CO_2. For 20 years the changes are negligible.

	GWP		GTP	
	H = 20	H = 100	H = 20	H = 100
VOC East Asia[a]	16.3 (±6.4)	5.0 (±2.1)	8.4 (±4.6)	0.7 (±0.4)
VOC EU + North Africa[a]	18.0 (±8.5)	5.6 (±2.8)	9.5 (±6.5)	0.8 (±0.5)
VOC North America[a]	16.2 (±9.2)	5.0 (±3.0)	8.6 (±6.4)	0.7 (±0.5)
VOC South Asia[a]	27.8 (±5.6)	8.8 (±1.9)	15.7 (±5.0)	1.3 (±0.5)
VOC four regions above	18.7 (±7.5)	5.8 (±2.5)	10.0 (±5.7)	0.9 (±0.5)
VOC global[b]	14	4.5	7.5	0.66

Notes:

[a] Fry et al. (2012) (updated by including stratospheric H_2O) and Collins et al. (2013).

[b] Fuglestvedt et al. (2010) based on Collins et al. (2002).

The values are given on a per kilogram of C basis.

Table 8.A.6 | GWP and GTP from the literature for BC and OC for time horizons of 20 and 100 years. For the reference gas CO_2, RE and IRF from AR4 are used in the calculations. The GWP_{100} and GTP_{100} values can be scaled by 0.94 and 0.92, respectively, to account for updated values for the reference gas CO_2. For 20 years the changes are negligible.

	GWP		GTP	
	H = 20	H = 100	H = 20	H = 100
BC total, global[c]	3200 (270 to 6200)	900 (100 to 1700)	920 (95 to 2400)	130 (5 to 340)
BC (four regions)[d]	1200 ± 720	345 ± 207	420 ± 190	56 ± 25
BC global[a]	1600	460	470	64
BC aerosol–radiation interaction +albedo, global[b]	2900 ± 1500	830 ± 440		
OC global[a]	–240	–69	–71	–10
OC global[b]	–160 (–60 to –320)	–46 (–18 to –19)		
OC (4 regions)[d]	–160 ± 68	–46 ± 20	–55 ± 16	–7.3±2.1

Notes:

[a] Fuglestvedt et al. (2010).

[b] Bond et al. (2011). Uncertainties for OC are asymmetric and are presented as ranges.

[c] Bond et al. (2013). Metric values are given for total effect.

[d] Collins et al. (2013). The four regions are East Asia, EU + North Africa, North America and South Asia (as also given in Fry et al., 2012). Only aerosol-radiation interaction is included.